UNIVERSITY GRANT COMMISSION

NEW DELHI

(WRO) WESTERN REGIONAL OFFICE, GANESHKHIND,

PUNE – 411007

MINOR RESEARCH PROJECT (File No.: 47-2077/11(WRO) Dated: 23 Feb 2012)

"SYNTHESIS OF TRANSITION METAL COMPLEXES INVOLVING 2-AMINOPYRIDINE AND ETHYLENEDIAMINE LIGANDS, THEIR CHARACTERIZATION AND BIOLOGICAL ACTIVITY"

BY

DR. KHAKRE PANDIT RAMCHANDRA

ASSISTANT PROFESSOR

DEPARTMENT OF CHEMISTRY

VASANTDADA PATIL COLLEGE, PATODA,

DIST. BEED – 414204 (MS)

AFFILIATED TO

DR. BABASAHEB AMBEDKAR MARATHWADA UNIVERSITY, AURANGABAD – (MS).

September-2023

Declaration

I, Dr. Khakre Pandit Ramchandra hereby declare that the Minor Research Project work entitled, "**Synthesis of transition metal complexes involving 2-aminopyridine and ethylenediamine ligands, their characterization and biological activity",** submitted to the University Grant Commission, WRO Pune. This Minor Research Project has not previously formed the basis for the award of any other Degree, Diploma, Associateship, Fellowship or other title and other University. The present work is completely original to the best of my knowledge.

Place: Patoda

Date:

Dr. Khakre Pandit Ramchandra

Assistant Professor

Department of Chemistry

Vasantdada Patil College, Patoda

Dist. Beed – 414204 (MS).

(Navgan Shikshan Sanstha Rajuri's)

VASANTDADA PATIL ARTS, COMMERCE & SCIENCE COLLEGE,
PATODA. TQ. PATODA. DIST. BEED. MAHARASHTRA

Reaccredited 'B' grade by NAAC
ISO 9001:2015 certified

PRINCIPAL
PROF. ABASAHEB HANGE KSHIRSAGAR

SECRETARY
DR. BHARATBHUSHAN

Cell No. 9423715583
Phone: Office- (02444) 243049, Website: www.pvpcollegepatoda.org, E-mail: pvp_patoda@rediffmail.com/pvppatoda@gmail.com

VPCP/2023-2024 / 708 Date: 20/ 09 / 2023

CERTIFICATE

This is to certify that **Dr. Khakre Padit Ramchandra**, Assistant Professor, Department of Chemistry, Vasantdada Patil College, Patoda, Dist. Beed, carried out Minor Research Project entitled "**Synthesis of transition metal complexes involving 2-aminopyridine and ethylenediamine ligands, their characterization and biological activity",** with financial assistance by University Grants Commission, New Delhi, under XI plan. Hence Certified.

Place: Patoda

Date: 20/09/2023

Principal

(Seal)

Index

1. Chapter -I

Introduction

1.1 Introduction:

Importance of coordination compounds, playing different roles, in living systems is well established. The studies on coordination complexes have become a challenge to the present day chemist [1]. Co-ordination chemistry in a broad sense constitutes a major part of inorganic chemistry. The field of co-ordination chemistry has always been a challenge to chemists and has become a fast emerging area of chemistry [2]. The rapidly developing field of bio-inorganic chemistry is centered on the study of coordination compounds present in living systems. Many biologically active compounds are complexes, and even the similar types of complexes have served as model compounds in investigation of bodily processes. In fact, the new field of bio-inorganic chemistry is concerned largely with coordination chemistry.

The complexes which are found in minerals, plants and animals are of great significance because they exhibit important functions in the environment where they are present. The synthesis of newer and newer organic chelating agents that can coordinate with transition metal ions has tempted the researchers to synthesize more and more co-ordination complexes. The rapid development in the field of bio-inorganic chemistry is centered on the study of co-ordination compounds present in living systems.

A complex defined by Rossotti and coworkers [3] is a species formed by the association of two or more simple species, each capable of independent existence. When one of the species is a metal ion, the resulting entity is known as a metal complex. The term ‘ligand’ is applied to the particular molecule or ion attached to the central metal ion [4]. Some ligands are attached to central metal ion by more than one atom in such a manner to form a ring. This is known as chelation and the resulting complex is called as metal chelate [5]. The stability of chelate depends on the size of the ring. Generally co-ordinated compounds of a saturated five membered ring are more stable than those formed of unsaturated five membered rings. However, a great stability to metal chelate is achieved with the formation of six membered ring [6].

The modern study of co-ordination compounds begins with Alfred Werner. Alfred Werner’s classical idea of coordination bond, in 1893, gave a great deal to the development of coordination chemistry [7]. The theory postulated that in coordination compounds, the metal exhibits two types of valencies, primary and secondary. The

primary valency is ionisable and non-directional, where as secondary valency is non ionisable and directional. The bonds between the ligand and the metal ion are due to the secondary valencies of metal ions. The development of electronic theory of valency by Lewis, Kossel, Langmuir, Sidgwick, Fajan and coworkers [8], cleared the ideas regarding primary (oxidation state) and secondary (co-ordination number) valencies in complexes.

In 1931, Pauling gave valence bond theory (VBT), which is based on revolutionary idea of hybridization of atomic orbitals [9]. According to this theory, the central metal ion makes available number of empty s, p, d hybrid orbitals equal to its coordination number. These orbitals undergo particular type of hybridization such as sp, sp^2, sp^3, dsp^2, d^2sp^3 and sp^3d^3 which gives shape to the molecule as linear, trigonal, tetrahedral, square planer and octahedral respectively. The filled ligand orbitals overlap with empty hybrid orbitals of metal ions to form coordinate covalent bond. This theory explains mainly electronic structure of central metal ion, shapes of complexes, magnetic properties of complexes and stereochemistry. However, it does not give proper explanation of maximum pairing, the spectra of the complexes and quantitative interpretation of magnetic properties.

Crystal field theory (CFT) developed by Bethe [10] in 1929, originally applied to crystalline solids was further developed by Van Vleck [11] and co-workers. According to this theory, the bond between metal and ligand is neither due to sharing of electron nor due to interaction of atomic orbitals. The bond between metal and ligand is purely electrostatic. The interaction of d-orbitals of central metal ion with the surrounding ligand orbitals produces crystal field effect. The electric field due to the ligands lifts the degeneracy of the five d-orbitals of central metal ion and splits them into two energy sublevels t_{2g}-triplet and e_g-doublet. The energies of these sub-levels depends upon the type of geometry and nature of ligand. The energy difference between t_{2g} and eg levels is known as crystal field stabilization energy (CFSE) and is denoted by 10Dq. The magnitude of 10Dq depends upon the nature of ligand and charge on the central metal ion. CFT interprets the magnetic and spectral properties of transition metal complexes quantitatively.

The molecular orbital theory (MOT), developed by Van Vleck [11], although more complicated than the VBT and CFT theories, explains more satisfactorily the nature of bonding involved in coordination complexes. The formation of covalent bond with metal

ion and donor group is occurred due to with or without replacement of hydrogen atom from an organic functional group**.**

An enzyme provides an arrangement of side-chain functional groups having an appropriate sized hole with the preferred groups on enzyme side chains needed to bind the required metal ion. The optimal number of such binding groups is chosen for the particular metal ion, together with the appropriate hydrophobic or hydrophilic environment in the binding site. Metal ions may be bound by main-chain amino and carbonyl groups, but specific binding is achieved by the amino acid side chains, particularly the carboxylate groups of aspartic and glutamic acid, and the ring nitrogen atom of histidine. Other side chains that bind metal ions include tryptophan (ring nitrogen), cysteine (thiol), methionine (thioether), serine, threonine, tyrosine (hydroxyl groups), and asparagine and glutamine (carbonyl groups, less often amino groups). Each ligand contains at least one functional group which may coordinate to metal ion through it. Depending on the functional group coordinating to the metal ion, they are classified as complexes such as, β-diketones, hydrazides, semicabazones, 8- hydroxyquinoline etc.

1.2 Application of transition metal complexes in various fields

Application of complex compounds in various fascinating area is current research interest to the inorganic chemist all over the world. The continued interest and quest in designing new ligands and their use as a models for protein metal binding sites in a substantial array of metalloproteinase in biological systems, as synthetic ionospheres, as a model to study the magnetic exchange phenomena, as therapeutic agents in chelation therapy for the treatment of metal ion toxication, as cyclic antibiotics that owe their antibiotic actions to specific metal complexation, to study the guest host interactions and in catalysis. Recognition of the importance of complexes containing ligands had led to inexpensive synthetic routes for these compounds [22-25]. Efforts are being invested in developing reliable ligands and their complexes with transition and non-transition metal ions which have medicinal, physiological and pharmaceutical application, also well known as antibacterial, antifungal, anticancer agents [26-32]. Nowadays, the research field dealing with co-ordination chemistry has expanded enormously.

The importance of metal complexes for, bioinorganic chemistry, biomedical application, supramolecular chemistry, catalysis, medical sciences, separation encapsulation processes and formation of compounds with unusual properties and structures has been well recognized and reviewed [33]. Among the several classes of ligands, a new tetradentate ligands derived from orthophenylenediamine, salicylaldehyde and isatin /acyl acetone /2-hydroxy napthalaldehyde containing oxygen and nitrogen donor sites have been recognized and synthesized [34] .The different types of ligands and their metal complexes have importance in generating new areas of fundamental chemistry and many opportunities of applied chemistry. The majority of complexes represent creative and focused efforts to design molecules which will have particular uses.

The transition metal complexes find extensive applications in technology, industry and medicine [35]. Some β-diketones complexes have been shown to be good substitutes for tetraethyllead, the anti-knock additive for gasoline. Together with triethylaluminum, some lanthanide complexes are used as Ziegler-Natta catalyst for 4-stereospecific polymerization of butadiene [36]. Some carboxylate complexes of transition metals were used as antioxidant in the chelation therapy to remove ^{144} Ce - contamination in the body [37]. The majority of macro-cycles represent creative and focused efforts to design molecules which will have particular uses. It has also been found that the toxicity decreases with chelation hence the transition metal complexes derived from ligands capable of forming chelates are of great importance. Many macrocyclic complexes find extensive applications in technology, industry and medicine. Complexes of thiazoles and benzothiazoles [38] possess effective antifungal activity. Presence of methoxy, halogen and napthyl groups enhance fungicidal activity towards curvularia. Pyradione complexes showed physiological activity against A. niger. Some complexes have quinazolinones [39] show antifungal activity against candida albicans, trichophytonrebrum, a. niger and microsporumgypseum. Metal complexes formed between furan or furyglycoxal with various amines have shown antifungal activity against helminthosporiumgramineum, syncephalostr-umracemasus and c. capsici. Transition metal complexes with C, N bonded organic ligands have great attention in past years, many of these complexes are palladium (II) compounds which are found to be very useful in liquid crystal,

catalysis, and in organic synthesis. Recently the term carbo-palladium have been coined although platinum complexes have been less substituted than their palladium (II) counterparts, their applications are nevertheless important, for example, as compounds with antitumor activity. Also, photophysical and photochemical properties of square planer platinum (II) complexes have been described [40] and more recently cyclometallated platinum (II) complexes have been prepared.

1.2.1 In medical field :

Metal complexes of nitroguanidine with various aldehyde and ketones were studied for their antineoplastic and tuberculostatic activities. Many other metal chelates were studied for anti-tumour and anti-neoplastic activities. 2-pyridine carbaaldehyde (2-pyca) and it's hydrazones are used to collect semen antipode for cyanide poisoning. The complexes derived from 2-pyca and amino acids are powerful chelates for antibacterial activities. Complexes of dehydroacetic acid with benzoyl hydrazone, salicylic aldehyde and thiosemicarbazone and their metal chelates have been studied for applications in biochemically relevant aspects, chemotherapy and also in the field of agriculture. The imino derivatives of 2-pyca can be used as

chemotherapeutic drugs. Platinum compounds such as cisplatin (cis-[Pt (NH_3) $_2Cl_2$]), carboplatin, nedaplatin, lobaplatin and oxaliplatin are among the most widely used cancer therapeutic agents. [41] Pt (II) forms complexes with estrogen hormones and is used as anticancer agent for the treatment of hormone dependant cancer like breast cancer [42].

Cobalt complexes of nitrogen bases ligand derived from salicyldehyde and diamines have been proposed as models of Vitamin B_{12} compounds for similar physicochemical behaviour such as ability to form stable organometallic compounds and also models of naturally occurring oxygen carrier capacity to take up oxygen reversibly. Cobalt complexes of nitrogen bases derived from salicylaldehyde and diamines have proved to be useful in food packages. They have excellent light resistance property and storage ability and hence prevent degradation of food in

presence of acidic gases like carbon dioxide.

Interest in nitrogen containing complexes of tin (IV) and organotin (II) moieties have been shown because of their potential fungicidal and bactericidal activity [43]. It has been

observed that reagents of selective interaction with particular metal ion are very less. Schiff base complexes of thiosemicarbazide and thiosemicarbazones have been paid much attention due to their antitubercular activity. Metal chelates are found to inhibit the tumour growth and such types of metal chelates are used in the treatment of cancer [44-45].

1.2.2 In industrial field:

The metal complexes carrying molecular oxygen are useful in biological and industrial processes. The industrial chemists are interested in developing the homogeneous analogues to metal catalyzed oxidation reaction where as the biochemists are interested in biological oxygen transport. The complex containing oxygen, nitrogen and sulphur as donor atoms extend more contribution. complex with sulphur as a donor atoms have been found to be more selective as analytical reagents due to its large size and less electro-negativity. They form stable and intense coloured chelates with central metal ions [46]. Hence they are successfully used in dyes and pigment industries. The transition metal complexes are useful for mass dyeing of linear polysters, polyethylene terephthallet fibers [47].

1.2.3 In analytical field :

Transition metal complexes have variety of applications in analytical chemistry, such as in chromatographic, solvent extraction, separation techniques, qualitative and quantitative analysis. Mono and diamine bases were used in developing qualitative tests for Cu (II), Ni (II), Co (II), Fe (II), Fe (III), Cd (III), Zn (II), Mg (II) and Pb (II). Schiff bases with ruthenium, rhodium and iridium complexes have been used as therapeutic agents and a number of kinetically inert ruthenium (II), rhodium and iridium complexes have been reported as inhibitors of protein kinases [48]. In chromatography, polymeric metal complexes from diamine, bissalicyaldehyde are used as supports and adsorbents and as covalent bond type polymers, the HPLC resolution of Cu, Ni, Pd chelates of tetradentate β-ketoimine were carried out. The efficiency of polymeric schiff base complexes for gas separation was studied by many workers [49].

1.2.4 As a catalysts:

The past few decades, have witnessed a great deal of interest in chemistry of transition metal complex chelates because of their importance as catalysts in reactions such as carbonylation, hydroformylation, reduction, oxidation, epoxydation and hydrolysis [50-55]. Ligands derived from thiosemicarbazide and their metal complexes are of great significance for their pharmacological properties such as antibacterial, antifungal, antitumoral, antiviral and anticancer [56-62]. The schiff base, thiosemicarbazones have been used for the analytical determination of metals [63]. Ruthenium thiosemicarbazones have been found to be very efficient catalyst in the oxidation of alcohols and alkenes [64]. Palladium thiosemicarbazones were used as catalyst in microwave promoted Suzuki Miyaura cross-coupling rections [65].

1.2.5 Biological field :

Transition metal complexes of ligands are useful for preventing superoxide mediated cell damage and for treatment of inflammatory disorders in mammals particularly in humans [66] Technetium complexes with phosphate coordination have been used as myocardial perfusion imaging agents. Some complexes were choosen for further imaging development based on myocardial uptake, rapid blood and liver clearances [67]. Silver complexes in oxidation state (I) showed inhibition against *C. mosaic virus*, Glycine salicyaldehyde Ag(I) complex, gave effective results up to 74 % towards *C.mosaic* virus. Fungicidal and bactericidal activity of transition metal chelates derived from physiologically active dehydroacetic acid was studied by some workers [68].

1.3 Literature survey of previous related studies of ligands

1.3.1 2-aminopyridine as a ligand

Transition metal complexes of N-donor heterocyclic ligands are of interest due to their applications in biology, pharmacology, magnetism, and so forth [69]. Pyridine and its derivatives are known for their use in the design and synthesis of multifunctional compounds as well as their biological and pharmacological applications as anticoagulants, antihistamines, antiseptics, antiarrhythmics, and antirheumatics [70– 72]. Amongst the pyridine derivatives, 2-aminopyridine (2-ampy), a potential bidentate ligand

with two nitrogen donor atoms, is of great pharmacological importance because it is used in the synthesis of pharmaceuticals such as antihistamines and anti-inflammatories [73]. 2-ampy has also been shown to have a major influence on the formation of transition metal molybdates in which it acts as a buffer and forms weaker complexes with the transition metals, thus preventing their hydrolysis [74]. A survey of the reported crystal structures of 2-ampy with different metal ions indicates that 2-ampy exhibits different bonding modes: it mostly acts as a mono dentate ligand through its pyridine nitrogen atom [72, 75–79], though coordination through the exocyclic amino N-atom(a less common mode) has also been reported [80, 81]. When it coordinates through the pyridine N-atom, the formation of additional H-bonds through the exo-cyclic amine N-atom is possible [82]. It also forms chelates with a bidentate coordination mode through the pyridine N and exocyclic amine N atoms [83]. Several mixed ligand complexes containing 2-ampy have also been synthesized with different properties and diverse applications [75, 77–80, 84–93].

1.3.2 Ethylenediamine as a ligand

Although predominantly occurring as a chelating agent, ethylenediamine (for simplicity, further denoted as en) has been observed to possess the capacity to act as a bridging ligand as well. Various coordination polymers have been reported so far with en linking neighboring metal centers such as: Co(II) (Lauchan et al., 2008), Zn(II) (Pritchard et al., 2001), or Ag(I) (Näther and Beck, 2004). Cd(II) coordination arrays with extended structures formed via small anionic bridges are numerous (Zhou et al., 2003; Xia et al., 2004; Abu-Youssef, 2005). Examples of en connecting Cd(II) centers, whether exclusively or together with other types of bridging ligands present, are also known in the literature (Shen et al., 2002; Yilmaz et al., 2005). Two polymeric compounds, $[Cd(en)Cl_2]n$ and $[Cd(en)Br_2]n$, synthesized and examined by means of thermogravimetry analysis, IR and Raman spectroscopy (Iwamoto and Shriver, 1971; De and Chaudhuri, 1984). Investigations revealed the presence of bridging trans en ligands.

One of the simplest bidentate ligands is ethylenediamine. Of the 691 crystal structures containing homoleptic $[M(en)_3]$ n+, 158 of them crystalize in one of the 65 Sohncke space groups. Among these are the nitrate salts, for which $[Ni(en)_3](NO_3)_2$ and

$[Zn(en)_3](NO_3)_2$ [94] crystallize as conglomerates in the hexagonal space group P6322 at room temperature. At lower temperatures, 109 K for $[Ni(en)_3](NO_3)_2$ [95] and 143 K for $[Zn(en)_3](NO_3)_2$ [96], the compounds undergo a reversible phase transition to a pair of enantiomorphic space groups. For crystals containing the enantiomer the low-temperature phase is P6522, and P6122 for those containing the enantiomer. The same phase transition also occurs in $[Ni(en)_3](NO_3)_2$ crystals under pressure, with a transition between 0.82 and 0.87 GPa at room temperature. Surprisingly, no other $[M(en)_3](NO_3)_2$ compounds with divalent transition metals can be found in the CSD, except for that of Cd(II), which, however, crystallizes as a racemate in the centrosymmetric space group I_2/a.

1.4 Literature survey of related studies of metals

Brief Account of Transition Metal Complexes:

1) Molybdenum Complexes:

Molybdenum disulfide has long been known as a desirable additive for use in lubricating oil compositions. However, one of its major detriments is its lack of oil solubility. Molybdenum disulfide is ordinarily finely ground and then dispersed in the lubricating oil composition to impart friction modifying and antiwear properties. Finely ground molybdenum disulfide is not an effective oxidation inhibitor in lubricating oils.

Molybdenum complexes are well known as active centers of several enzymes such as oxotransferases [97–100]. Some molybdates show antiviral, antitumoral or antibiotic activity [101–103]. They are also known as efficient catalysts for the oxidation of various organic compounds with different oxygen donors like ROOH [104–116] and H_2O_2 [117–125]. Molybdenum(VI) dioxo or oxodiperoxo compounds are commonly encountered in oxidation catalysis. It has been shown that mononuclear peroxo and mono-oxo bridged dinuclear molybdenum complexes are active catalysts for the epoxidation of olefins and nonfunctionalized olefins with t-butylhydroperoxide TBHP as oxygen donor [104, 109–111]. The epoxidation of olefins catalyzed by a large family of complexes with $MoO_2X_2(N–N)_2$ or $MoO_2X_2(N– O)_2$ formula where N–N or N–O are bidenate ligands and X = Cl, Br or Me has been previously reported [106, 107, 111, 112]. All these catalysts show high activity and selectivity.

Molybdenum oxo-peroxo complexes were applied as catalysts for selective oxidation of arylalkyl, diaryl and dialkylsulfides to corresponding sulfoxides with TBHP as oxidant [126–129].

2) Ruthenium Complexes:

Ruthenium(II) polypyridyl complexes have received attention as DNA-binding substrates due to rich photochemical and photophysical properties [130]. In two decades of research on the excited-state properties of ruthenium complexes [131], a variety of substituted 2,2′-bipyridine and 1,10-phenanthroline systems as well as other α,α′-diimine systems have been investigated as ligands for ruthenium(II) complexes. There has been considerable interest in DNA-binding properties of transition metal complexes [132–134].

Ruthenium polypyridyl complexes are promising DNA probes due to their intense MLCT luminescence, excited-state redox properties, and DNA-binding properties [135]. When such binding is through intercalation, complexes can be quite useful. Many studies have focused on the interaction of ruthenium complexes containing planar ligands which have good biological activities [136–139]. Most of the well-known platinum anticancer complexes have amines as ligands [140]. Inventions [141] of platinum-diamine complexes with excellent antitumor activity and lower renal toxicity than cisplatin have been reported.

These studies suggest that at least one ligand must be a N-donor and should possess one hydrogen. Ruthenium(II) ethylenediamine complexes have similar DNA-binding properties to complexes containing phen or bpy as co-ligands [142], hence we concentrate on ethylenediamine co-ligands. Several transition metal complexes containing ethylenediamine as co-ligands have good DNA-binding properties and cytotoxicities [143].

3) Rhodium Complexes:

In spite of the recent advances in the field of intramolecular alkene hydroamination [144] the intermolecular hydroamination, and in particular, the anti-Markovnikov functionalization of unactivated olefins with amines, still remains an important challenge in catalysis. Reaction products can be amines, as a consequence of a formal N-H bond

addition to the unsaturated carbon-carbon bond, or enamines, as a result of an oxidative amination [145]. The control of the regioselectivity is an important issue as both anti-Markovnikov products are of industrial significance.

The first reported late transition metal catalysts for intermolecular hydroamination were rhodium salts used by DuPont in the hydroamination of ethylene with secondary amines [146] Later on, Taube studied the reaction mechanism with complex $[RhCl(C_2H_4)(piperidine)_2]$ that exhibited a superior catalytic activity [147-149] described the iridium catalytic system $[IrCl(PEt_3)_2(C_2H_4)_2]/ZnCl_2$, and confirmed that the hydroamination of styrene with aniline takes place through a N-H activation mechanism. Interestingly, although the analogue rhodium compound showed very low activity, the system $[\{RhCl(PEt_3)_2\}_2]/Li(NHC_6H_5)$, reported by Brunet, presents a moderate catalytic activity giving simultaneously the hydroamination and the oxidative amination products, both with Markovnikov selectivity [150].

4) Palladium Complexes:

The similarity between the coordination chemistry of palladium(II) and platinum(II) compounds has led to a large research effort towards Pd(II) antitumor drugs that are efficient against Pt(II) resistant therapies and have less side effects [151]. A key factor that might explain why platinum is most useful comes from the ligand-exchange kinetics. The hydrolysis in palladium complexes is too rapid, 105 times faster than that of the corresponding platinum analogues [152]. These complexes dissociate readily in solution leading to very reactive species that are unable to reach their pharmacological targets. Accordingly, compared to cisplatin, the corresponding *cis*-palladium, *cis*-$[Pd(NH_3)_2Cl_2]$, does not show antitumor activity [153, 154]. Therefore, if an antitumor palladium complex is to be designed, it must be stabilized by a chelate or a strongly coordinating nitrogen ligand [155]. Studies of platinum and palladium compounds

The synthesis and molecular structure of an enantiomerically pure, *trans*-palladium(II) complex, *trans*-$[Pd\{(R)\text{-}(+)\text{-bornyl-amine}\}_2Cl_2]$ that bears the bulky amine ligand R-(+)-bornylamine (*endo*-(1R)-1,7,7-trimethylbicyclo[2-2-1]-heptan-2-amine) [156]. The complex showed similar antitumor activity against HeLa cells when compared with the activity of the standard references, cisplatin, carboplatin, and oxaliplatin. In addition, a

palladium complex which contains the bulky nitrogen ligand harmine (7-methoxy-1-methyl-9H-pyrido[3,4-b]indole), *trans*- [Pd(harmine)(DMSO)Cl2], exhibited a greater cytotoxic activity against P_{388}, L_{1210}, and K_{562} cell lines than cisplatin [157, 158].

1.5 Characterization of the Ligands and Metal Complexes:

Melting Point Determination:

Melting points were determined using a MEL-TEMP II melting point instrument and were not corrected. All samples are placed in the micro haemotocrit tube (soda lime glass). The melting points of the sample were recorded after they have completely melted.

Carbon, Hydrogen and Nitrogen (CHN) Analyses

Microanalyses for carbon, hydrogen and nitrogen in the compounds were carried out on a Perkin-Elmer 2400 elemental analyzer. All compounds (1.75–2.00 mg) were weighted in aluminium foil capsules. The instrument was calibrated with sulfamethinezine.

Infra Red (IR) Spectroscopy

The Infrared spectra were recorded on a Perkin Elmer Spectrum 400 ATR-FT-IR spectrometer. All the spectra were run in the range of 400-4000 cm^{-1} at room temperature.

Nuclear Magnetic Resonance (NMR) Spectroscopy

The ^{1}H NMR spectra of the complexes were recorded using a Bruker Apex 600MHz; FT-NMR spectrometers chemical shifts are given in δ values (ppm) using TMS as the internal standard. Deuterated dimethylsulphoxide (DMSO) was used as solvent.

Ultraviolet-Visible (UV-Vis) Spectroscopy.

The spectra (solid) were obtained from reflectance electronic technique by using UV-3600 Shimadzu UV-Vis-NIR Spectrophotometer and were scan from 200-1000, while the

spectra (DMSO) were recorded in quartz cuvettes on a Shimadzu 1601 spectrophotometer in the region of 200-1000 nm.

1.6 Aim of present investigation

The literature survey reveals that the most of the work which have been reported is related the Transition metal complexes and aliphatic, aromatic amines and related compounds with first and second series of transition elements, however, a little work is reported on precious metal complexes.

With this aim in mind, the present study deals with the synthesis of solid complexes of Ruthenium, Rhodium, Palladium and Molybdenum metal ions with Nitrogen containing ligands such as 2-aminopyridine and ethylenediamine.

1) ethylenediamine

2) 2-aminopyridine

The characterization of ligands and their corresponding metal complexes were carried out using physicochemical techniques involving elemental analysis, thermal, spectral and x-ray powder diffraction analysis and studied antimicrobial activity, of these metal complexes.

2. Chapter -II

Synthesis of Metal Complexes

2.1 Section A

SYNTHESIS AND CHARACTERIZATION OF ETHYLENEDIAMINE LIGANDS AND THEIR METAL COMPLEXES

2.1.1 Basic requirements:

1) Apparatus:

The experimental work was carried out using borosilicate glass apparatus. All beakers, flasks and other glassware used for experimental work scrupulously cleaned before use by means of chromic acid cleaning agent followed by tap water and portions of de-ionised water. Finally they were weighed on one pan analytical balance with 0.01 mg sensitivity.

2) Chemicals:

All the chemicals used for experimental work were of AR- grade. The purity of ligands was checked by melting points and by TLC. And the complexes are characterized by spectral methods.

3) Solvents:

are the chemical for proper dissolution of reactant.

i) Water:

Throughout the experimental work, the glass distilled water was used. The glass distilled water was obtained by distillation of metal distilled water in presence of crystals of potassium permanganate in alkaline condition.

ii) Super dry ethanol:

For the synthesis of transition metal complexes, ethanol or methanol was used as solvent. Super dry ethanol and anhydrous methanol were obtained by distillation after treatment with magnesium and iodine crystals. Distilled ethanol and methanol was stored in air tight polyethylene vessels and protected from atmospheric moisture. All other solvents used during the experimental work were of AR grade.

iii) Other solvents:

The solvents like tertahydrofuran, ethyl acetate, acetone, dimethylformamide (DMF), pet ether and carbon tetrachloride were purified by reported methods.

4) Reactants and reagents:

The reagents such as Ethylenediamine and 2-aminopyridine, metal salts and other chemicals used for the synthesis of metal complexes were of AR grade. The purity of chemicals was checked by routine tests like melting point, boiling point, thin layer chromatography (TLC) etc. The purification of liquid chemicals and solvents were done by distillation.

5) Measurement of mass:

The samples weighing up to 100 mg or more, single pan analytical balance EMettler Zurich, type-MG 60NO72840 Swiss made with maximum capacity ranging between 160-200 gm having precision $\pm$0.01 mg was used.

2.1.2 Ethylenediamine ligands:

1,2-Diaminoethane (CAS No. 107-15-3), commonly known as ethylenediamine (EDA), is a synthetic colourless to yellowish liquid at normal temperature and pressure. It is strongly alkaline and is miscible with water and alcohol.

Ethylenediamine, with EDA used as a common abbreviation. Other common synonyms include dimethylenediamine, 1,2-ethanediamine, 1,2- ethylenediamine, beta-aminoethylamine, and ethane-1,2- diamine. EDA's structural formula is shown below:

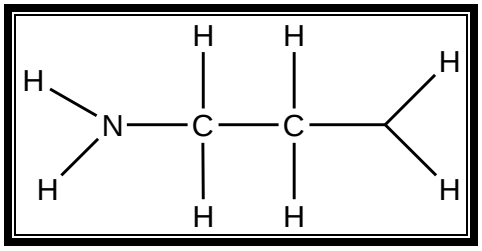

Fig. 2.1.1 Structure of ethylenediamine

EDA is a colourless to yellowish hygroscopic liquid with an ammonia-like odour. Its molecular weight is 60.12. It is a strongly alkaline (pH of 25% EDA in water is 11.9), very volatile, pungent material, which fumes profusely in air. It has a melting point of about 8.5 °C, a boiling point of 116 °C (at 101.3 kPa), and a vapour pressure of 1.7 kPa at 25°C. EDA is miscible with water and alcohol.

2.1.3 Characterization of ligands:

Ethylenediamine ligand was found to be stable to air and moisture. Ethylenediamine is purchased from s.d. fine chemical pvt ltd, Mumbai. It was used as ligand for synthesis of complexes with Molybdenum, Rhodium, Ruthenium and Palladium element.

1) Physical parameters of the ligands:

The EDA ligands are yellow and white in colour. The results obtained are in good agreement with the results of elemental analysis using elemental analyzer 'PERKIN ELMER' model no 2400. The sample weight and percentage of carbon, hydrogen and nitrogen found and calculated theoretically and melting points are given in (Table 2.1.2).

2) ^{1}HNMR spectral study of ligands :

The ^{1}HNMR technique is highly useful to prove the structure of the compounds. Nuclear magnetic resonance spectroscopy can detect nuclei under the influence of different environment in a molecule. In the analysis of organic molecules, proton nuclear magnetic resonance spectra plays very important role. It is most valuable technique in structural investigation.

3) Scanning of the ^{1}H NMR spectra :

Nuclear magnetic resonance spectroscopy is related with magnetic properties of certain atomic nuclei. The present discussion is related to proton (hydrogen atom) nucleus compound. The ^{1}HNMR of Ethylenediamine ligands were recorded on BrukerAvance II 400 MHz spectrophotometer in DMSO solvent using TMS (Tetra methyl silane) as an internal standard at SAIF, Chandigarh.

4) Discussion of 1HNMR spectral data of ligands :

The ligand ethylenediamine is known compound, and due to presence of two amino group it act as a lingand. The 1H-NMR of ethylenediamine shows peaks for CH_2 and NH_2 group. Two CH_2 group shows peak at 2.91 ppm due to presence of one alpha nitrogen and two beta nitrogen. And peak at 2 ppm due to presence of two amino group in the compound.

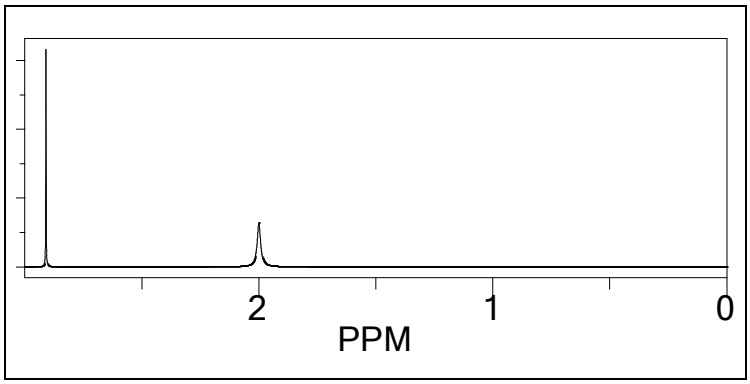

Fig 2.1.1 ^{1}H-NMR spectra of ethylenediamine.

5) Infrared spectra of ethylenediamine

From figure 2.1.2 the peaks is clearly shows presence of NH near 3300-3500 cm^{-1}, peak of C-N at 1270 cm^{-1} and peaks at 1000-1250 cm^{-1} is due to presence of amines.

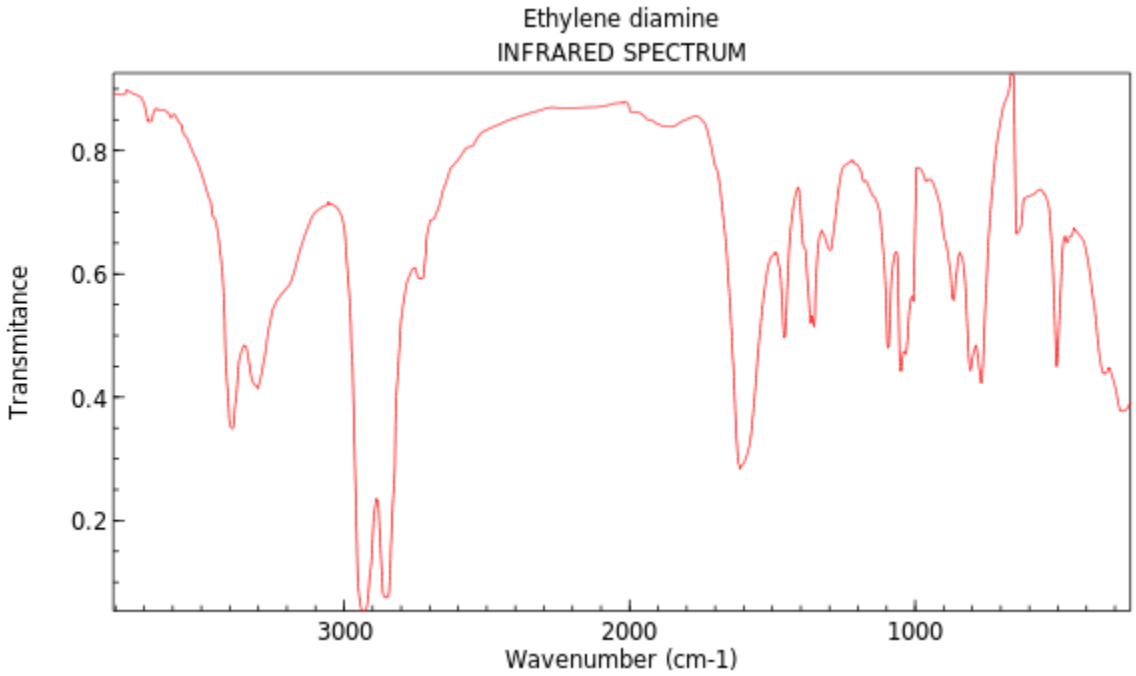

Fig 2.1.2 FTIR spectra of ethylenediamine

2.1.4 Synthesis of metal complexes with ethylenediamine ligand:

The metal complexes were synthesized by various methods. In the present work, the transition metal complexes were synthesized by refluxing methanolic solutions of ligands and metal chloride in 2:1 molar ratio.

1)Synthesis of bis(ethylenediamine)dichloro Molybdenum Chloride

0.02 mole of ligand in slight excess was taken in round bottom flask containing 30 ml. of anhydrous methanol (15 ml chloroform + 15 ml. methanol) and refluxed for few minutes so as to dissolve ligand completely. A solution of 0.01 mole of metal chloride in 20 ml. of anhydrous methanol was then added drop-wise to the solution of the ligand. The contents were refluxed for three hours and then cooled to observe the occurrence of precipitation which rarely found in the cold reaction mixture, Therefore, the reaction mixture was refluxed for 8-9 hours and then a ten percent methanolic solution of ammonia was added drop wise to increase the P^H till the metal complex precipitates out completely. The precipitate was digested for one hour. Any subsequent change in the PH if observed was readjusted and contents digested again for one hour. The solid metal complex separated out was then filtered in hot condition. It was washed with portions of hot methanol, followed by petroleum ether (40-60^0 C) and dried in vacuum desiccator over anhydrous granular calcium chloride. The melting points decomposition temperatures of the complexes were determined by Thiele's melting apparatus. The PH range of precipitation, colour and melting points for all the synthesized metal complexes are presented in Table 2.1.1.

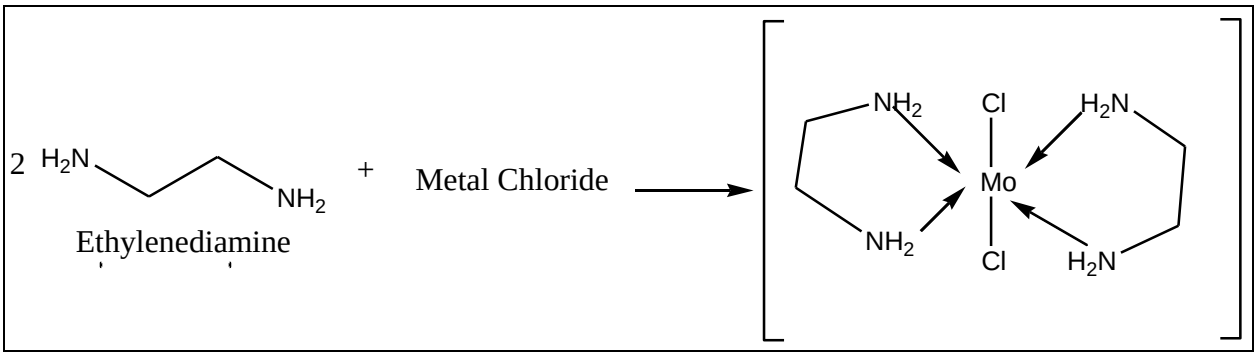

Scheme 2.1.1 Synthesis of bis(ethylenediamine)dichloro Molybdenum complex.

2)Synthesis of bis(ethylenediamine)dichloro rhodium Chloride

0.02 mole of ligand in slight excess was taken in round bottom flask containing 30 ml. of anhydrous methanol (15 ml chloroform + 15 ml. methanol) and refluxed for few minutes so as to dissolve ligand completely. A solution of 0.01 mole of rhodium chloride in 20 ml. of anhydrous methanol was then added drop-wise to the solution of the ligand. The contents were refluxed for three hours and then cooled to observe the occurrence of

precipitation which rarely found in the cold reaction mixture, Therefore, the reaction mixture was refluxed for 8-9 hours and then a ten percent methanolic solution of ammonia was added drop wise to increase the P^H till the metal complex precipitates out completely. The precipitate was digested for one hour. Any subsequent change in the PH if observed was readjusted and contents digested again for one hour. The solid metal complex separated out was then filtered in hot condition. It was washed with portions of hot methanol, followed by petroleum ether (40-60^0 C) and dried in vacuum desiccator over anhydrous granular calcium chloride. The melting points decomposition temperatures of the complexes were determined by Thiele's melting apparatus. The PH range of precipitation, colour and melting points for all the synthesized metal complexes are presented in Tables 2.1.1.

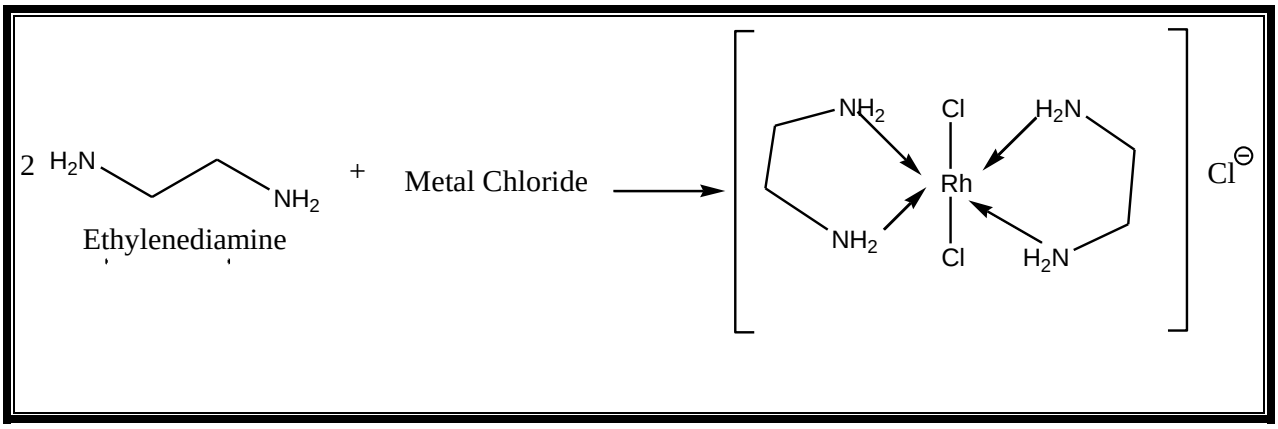

Scheme 2.1.2 Synthesis of bis(ethylenediamine)dichloro Ruthenium Chloride complex.

3)Synthesis of bis(ethylenediamine)dichloro Ruthenium Chloride

0.02 mole of ligand in slight excess was taken in round bottom flask containing 30 ml. of anhydrous methanol (15 ml chloroform + 15 ml. methanol) and refluxed for few minutes so as to dissolve ligand completely. A solution of 0.01 mole of ruthenium chloride in 20 ml. of anhydrous methanol was then added drop-wise to the solution of the ligand. The contents were refluxed for three hours and then cooled to observe the occurrence of precipitation which rarely found in the cold reaction mixture, Therefore, the reaction mixture was refluxed for 8-9 hours and then a ten percent methanolic solution of ammonia was added drop wise to increase the P^H till the metal complex precipitates out completely. The precipitate was digested for one hour. Any subsequent change in the PH

if observed was readjusted and contents digested again for one hour. The solid metal complex separated out was then filtered in hot condition. It was washed with portions of hot methanol, followed by petroleum ether (40-60^0 C) and dried in vacuum desiccators over anhydrous granular calcium chloride. The melting points decomposition temperatures of the complexes were determined by Thiele's melting apparatus. The PH range of precipitation, colour and melting points for all the synthesized metal complexes are presented in Tables 2.1.1.

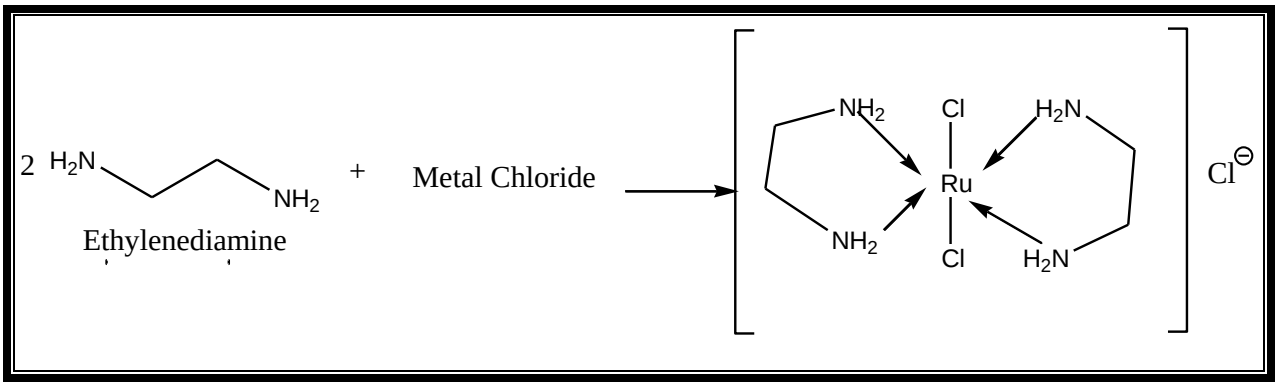

Scheme 2.1.3 Synthesis of bis(ethylenediamine)dichloro Ruthenium Chloride complex.

4)Synthesis of bis(ethylenediamine)dichloro palladium (II)

0.02 mole of ligand in slight excess was taken in round bottom flask containing 30 ml. of anhydrous methanol (15 ml chloroform + 15 ml. methanol) and refluxed for few minutes so as to dissolve ligand completely. A solution of 0.01 mole of metal chloride in 20 ml. of anhydrous methanol was then added drop-wise to the solution of the ligand. The contents were refluxed for three hours and then cooled to observe the occurrence of precipitation which rarely found in the cold reaction mixture, Therefore, the reaction mixture was refluxed for 8-9 hours and then a ten percent methanolic solution of ammonia was added drop wise to increase the P^H till the metal complex precipitates out completely. The complexes of different metals were precipitated at different P^H range, and found to be characteristic of that complex. The precipitate was digested for one hour. Any subsequent change in the PH if observed was readjusted and contents digested again for one hour. The solid metal complex separated out was then filtered in hot condition. It was washed

with portions of hot methanol, followed by petroleum ether (40-60^0 C) and dried in vacuum desiccator over anhydrous granular calcium chloride. The melting points decomposition temperatures of the complexes were determined by Thiele's melting apparatus. The PH range of precipitation, colour and melting points for all the synthesized metal complexes are presented in Tables 2.1.1.

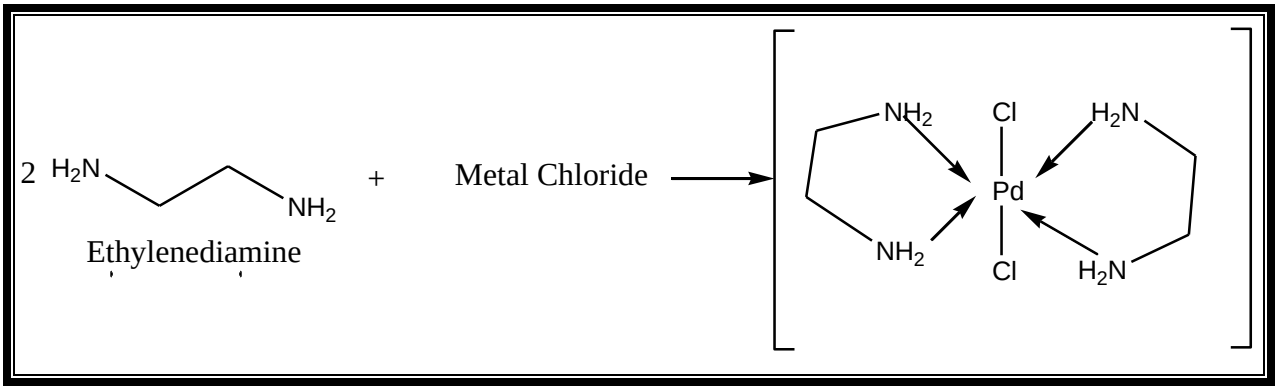

Scheme 2.1.4 Synthesis of bis(ethylenediamine)dichloro Palladium Chloride complex.

Table 2.1.1 P^H range of precipitation of metals with ethylendiamine.

Sr. No.	Metal	Ligand	P^H range of precipitation	Colour	Melting point/ Decomposition temp. ^oC
1	Molybdenum	Ethylenediamine	8.0 – 9.0	Yellow	>300
2	Rhodium	Ethylenediamine	6.0 – 7.0	Brown	>300
3	Ruthenium	Ethylenediamine	8.0 – 9.0	Violet	>300
4	Palladium	Ethylenediamine	7.0 – 8.0	Brown	>300

2.1.5 Characterization of metal complexes:

All the metal complexes are stable to air and moisture. The solubility of these complexes was examined in different solvents like water, polar and non-polar organic solvents. All the transition metal complexes are insoluble in water. Majority of complexes are sparingly soluble in chloroform, methanol and dioxane and easily soluble in DMSO and DMF. The synthesized metal complexes were characterized by elemental analysis,

solution conductivity, mass spectrometry, magnetic susceptibility, electronic and infrared absorption spectroscopy and also by thermo gravimetric and X-ray powder diffraction analysis.

1) Colour and melting points/decomposition temperature of complexes:

The melting points / decomposition temperatures of the complexes were determined by melting point apparatus. The observed values of melting points decomposition temperatures and colour of complexes are tabulated in Table no. 2.1.2.

2) Elemental analysis of metal complexes:

Analysis of Carbon, Hydrogen and Nitrogen:

The C, H and N content of metal complexes were confirmed using elemental analyzer 'PERKIN ELMER' model no. 2400. The percentage of C, H and N found in metal complexes and those calculated theoretically are tabulated in Table 2.1.2. The molecular stoichiometry of each compound is established on the basis of elemental analysis [21].

Table 2.1.2 Analytical data of complexes.

Sr. No.	Molecular Formula	Mol. Wt.	% Found (Calculated)			
			C	H	N	M
1	$[C_4H_{16}Cl_2N_4Mo]$	287.04	16.74 (16.24)	5.62 (5.21)	19.52 (19.17)	33.42 (32.90)
2	$[C_4H_{16}Cl_2N_4Ru]Cl$	327.63	14.91 (14.66)	5.11 (4.92)	17.85 (17.10)	31.24 (30.85)
3	$[C_4H_{16}Cl_2N_4Rh]Cl$	329.46	14.88 (14.58)	5.18 (4.89)	17.96 (17.01)	32.15 (31.23)
4	$[C_4H_{16}Cl_2N_4Pd]$	297.52	17.23 (16.15)	6.02 (5.42)	19.13 (18.83)	35.95 (35.77)

2.2 Section B

SYNTHESIS AND CHARACTERIZATION OF ETHYLENEDIAMINE LIGANDS AND THEIR METAL COMPLEXES

2.2.1 Basic requirements:

1) Apparatus:

The experimental work was carried out using borosilicate glass apparatus. All beakers, flasks and other glassware used for experimental work scrupulously cleaned before use by means of chromic acid cleaning agent followed by tap water and portions of deionised water. Finally they were weighed on one pan analytical balance with 0.01 mg sensitivity.

2) Chemicals:

All the chemicals used for experimental work were of AR- grade. The purity of synthetic ligands was checked by melting points and by TLC. And the complexes are characterized by spectral methods.

3) Solvents:

are the chemical for proper dissolution of reactant.

i) Water:

Throughout the experimental work, the glass distilled water was used. The glass distilled water was obtained by distillation of metal distilled water in presence of crystals of potassium permanganate in alkaline condition.

ii) Super dry ethanol:

For the synthesis of transition metal complexes, ethanol or methanol was used as solvent. Super dry ethanol and anhydrous methanol were obtained by distillation after treatment with magnesium and iodine crystals. Distilled ethanol and methanol was stored in air tight polyethylene vessels and protected from atmospheric moisture. All other solvents used during the experimental work were of AR grade.

iii) Other solvents:

The solvents like tertahydrofuran, ethyl acetate, acetone, dimethylformamide (DMF), pet ether and carbon tetrachloride were purified by reported methods.

4) Reactants and reagents:

The reagents such as 2-aminopyridine, metal salts and other chemicals used for the synthesis of metal complexes were of AR grade. The purity of chemicals was checked by

routine tests like melting point, boiling point, thin layer chromatography etc. The purification of liquid chemicals and solvents were done by distillation.

5) Measurement of mass:

The samples weighing up to 100 mg or more, single pan analytical balance EMettler Zurich, type-MG 60NO72840 Swiss made with maximum capacity ranging between 160-200 gm having precision $\pm$0.01 mg was used.

2.2.2 2-aminopyridine ligand:

2-Aminopyridine is an organic compound with the formula $H_2NC_5H_4N$. It is one of three isomeric aminopyridines. It is a colourless solid that is used in the production of the drugs piroxicam, sulfapyridine, tenoxicam, and tripelennamine. It is produced by the reaction of sodium amide with pyridine, the Chichibabin reaction.

2-Aminopyridine

Formula: $C_5H_6N_2$

Molecular weight: 94.1145

Other names: 2-Pyridinamine; Pyridine, 2-amino-; α-Aminopyridine; α-Pyridinamine; α-Pyridylamine; β-Pyridylamine; o-Aminopyridine; 2-Pyridylamine; Amino-2 pyridine; 1,2-Dihydro-2-iminopyridine;

Chemical structure:

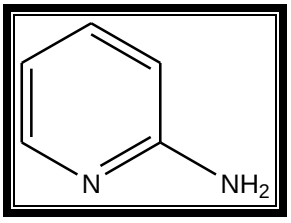

Fig 2.2.1 Structure of 2-aminopyridine

2.2.3 Synthesis of Metal complexes with 2-aminopyridine ligand:

1) Preparation of bis(2-aminopyridine)Molybdenum complexes

1·88 g (0·02 mmol) of 2-aminopyridine, and 1.96 g (0·01 mmol) of diammonium molybdate, $(NH_4)_2MoO_4$ were added under anhydrous to a dry 100 mL Schlenk flask.

They were dissolved in 30 mL of dry alcohol, and the reaction mixture was refluxed for 4 h. The mixture was filtered to furnish crystals.

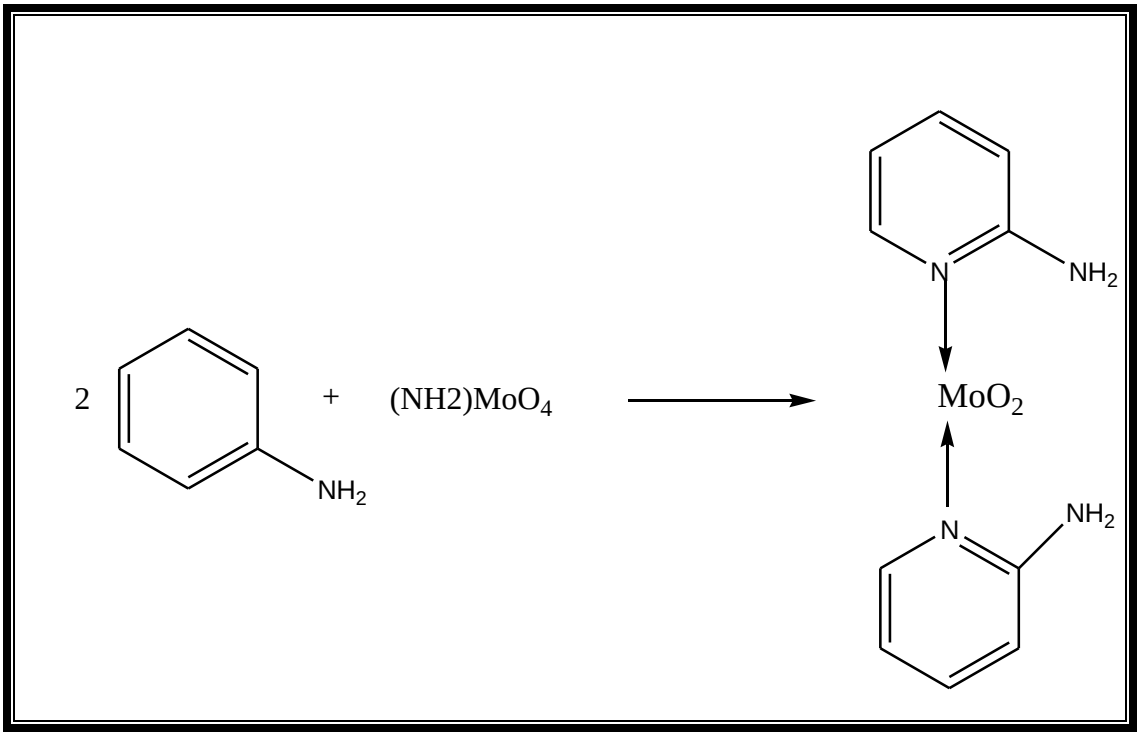

Scheme 2.2.1 Synthesis of bis(2-aminopyridine)Molybdenum complexes

2) Synthesis of bis(2-aminopyridine)Rhodium complexes

1·88 g (0·02 mmol) of 2-aminopyridine, and 2.09 g (0·01 mmol) of Rhodium (III) chloride were added under anhydrous to a dry 100 mL Schlenk flask. They were dissolved in 30 mL of dry alcohol, and the reaction mixture was refluxed for 4 h. The mixture was filtered to furnish crystals

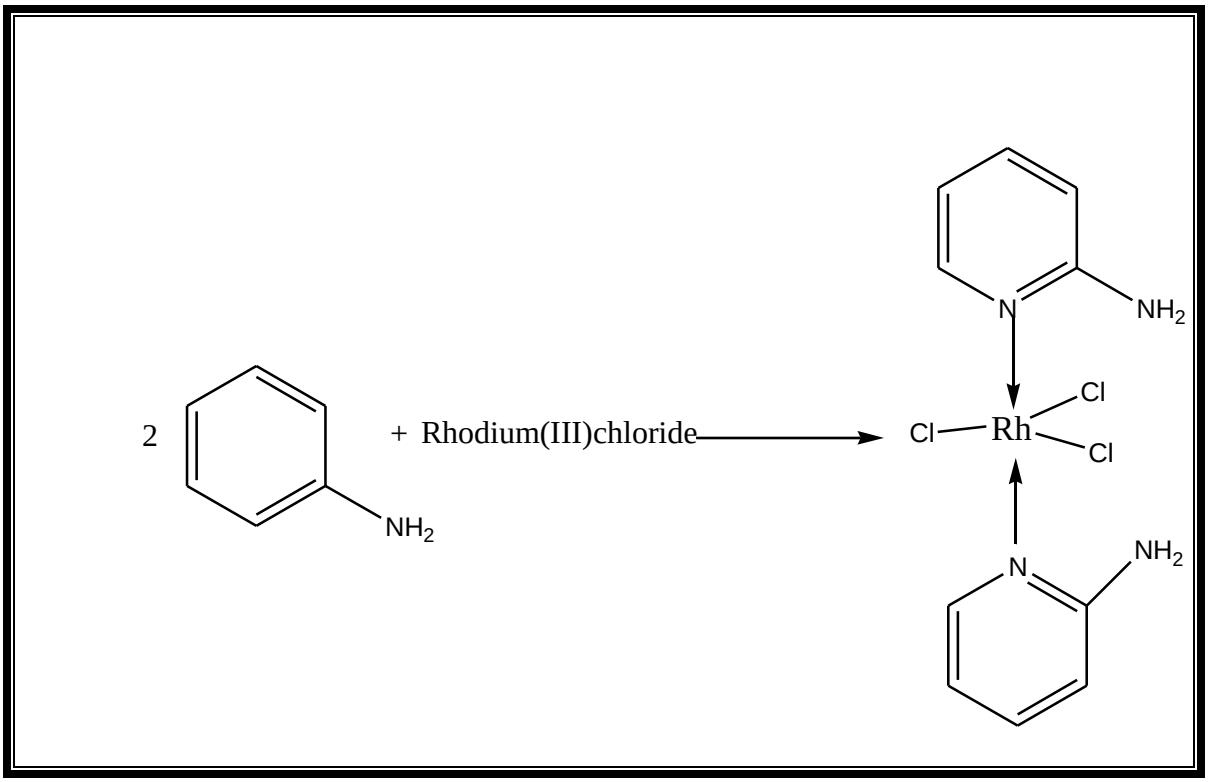

Scheme 2.2.2 Synthesis of bis(2-aminopyridine)Rhodium complexes

3) Synthesis of bis(2-aminopyridine)Ruthenium complexes

1·88 g (0·02 mmol) of 2-aminopyridine, and 2·07 g (0·01 mmol) of ruthenium (III) chloride were added under anhydrous to a dry 100 mL Schlenk flask. They were dissolved in 30 mL of dry alcohol, and the reaction mixture was refluxed for 4 h. The mixture was filtered to furnish crystals

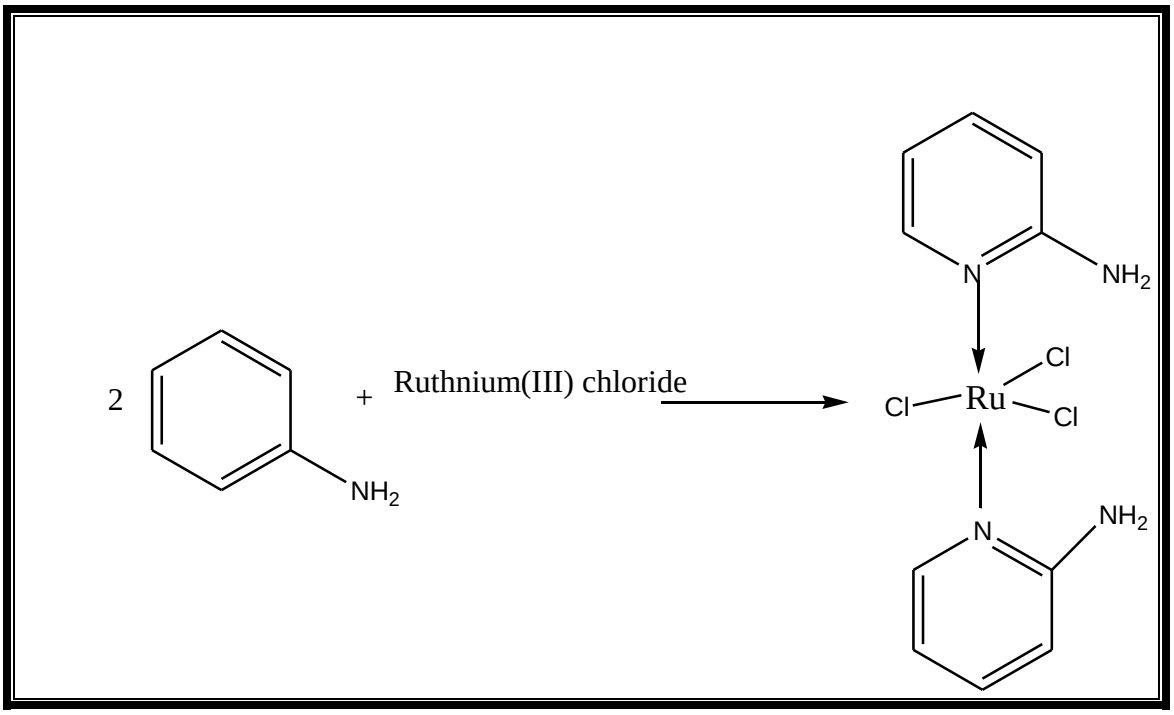

Scheme 2.2.3 Synthesis of bis(2-aminopyridine)Ruthenium complexes

4) Synthesis of bis(2-aminopyridine)Palladium complexes

1·88 g (0·02 mmol) of 2-aminopyridine, and 1.77 g (0·01 mmol) of Palladium dichloride were added under anhydrous to a dry 100 mL Schlenk flask. They were dissolved in 30 mL of dry alcohol, and the reaction mixture was refluxed for 4 h. The mixture was filtered to furnish crystals

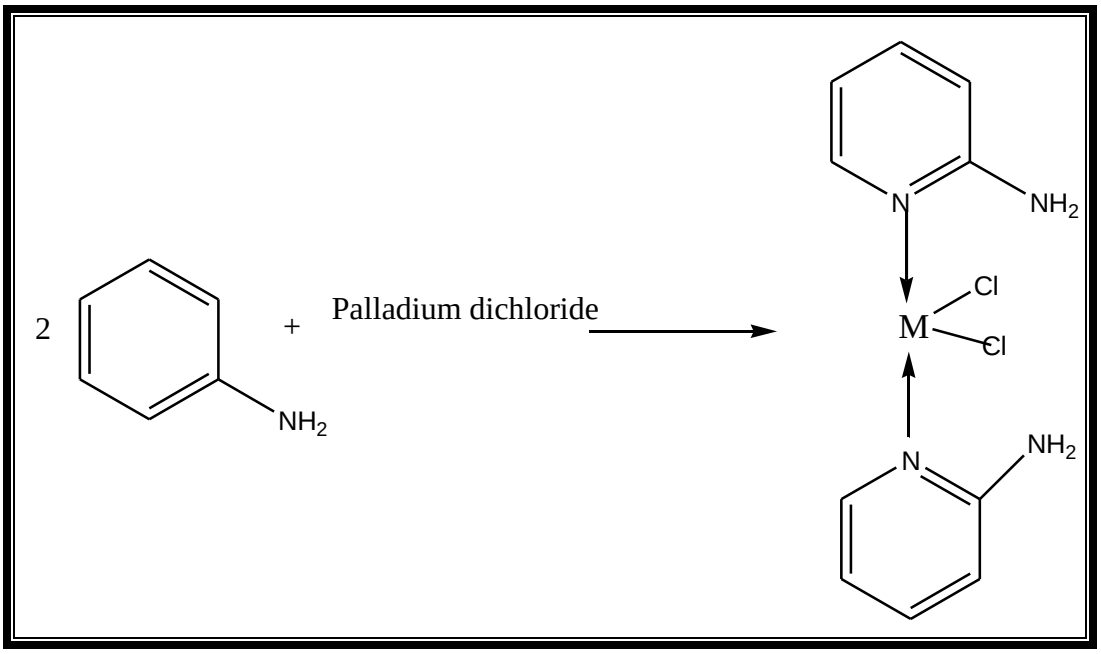

Scheme 2.2.4 Synthesis of bis(2-aminopyridine)Palladium complexes

Table 2.2.1 P^H range of precipitation of metals with ethylendiamine.

Sr. No.	Metal	Ligand	P^H range of precipitation	Colour	Melting point/ Decomposition temp. ^oC
1	Molybdenum	2-aminopyridine	8.0 – 9.0	Yellow	>300
2	Rhodium	2-aminopyridine	6.0 – 7.0	Brown	>300
3	Ruthenium	2-aminopyridine	8.0 – 9.0	Violet	>300
4	Palladium	2-aminopyridine	7.0 – 8.0	Brown	>300

3. Chapter -III

Characterization of metal complexes

3.1 Section A:

Theoretical Experimental Techniques:

The different techniques are used to study structural features, nature of bonding and properties of the metal complexes. All such physiochemical techniques helps to ascertain the exact structure of metal chelates.

3.1.1 Magnetic susceptibility:

One of the most valuable fields of magnetochemistry is the investigation of transition metal complexes. The measurement of magnetic properties can provide information of the electronic structure, oxidation state and in some cases the symmetry properties of the transition metal central ion and nature of bonding in the complexes.

All substances possess magnetic properties and are affected in some way by the application of a magnetic field. The chemistry of the transition elements provides the most interesting field for magnetic investigation. This is due to the fact that the influences of neighbouring groups on the *d* electrons of the metal ions are sufficiently strong to affect significantly their magnetic properties. The study of magnetic properties provides the mechanism of these interactions and can yield valuable information about the bonding and structures of transition metal complexes. Thus magnetochemistry is one of the most valuable techniques in the investigation of transition metal complexes.

The magnetic moment can be calculated by determining the magnetic susceptibility. This is a most useful parameter in the establishment of number of unpaired electrons and their distribution in orbitals around the central metal ion. The number of unpaired electrons and electronic configuration of the central metal ion decides the geometry of the metal complexes. The proper interpretation of observed magnetic data on the basis of valence bond and crystal field theories, is useful to obtain valuable information about oxidation state of the metal ion, type of bonding

and structure of transition metal complexes. The magnetic properties of the metal complexes shows whether inner or outer d-orbitals are used and whether d-electrons are paired or unpaired in the complexes. This is useful in distinguishing the high spin and low spins metal complexes.

The ratio of intensity of magnetization induced due to the applied magnetic field is called as magnetic susceptibility. The intensity of magnetic field induced inthe substance depends on paired or unpaired electrons present in the orbitals of metal ion, based upon which the substances are classified as diamagnetic and paramagnetic. The induced magnetization in diamagnetic substance is always opposite in direction to the lines of forces of the external field, which results in a negative susceptibility of the diamagnetic material which ranges from 10^{-6} to 10^{-5} CGS units. Paramagnetism arises in substances containing unpaired electrons and induced magnetic field is parallel to the lines of force of external field. They have positive susceptibility in the order of 10^{-5} to 10^{-3} CGS units. The diamagnetic susceptibility is independent of the temperature while paramagnetic susceptibility varies inversely with the absolute temperature.

1) Experimental method:

The determination of magnetic susceptibility involves measurement of the force exerted by a homogeneous magnetic field on the sample under study. If the force acting on the sample under investigation is known, the magnetic susceptibility of the compound can be determined and from this, the value of the magnetic moment can be calculated.

Gouy's method was used for the measurement of magnetic susceptibility of the compounds at room temperature. Gouy's balance consists of an electromagnet with a suitable power supply and a single pan-semi microbalance, E-Mettler-Zurich, Swiss-make-H-1640 with maximum capacity 80 gm and a precision ± 0.01 mg.

The electromagnet consists of cylindrical poles, 15 cm in diameter tapering at ends at an angle of 450 and ending in circular faces, 3.5 cm in diameter. A gap of 4 cm is maintained between the two poles. The magnetic assembly having an electromagnet with capacity up to 7000 oresteds was placed around the tube, with a current of 6 amps fed by a suitable power supply.

The specimen tube made up of Pyrex glass, 14 cm in length and 3.5 mm in diameter with a Teflon stopper was used to hold the sample tube. The tube was supported and suspended freely in the magnetic field with the help of clean silver chain in such a way that its lower end was located at the center of the pole gap. The empty clean and dry tube was weighed successively when current is off and on with 4 amps and 6 to poles remain

unchanged during every measurement. The mean of five readings gave the value W g for the empty tube. amps. The field strength of the magnet and position of tube with respect

2) Calibration of the specimen tube :

For accurate measurement of the magnetic moments, the tube constant was determined by using substance of known magnetic susceptibility at room temperature. The standard substance used was mercury tetrathiocyanatocobalt (II), which was prepared by the standard method given in the literature. The measurement of the force developed on the specimen tube was recorded with two independent fillings of the substance. The compound under investigation was filled in glass tube and packed in such a way to eliminate any air pockets. The gram susceptibility of the standard substance was taken as 16.44×10^{-6} CGS units. The tube constant (β) was determined

at room temperature, and was used for the calculation of magnetic susceptibility of metal complexes.

A typical data of the calibration is as follows:

Weight of empty tube = 13.42435 gm.

Weight of empty tube in the presence of magnetic field = 13.42150gm

Force on the empty tube in the presence of magnetic field = 0.00285gm

Table 3.1.1 Standard value for magnetic susceptibility.

Weight of Hg[Co(NCS)4] (gm)	Temperature, ^{o}K	Force on the sample (gm)	B x 10^{6}
0.28280	299	0.0200	232.46

3) Sources of error :

The main source of error in the Gouy's method for solids arises from the improper packing of the sample. This can be reduced by repeating the measurements on homogeneously repacked samples until relatively constant values of gram susceptibility (χg) are obtained. Agreement within 1 % is to be considered good.

4) Measurement of magnetic susceptibilities of metal complexes (Gouy balance method) :

The finely powdered metal complex was filled in the experimental tube up to reference mark. The precaution was taken to ensure tight and uniform packing without any air gap in the column of sample. The teflon stopper was tightly fixed on the tube and the tube was suspended between the electromagnetic poles with the help of silver chain suspension from the pan of the balance. Similar measurements were recorded which are described earlier.

From the experimental data, the magnetic susceptibility (χg) of metal complexes was calculated from the following expression.

$$\chi g = \frac{\beta \Delta \omega}{W}$$

Where,

χg = susceptibility per gram of the substance.

β = tube constant (characteristic of the tube.)

Δω = force exerted by W gm of substance.

W = weight of the substance.

The molar susceptibilities (χM) of complexes were then calculated by the expression.

$$\chi M = \chi g \times Molcular\ weight$$

The magnetic moments (μeff) of the complexes were calculated from the value of χM by the equation.

$$\mu eff = \sqrt{xAT}$$

where,

μeff = Magnetic moment of the metal ion in Bohr magnetrons (B. M.)

T = Temperature in Kelvin scale.

χA = χcorr. = χM. – χ diamagnetic (L)

Magnetic susceptibilities obtained by subtracting the diamagnetic susceptibility of ligand molecule calculated by using Pascal's constants.

χ diamagnetic (L) = Σ χ (atomic correction) + Σ χ(multiple bonds)

The reproducibility of magnetic susceptibility measurements of the complexes was within ± 2%. The diamagnetic susceptibility, (χ diamagnetic) of ligand molecules

have calculated from Pascal's constants.

3.1.2 Electronic absorption spectroscopy :

When continuous radiation passes through a transparent material, a portion of radiation may be absorbed and when residual radiation is passed through a prism, it gives a spectrum, called absorption spectrum. The absorption of ultraviolet (UV) or visible light results in a change in the energy of electrons of the absorbing molecule. The electronic spectrum consists of several absorption bands. Each band corresponds to a definite change in the electronic energy and individual lines within the band are due to specific transitions.

The structure of metal complexes can be predicted from the interpretation of their electronic absorption spectra and comparing them with the spectra of corresponding ligands. The complexes can be identified by their characteristic absorption bands, which is based on the positions of maxima and minima in the absorption spectra along with the molar extinction coefficient values. In the spectra of transition metal ions, basically bands are of three types, I) Bands due to d-d transitions.

II) Charge transfer bands.

III) Bands due to electron transfer within the ligand.

In the transition metal complexes, a visible spectra arises when an electron is excited between t2g and eg orbitals with different energy levels. Charge transfer bands may arise from the transition of an electron from an orbital of ligand to the central metal atom. The molar extinction coefficient of a charge transfer band is about hundred times than that of d-d transition bands. By recording absorption spectra of known molecule, the wavelength of radiation absorbed is correlated with the characteristic structural features. This information is then used in determining the structure of unknown molecules from their spectra. In more stable complexes, the change in the spectrum of the ligand will depend on the degree of covalency of the metal ligand bond. The magnitude of the shift depends on the coordination number of the central atom and its ionic radius. In complexes, stability increases back coordination and charge transfer bands also

appear besides the bands of the ligands. The UV/Vis spectroscopy is, therefore a powerful tool, for structure elucidation.

The correct interpretation of the absorption bands gives an insight into the energy of orbital, mode of bonding in the complexes and their geometries. By this means, it is possible to distinguish tetrahedral, octahedral, and square planar complexes and whether the shape is distorted or regular. Both the intensity and wavelength of absorption band is associated with resonance states of molecule. The intensity of absorption band is associated with energy difference between the ground and excited state of molecule. In general, there is an increase in intensity as the length of conjugation chain increases.

Most organic molecules absorb in the near UV region (200-400 nm) in which the solution is colorless where as transition metal complexes absorb in the visible region (400-800 nm) because of coloured solutions.

3.1.3 Scanning of UV/ Vis. Spectra :

All Ru(III), Rh(III), Pd(II), Pt(IV) and Ir(III) complexes of Schiff bases in the present study are soluble in DMF/DMSO.Therefore absorption spectra of solutions were recorded on JascoUV-530 spectrometer in the region 190-1100 nm using quartz optic tube of 2cm path length. Absorption spectroscopy of ligand is based on n→π* and π→π* transition.Many inorganic species show ligand to metal charge transfer (LMCT) transition and metal to ligand (MLCT) transitions (not as common as LMCT) .Transition probably in ligand field transitions (d-d) transition is determined by the spin selection rule and the orbital selection rule.

3.1.4 Infrared spectroscopy :

IR radiation refers to that part of electromagnetic spectrum which is in between visible and microwave region. IR radiation occurs when the frequency of alternating field associated with the incident radiation matches a possible change in the vibration or rotational frequency of absorbing molecule. When the carbon skeleton of a molecule vibrates, all the bonds stretch and relax in combination .However some bonds stretch essentially independent of the rest of the molecule. This occurs if the bond is either,

1) Much stronger or weaker than others nearby, or

2) Between atoms that are much heavier or lighter than their neighbors.

Indeed, the relationship between the frequency of the bond vibration, the mass of the atoms is same as Hook's law for a simple harmonic oscillator.

$\upsilon = 1/2\ \pi c\sqrt{f/c}$

The absorption of Infra-red radiations causes an excitation of molecule from a lower to higher vibrational level. Each type of bond has a different natural frequency of vibration and since same type of bond in two different compounds is in two different environments, no two molecules of different structure have exactly the same infrared absorption pattern or infrared spectrum. Thus, the infrared spectrum can be used for molecules as a fingerprint, used for humans. Absorption of energy from infrared radiation occurs when the frequency of alternating field associated with the
incident radiations matches a possible change in the vibration or rotational frequency of the absorbing molecule. It is suggested that, when metal ion combines with the ligands to form complex, its vibration spectrum is expected to change. The change in the vibration can be related to molecular symmetry or with the change in the individual frequency. A molecule can undergo two types of vibrations, stretching (υ) and bending (δ-deform). Stretching vibrations have higher frequencies than deformation. Some of the important applications of IR spectroscopy are the identification of major types of bonds, various functional groups, hydrogen bonding in metal complexes and cis-trans isomers. One of the best features of IR spectroscopy in qualitative analysis is that, the absorption or lack of absorption in the specific frequency region can be corrected with specific stretching and bending modes and in some cases, with the relationship of these groups to rest of the molecule. IR absorption occurs not only with organic molecules but also with covalently bonded metal complexes, which are generally active in the longer wavelength IR region. The inorganic complexes derived from organic chelating groups have a
tendency to absorb in the IR region 400-660 cm-1 which is of greatest significance in the study of metal complexes. IR studies thus provide much useful information about metal complexes.

1) **Scanning of IR spectra :**

The infrared spectra of ligands and metal complexes were recorded on a Jasco FTIR-4100 spectrometer over the range 4000cm-1 to 400 cm-1 using KBr pellet technique.

3.1.5 Thermal analysis

Thermogravimetric analysis (TGA) is an experimental technique in which the weight or strictly speaking, the mass of the sample is measured as a function of sample temperature or time. The sample is typically heated at constant heating rate (so-called dynamic

measurement) or held at a constant temperature (isothermal measurement), but may also be subjected to non-linear temperature programs such as those used in sample controlled TGA (so-called SCTGA) experiments. The choice of temperature programme will depend upon the type of information required about the sample. Additionally, the atmosphere used in the TGA experiment plays an important role and can be reactive, oxidizing or inert. Changes in the atmosphere during a
measurement may also be made.

TGA is commonly employed in research and testing to determine characteristics of materials such as polymers, to determine degradation temperatures, absorbed moisture content of materials, the level of inorganic and organic components in materials, decomposition points of explosives, and solvent residues. It is also often used to estimate the corrosion kinetics in high temperature oxidation.

Thermogravimetric techniques have a very wide field of applications. The technique can be used in the examination of absorptive surfaces, together with the nature and processes involved in thermal decomposition and oxidation processes. The technique has also been applied to the examination of water of crystallization and in forensic work involving the identification and comparison of varnishes and other surface coatings. Thermo gravimetric analysis has also been involved in determining the age of art treasures, particularly paintings and in determining the stability of explosives. The technique is commonly used to control the dehydration procedures for crops particularly in the control of the drying processes used for tobacco. Thermo gravimetric analysis is also used extensively in the pharmaceutical industry in the examination of drug stability and the rate of degradation of certain drugs when exposed to air.

The majority of compounds, including complexes suffer physical and chemical changes when subjected to heat. Under defined experimental conditions, these changes are characteristic of the substance examined and can be used for its qualitative and quantitative analysis. The techniques in which changes in properties of substance are measured as a function of temperature, in controlled temperature program are known as thermo-analytical techniques. These methods are based upon the measurement of dynamic relationship between the temperature and some properties of substance such as mass, heat of reaction or volume.

When the sample to be analyzed is heated, various physicochemical changes like thermal decomposition, oxidation, dipole moment, electrical potential, magnetic susceptibility, crystal structure, electrical conductivity, water evaporation, sublimation may take place with a consequent change in the weight of the sample. Thermal decomposition studies of the substance are very useful in predicting the thermal stability of the substance. Chemical changes in the substance can be studied with the help of thermogravimetric analysis (TGA) and differential thermal analysis (DTA) and therefore thermal properties are among the important properties of substances. In the present study, we have used TGA and DTA techniques.

1) Thermo gravimetric analysis (TGA) :

Thermogravimetry is a technique in which the change in the weight of a substance when heated or cooled at a controlled rate is recorded as a function of temperature and/or time. A plot of sample weight change as a function of temperature provides both qualitative and quantitative information of sample. It directly records the loss in weight as a function of temperature for transitions that involve dehydration or decomposition. Thermogravimetric curves are characteristic of a given compound or a material due to the unique sequence of physical transition and chemical reactions that occur over definite temperature ranges. Changes in weights are the results of breaking or formation of various bonds and evolution of volatile or heavier reaction products. Kinetic studies of thermal decomposition reactions of a substance are of

great importance in calculating various parameters like energy of activation (Ea), free energy change (ΔF), pre-exponential factor (Z), order of reaction (n), and entropy of activation (ΔS), which directly govern the factors of thermal stability of any substance.

The course and character of the TG curves are influenced by several experimental factors such as rate of heating, the atmosphere of the furnace, the geometry of the furnace and sample holder, particle size, heat of reaction and compactness of the sample.

2) Differential thermal analysis (DTA) :

The technique firstly developed by E.S.Watson and M.J O' Neill in 1962 and introduced commercially at the 1963 Pittsburgh conference on analytical chemistry. The first adiabatic differential scanning calorimeter that could be used in biochemistry was developed by P. L. Privaiov and D. R. Monaselidze in 1964. The term DSC was coined to

describe this instrument which measures energy and allows precise measurement of heat capacity. It may be stated that a single thermal property is not sufficient to characterize a chemical reaction or system, but that as many thermal methods as possible be employed.

Differential thermal analysis (DTA) is a thermal technique in which the heat effects, associated with physical or chemical changes are recorded as a function of temperature or time as the substance is heated at a uniform rate. Heat or enthalpy changes, either exothermic or endothermic are caused by phase transitions. Generally phase transitions, dehydration reactions, and some decomposition reactions produce endothermic effect, where as crystallization, oxidation and some decomposition reaction produce exothermic effects. The heat effects occurring during these chemical and physical changes are measured by differential thermal analysis. Each substance will give a DTA curve whose number, size; shape and position of various endothermic and exothermic features serve as a means of qualitative information of the sample. The endotherms or exotherms can be used to calculate the heat of reaction or heat of phase transition. The area (A) of DTA peak is given by

$$A = \pm \frac{G\, m\Delta H}{K}$$

Where, G = sample geometry,

m = sample mass,

K = constant,

ΔH (enthalpy change) = - ve → exothermic

= + ve → endothermic

DTA is used to study the thermal stability of large number of metal complexes and organic compounds.

The thermogravimetric studies of metal complexes find extensive applications in determining the purity, metal-ligand bond strength and melting points. The simultaneous use of TG and DTA for the study of metal complexes provides the useful information. The TG is most useful when it complements DTA. The similarity in the values of thermodynamic and kinetic parameters indicates the basic steps involved in the thermal

degradation of chelates are same. The simultaneous use of TGA and DTA plays an important role in the study of thermal behaviour of the inorganic substances.

3) Scanning of TG-DTA curves:

The simultaneous thermo gravimetric and differential thermal analyses of representative metal complexes were performed on SDT Q600 V20.9 Build 20. in an inert nitrogen atmosphere over a temperature range of 0°C to 1000°C. The heating rate was 10°K min-1 and flow rate of air 10 ml/min. The reference substance used was α-Al2O3 in platinum crucible and samples weighed in the range 4 to 7 mg.

3.1.6 Powder X-ray diffraction:

X-ray powder diffraction (XRD) is a rapid analytical technique primarily used for phase identification of a crystalline material and can provide information on unit cell dimensions. Max von Laue, in 1912, discovered that crystalline substances act as three-dimensional diffraction gratings for X-ray wavelengths similar to the spacing of planes in a crystal lattice.

X-ray diffraction is now a common technique for the study of crystal structures and atomic spacing. X-ray diffraction is based on constructive interference of monochromatic X-rays and a crystalline sample. These X-rays are generated in a cathode ray tube by heating a filament to produce electrons, accelerating the electrons toward a target by applying a voltage, and bombarding the target material with electrons. When electrons have sufficient energy to dislodge inner shell electrons of the target material, characteristic X-ray spectra are produced. These spectra consist of several components, the most common being Kα and Kβ. Kα consists, in part, of Kα1 and Kα2. Kα1 has a slightly shorter wavelength and twice the intensity as Kα2. The specific wavelengths are characteristic of the target material (Cu, Fe, Mo, Cr).

Filtering, by foils or crystal monochromaters, is required to produce monochromatic X-rays needed for diffraction. Kα1and Kα2 are sufficiently close in wavelength such that a weighted average of the two is used. Copper is the most common target material for single-crystal diffraction, with CuKα radiation = 1.5418A. These X-rays are collimated and directed onto the sample. As the sample and detector are rotated, the intensity of the reflected X-rays is recorded.

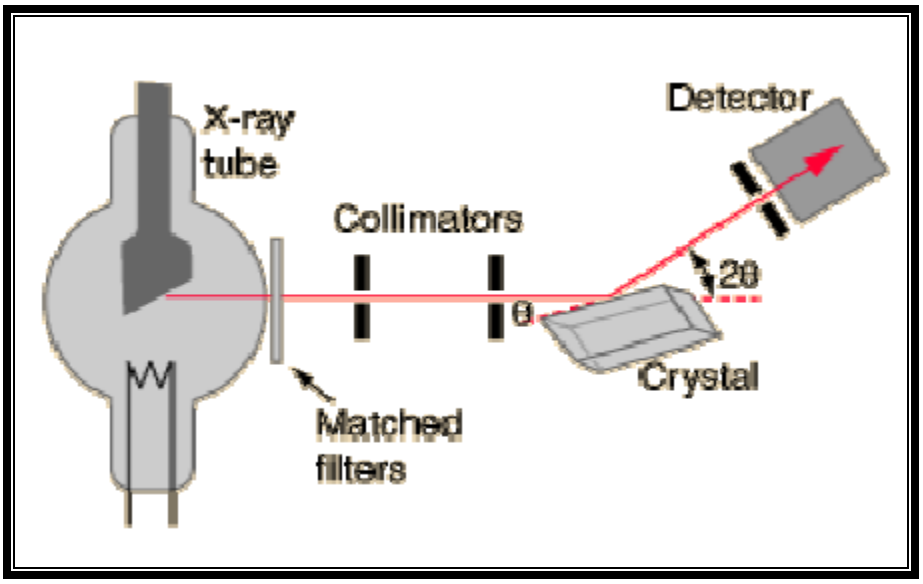

Fig. 3.1.1 schematic diagram of X-ray spectrometer.

When the geometry of the incident X

Bragg,s Equation, $n\lambda = 2d\sin\theta$ constructive interference occurs and a peak in intensity occurs.

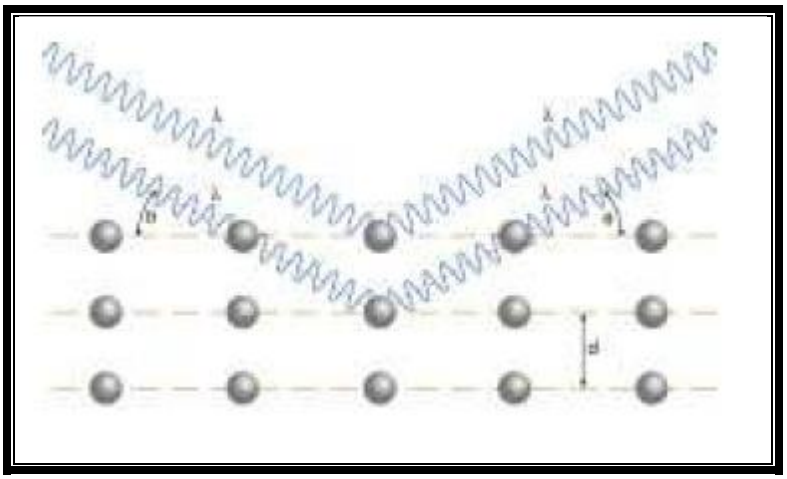

Fig. 3.1.2 Schematic diagram of Bragg's law.

This law relates the wavelength of electromagnetic radiation to the diffracti angle and the lattice spacing in a crystalline sample. These diffracted X detected, counted and processed b all possible diffraction directions of the lattice should be attained due to the orientation of the powdered material. Conversion of the diffraction peaks to d allows identification of the mineral because each mineral has a set of unique d spacing. Typically, this is achieved by comparison of d

reference patterns. Schematic diagram of X-ray diffractometer.

X-rays impinging the sample satisfies the Schematic diagram of Bragg's law.

Xprocessed by scanning the sample through a range of 2θ angles, d-spacing with standard reference pattern.

The X–ray diffraction is a powerful method to understand the structure of the compounds. X–ray method, can determine the structure and symmetry properties of complexes. It gives information of inter atomic distance, bond angles and electronic arrangement in a complex.

It is possible to observe the molecules indirectly by using X-ray radiation of very small wavelength of the order of 10-8 cm and involves the studies of crystalline solids by the phenomenon of X-ray diffraction. When the beam of monochromatic Xray strikes the plane of atoms in the crystal, an interference phenomenon is observed. Bragg's equation gives the relation between inter planar distance and the diffraction angle.

$$n\lambda = 2d \sin\theta$$

Where,

n = order of reflection.

λ = Wavelength of X-rays.

d = inter planar distance and

θ = Angle of diffraction.

Constructive interference of the radiation from successive planes occurs when the path difference is an integral multiple number (n) of wavelength. This is the Bragg's law. All crystals of a substance possess the same elements of symmetry.

Bragg pictured the diffraction effect or a reflection of X-rays from the lattice planes of the crystal. The atoms in the plane are being responsible for scattering of the X-rays to an extent, dependent upon the number of its electrons. This has made a new and significant tool available to the crystallographers and as a result, an extensive amount of work on single crystal was carried out to reveal the internal structure of the compound and is a convenient and practical means for qualitative identification of crystalline compounds. Now a day, XRD is a well established and powerful technique to understand the internal structure of solids.

The procedure in analyzing the powder diffractogram of an unknown sample is consisting of measuring the intensities of the peaks, the diffraction angles θ or 2θ. Once θ is determined, it is used for calculating the inter planer spacing d of reflection planes from the values of λ of X-rays used, and then the dimensions of unit cell are determined. Powder diffraction technique is very important method for the identification of unknown compound and applicable to all crystalline substances.

1) Scanning of X-ray powder diffraction and indexing of the data:-

The X-ray powder diffraction pattern of representative metal complex was scanned on Philips 50-70 PW –3710 diffractometer attached to a digital computer along with graphical assembly in which Cu-K radiation source connected with the tube Cu-Ni-40 Kv/40 mA producing 1.543 A0 wavelength radiations was used with scanning rate 20/min. Each test sample of 200-300 mesh size weighing minimum amount, 10 mg, was spread in the form of thin film and spectra were scanned in the range of 2θ = 5 to 1000.

`The data obtained was deduced using computer program Powder-X. The preliminary data in the form of 2θ and intensity ratio were fed to the computer and corresponding h, k, l values were assigned to each peak. The programme calculates the lattice parameters a, b, c (A0) and α, β, γ (degree) along with standard deviation in each. The crystal volume is also obtained from the unit cell data.

The pyknometric densities of each of the complexes were determined using specific gravity bottle by the principle of Archimedes. The density is related to the formula factor as follows:

$$D = \frac{Z\ X\ F\ X\ M}{V}$$

Where,

Z = Number of formula units in the cell.

F = Formula weight of compound.

M = Mass of hydrogen atom in amu.

V = Crystal volume.

The calculated densities were correlated with the experimentally obtained densities. The observed densities were used to fix the value of Z to the nearest whole number. By using

literature values for definite crystal system, probable space group was assigned to each of the complexes.

Once the dimension of the unit cell, the density and the chemical composition of crystals are known, the number of atoms per unit cell can be established. From the space group, number of atoms in equivalent position contained by the unit cell can be deduced. In this way the unit cell represents the lattice structure of a crystal.

3.1.7 ^{1}HNMR spectroscopy :

Nuclear magnetic resonance involves the interaction between an oscillating magnetic field of electromagnetic radiation and the magnetic energy of the hydrogen nucleus or some other type of nuclei. The sample absorbs electromagnetic radiation in the radio wave region. Proton nuclear magnetic resonance (^{1}H NMR) spectroscopy is concerned with the proton (^{1}H) nuclei having spin quantum number I=1/2. In this technique, the absorption of radiofrequency radiation by an organic molecule induces changes in the magnetic properties of 1H atomic nuclei in that

molecule. The frequency at which proton absorbs energy depends on the electronic environment. So, by ^{1}H NMR spectroscopy, it is possible to locate the protons with different environment which absorbs at different frequencies. The resulting spectrum can be integrated for the number of chemically equivalent protons present in the molecule.

As any spinning charged body generates magnetic field, the proton possessing both electric charge and mechanical spin also generates magnetic field and behaves like tiny spinning bar magnet. Like all bar magnets, the proton orient itself under the influence of external magnetic field, either aligned (α-spin state) with the field or opposite to the field (β-spin state). Thus, it is said to have precessional motion with frequency (ν) directly proportional to the strength of external field (B_0). If the precessing proton is irradiated with beam of radiofrequency radiation, it will absorb the radiation energy from the source only when its precessional frequency is same as that of the frequency of incident rf-radiation. When such situation arises, flipping of the spin of proton from α-spin to β-spin takes place, and the proton is said to be in a state of resonance with the radiofrequency radiation and hence the term proton nuclear magnetic resonance. At resonance, there is a continuous excitation and relaxation of proton. In ^{1}H NMR, the precessional frequency of proton under resonance is measured. Actually protons differently situated in the molecule

are magnetically non-equivalent and come successfully into resonance as the field is varied. The energy of resonance is dependent upon the electronic environment about the nucleus. The electron density around proton, shields the nucleus from the influence of applied field (B_0), so that the field experienced by the nucleus is different than the applied field. This affects the precessional frequency of the nucleus. More the electron density, greater the shielding effect, lower would be the precessional frequency. The opposite of this character is deshielding effect caused by less electron density. Greater the deshielding effect, higher the precessional frequency.

The effective field is given by Beff. = B_0 (1- δ)

Where - δ is shielding constant.

The value of δ is different for different protons of different functional groups. The required applied field will also be different for different functional group protons. The areas under the peaks are in direct ratio to the number of equivalent protons.Since the precessional frequency (ν) is proportional to applied magnetic field (B_0), by holding the radio frequency constant at 60 or 100 MHz, and varying B0, an increase or decrease in the precessional frequencies of all the proton nuclei can be achieved until each turn reach 60 to 100 MHz and come to resonance with the radio frequency source. In a typical proton spectra, the differences in the position of absorption peaks are small, usually of the order of a few hundred Hz compared to the absolute value of the frequency which is around 107 Hz. The position of an absorption peak in the spectra is therefore denoted not by its absolute frequency value, but by the relationship to that of a reference compound, Hz up field or downfield from the reference. The normal reference compound is tetramethylsilane [$(CH_3)_4$ Si. TMS] in which all the protons are equivalent and highly shielded and exhibit a single band at high applied field well beyond the band due to protons in most organic compounds. The proton nuclei in vast majority of organic compounds absorb downfield from the TMS peak. In a proton spectrum, the position of an absorption peak relative to that of reference compound TMS is referred as chemical shift.

In order to make direct and rapid comparison between spectra recorded on instruments operating at different frequencies, the chemical shift is normally quoted on the δ (delta) scale which is independent of the instruments operating frequency. The δ value is

obtained by dividing the position in Hz by the instrument frequency in MHz and is expressed in parts per million (ppm). These values can be calculated using the expression:

$$\delta x = \frac{\nu - \nu TMS}{\nu_{\circ}}$$

Where δx = Chemical shift

νx and νTMS = Frequencies in Hz of the signal for sample x and TMS respectively.

ν_0 = Operating frequency of the instrument in MHz.

Factors such as electro negativity, density of electron cause particular nuclei to appear at different chemical shift (δ). The scale is from up field to downfield (δ = 0 to δ = x).

3.1.8 Mass spectroscopy:

Mass spectrometry (MS) is an analytical technique that ionizes chemical species and sorts the ions based on their mass to charge ratio. In simpler terms, a mass spectrum measures the masses within a sample. Mass spectrometry is used in many different fields and is applied to pure samples as well as complex mixtures. A mass spectrum is a plot of the ion signal as a function of the mass-to-charge ratio. These spectra are used to determine the elemental or isotopic signature of a sample, the masses of particles and of molecules, and to elucidate the chemical structures of

molecules, such as peptides and other chemical compounds. Mass spectrometry is the most accurate method for determining the molecular mass of compound. In this technique molecules are bombarded with a beam of energetic electrons. The molecules are ionized and broken up into many fragments, some of which are positive ions. Each kind of ion has a particular ratio of mass to charge i.e. m/e ratio. For most of ions, the charge is one and thus, m/e ratio is simply the molecular mass of the ion. The molecular ion is called parent ion and is usually designated as M+. The set of ions is analyzed in such a way that a signal is obtained for each value of m/e. the

intensity of each signal represents the relative abundance of the ion producing the signal. The largest peak in the structure is called the base peak and its intensity is taken as

100.the intensities of other peaks are represented relative to the base peak. The mass spectrum is a plot representing the m/e values of various ions against their corresponding relative abundances. The peak on the extreme right corresponds to the molecular mass of the original molecule. In aromatic compounds, $M^{++\,1}$ and $M^{++\,2}$ peaks are also noticed.

3.2 Section B
Elemental Analysis and Solution Conductivity

3.2.1 Mo (VI) complexes:

1) Elemental analysis and solution conductivity:

In the present investigation, all Mo (VI) complexes synthesized from two molecules of ethylenediamine (L1) and 2-aminopyridine (L2) are coloured and stable to air and moisture at room temperature. Most of them decomposes at high temperature without melting. These are insoluble in water but soluble in dimethyl sulphoxide (DMSO) and dimethyl formamide (DMF).

The observed solution conductivity of Mo (VI) complexes are presented in (Table 4.1).The low solution conductivity of 12.4M and 12.614M for L1 and L2 respectively, solutions of Mo(VI) complexes in DMSO indicate their non electrolytic nature. Data reveals that the observed percentages of C, H, N, and metal ion are in good agreement with values predicted and calculated for Mo(VI) complexes, assuming 1:2 ratio with ligands. The first ligand are Ethylenediamine (L1), and second compex with ligand 2-aminopyridine (L2).

2) Magnetic susceptibility and electronic absorption spectral studies of Mo(VI) complexes:

A broad and intense absorption band at 381, 291 nm for L1 and 383, 293nm for L2 which can be assigned to the $\pi \rightarrow \pi^*$ and $n \rightarrow \pi^*$ transition of amine groups in both the complexes. The ligands ethylenediamine shows absorption bands at 381, 291, 233 and 245nm are indicative of benzene and other chromophore(>C=N, azomethine) moieties present in the ligand. A moderately intensive band observed in the range 381, 291 nm is due to the existence of ligand to metal charge transfer.

The ligands 2-aminopyridine shows absorption bands at 383, 382, 345 and 293nm are indicative of benzene and other chromophore(>C=N, azomethine) moieties present in the ligand. A moderately intensive band observed in the range 383, 293 nm is due to the existence of ligand to metal charge transfer.

The absorption bands of the complexes shifted to longer wavelength compared to that of ligand.

The electronic absorption spectra of Mo(VI) complexes have been recorded in DMF. The magnetic moment of Ru(III) complexes in the present investigation were observed in the range 1.5 B.M. which are almost close to the spin only value of 1.72 B.M. However these values are fairly in good agreement with the magnetic moment reported for mononuclear high spin octahedral Mo(VI) complexes with L1.

Electronic spectrum of Mo(VI) complexes display four electronic spectral bands at 26246.32, 35683.63, 37432.34, 40311.12cm^{-1}. These four bands may be assigned to transitions $2T_2g \rightarrow 4T_1g$, $2T_2g \rightarrow 4T_2g$, $2_{T2}g \rightarrow 2A_2g$, $2T_1g$ and $\pi \rightarrow T_2g$ (π^*) respectively for octahedral geometry for ethylenediamine ligands and spectral bands for 2-aminopyridine are observed at 26256.45, 26267.42, 32532.11 and 35433.22cm^{-1}. These four bands may be assigned to transitions $2T_2g \rightarrow 4T_1g$, $2T_2g \rightarrow 4T_2g$, $2T_2g \rightarrow 2A_2g$, $2T_1g$ and $\pi \rightarrow T_2g$ (π^*) respectively for square planar geometry

3.2.2 Ru (III) complexes:

1) Elemental analysis and solution conductivity:

In the present investigation, all Ru (III) complexes synthesized from two molecules of ethylenediamine are coloured and stable to air and moisture at room temperature. Most of them decomposes at high temperature without melting. These are insoluble in water but soluble in dimethyl sulphoxide (DMSO) and dimethyl formamide (DMF).

The observed solution conductivity of Ru (III) complexes are presented in (Table 3.2.1). The low solution conductivity of 13.7M solutions of Ru(III) complexes in DMSO indicate their non electrolytic nature. Data reveals that the observed percentages of C, H, N, and metal ion are in good agreement with values predicted and calculated for Ru(III) complexes, assuming 1:2 ratio with ligands. The first ligand are ethylenediamine (**L1**), and second compex with ligand 2-aminopyridine (**L2**).

2) Magnetic susceptibility and electronic absorption spectral studies of Ru(III) complexes:

A broad and intense absorption band at 370, 380 nm which can be assigned to the п→п* and n→п* transition of amine groups. The ligands ethylenediamine shows absorption bands at 374, 386, 345, 233nm are indicative of benzene and other chromophore(>C=N, azomethine) moieties present in the ligand .A moderately intensive band observed in the

range 233, 345 nm is due to the existence of ligand to metal charge transfer. The absorption bands of the complexes shifted to longer wavelength compared to that of ligand.

The electronic absorption spectra of Ru(III) complexes have been recorded in DMF. The magnetic moment of Ru(III) complexes in the present investigation were observed in the range 1.31 to 1.4 B.M. which are almost close to the spin only value of 1.72 B.M. However these values are fairly in good agreement with the magnetic moment reported for mononuclear high spin octahedral Ru(III) complexes.

Electronic spectrum of Ru(III) complexes display four electronic spectral bands at 26737.92, 26749.91, 33546.45, 37212.01cm^{-1}.These four bands may be assigned to transitions $2T_2g \rightarrow 4T_1g$, $2T_2g \rightarrow 4T_2g$, $2T_2g \rightarrow 2A_2g$, $2T_1g$ and $\pi \rightarrow T_2g$ (π^*) respectively for octahedral geometry for ethylenediamine ligands and spectral bands for 2-aminopyridine are observed at 26259.37, 26783.41, 35666.10, 37565.43 cm^{-1}. These four bands may be assigned to transitions $2T_2g \rightarrow 4T_1g$, $2T_2g \rightarrow 4T_2g$, $2T_2g \rightarrow 2A_2g$, $2T_1g$ and $\pi \rightarrow T_2g$ (π^*) respectively for square planar geometry

3.2.3 Rh (III) complexes :

1) Elemental analysis and solution conductivity:

All the Rh(III) complexes synthesized from ligands are coloured and stable to air and moisture. These are insoluble in polar solvents but sparingly soluble in DMF and DMSO. Most of them decompose at higher temperature without melting. The observed solution conductivities of Rh(III) complexes are presented in Table 4.2.The low solution conductivity of 13.3 and 12.52M solutions of Rh(III) complexes in DMSO indicate their non,electrolytic nature. The elemental analysis (Table 4.1) shows that the metal to ligand ratio in Rh(III) complexes with ligand L1 and L2 is 1:2. The L1 means ethylenediamine and L2 means 2-aminopyridine.

2) Magnetic susceptibility and electronic absorption spectral studies of Rh(III) **complexes:**

The Rh(III) complexes are found to be diamagnetic in nature. The electronic absorption spectra of Rh(III) complexes have been recorded in DMF. Electronic spectrum of Rh(III) complexes when L1 ligand was present, display four electronic spectral bands at

26737.97, 26574.67, 34645.76 and 39432.98 cm^{-1}. These four bands may be assigned to transitions $2T_2g \rightarrow 4T_1g$, $2T_2g \rightarrow 4T_2g$, $2T_2g \rightarrow 2A_2g$, $2T_1g$ and $\pi \rightarrow T_2g$ (π^*) respectively for octahedral geometry. And the bands 26743.78, 26783.76, 33544.00 and 36232.67 for L2 ligands describe the square planar geometry.

3.2.4 Pd(II) complexes:

1) Elemental analysis and solution conductivity:

All the Pd(II) complexes synthesized from ligands L1 and L2 are coloured and stable to air and moisture. These are insoluble in polar solvents but sparingly soluble in DMF and DMSO. Most of them decompose at higher temperature without melting. The observed solution conductivities of Pd(II) complexes are presented in Table 3.2.1. The low conductivity values in DMF reveals their non,electrolytic nature. The elemental analysis shows that the metal to ligand ratio in Pd(II) complexes with ligand L1 and L2 is 1:2.

2) Magnetic susceptibility and electronic absorption spectral studies of Pd(II)complexes:

The Pd(II) complexes are found to be diamagnetic in nature. The electronic absorption spectra of Pd(II) complexes have been recorded in DMF.Electronic spectrum of Pd(II) complexe with L1 display four electronic spectral bands at 35587.19, 26245,65, 34256.71 and 38978.22cm^{-1}. These four bands may be assigned to $2T_2g \rightarrow 4T_1g$, $2T_2g \rightarrow 4T_2g$, $2T_2g \rightarrow 2A_2g$, $2T_1g$ and $\pi \rightarrow T_2g$ (π^*) respectively octahedral and spectral bands observed for ligand L2 was at 35672.67, 39840.43, 35232.12, 38375.21 assigned for $2T_2g \rightarrow 4T_1g$, $2T_2g \rightarrow 4T_2g$, $2T_2g \rightarrow 2A_2g$, $2T_1g$ and $\pi \rightarrow T_2g$ (π^*) respectively, the structure should be square planar for this ligand. The Palladium with both ligand was diamagnetic in nature.

Mehta and Shaikh studied Palladium(II) complexes of Thiosemic, arbazone ligands and reported that three electronic absorption bands are observed around 21500, 23600 and 27700 cm,1 are assigned to 1A1g→1A2g, 1A1g→1B1g,and 1A1g→1Eg electronic transitions respectively.

Shukla et al studied palladium complexes with schiff bases derived from 1,3, diaminopropane and reported that three electronic absorption bands are observed around 25000, 35000 and 37000 cm,1 are assigned to 1A1g→1A2g, 1A1g→1B1g,and 1A1g→1Egelectronic transitions respectively.

Hegazy W. H. and ssD.M. Gaffar synthesized Pd(II) complexes of some unsymmetrical tetradentate schiff bases and reported that the Pd(II) complexes in DMSO show two transitions at 20619,20877 and 25974,26178cm-1 and these two transition are assignable to square planner geometry.

Table 3.2.1 Solution conductivity, magnetic and electronic absorption spectral data of Metal complexes.

Metal complex	**Mol. Cond. Ohm^{-1}cm^{2}mol^{-1}**	**μeffe. (B.M.)**	**Absorption maxima (cm^{-1}) nm**			
			$^2T_{2g} \rightarrow {}^4T_{1g}$	$^2T_{2g} \rightarrow {}^4T_{2g}$	$^2T_{2g} \rightarrow {}^4A_{2g}$ $^2T_{1g}$	$T_{2g}(\pi^*) \rightarrow {}^2E_g$
L1-Mo	12.4	1.5	26246.32(381)	35683.63(291)	37432.34(233)	40311.12(245)
L1-Ru	13.7	1.31	26737.92(374)	26749.91(386)	33546.45(345)	37212.01(233)
L1-Rh	13.3	1.29	26737.97(374)	26574.67(383)	34645.76(333)	39432.98(246)
L1-Pd	13.2	1.06	35587.19(281)	26245.65(384)	34256.71(341)	38978.22(265)
L2-Mo	12.614	1.02	26256.45(383)	26267.42(382)	32532.11(345)	35433.22(293)
L2-Ru	13.8	1.4	26259.37(383)	26783.41(374)	35666.10 (293)	37565.43(321)
L2-Rh	12.52	1.12	26743.78(386)	26783,76(374)	33544.00(345)	36232.67(312)
L2-Pd	13.9	1.6	35672.67(291)	39840.43(251)	35232.12(294)	38375.21(216)

3.3 Section C:
Infra-Red Spectral Study

3.3.1 Theoretical consideration:

Infrared spectroscopy is one of the important techniques in the study of metal complexes. This offers the possibility of chemical identification and provides useful information about the structure of molecule. The vibrational frequency of bonds and functional groups of ligands are influenced by the neighboring groups. The interaction of functional group with its surrounding can be identified by this technique. In this spectroscopy, stretching and bending of bonds are recorded. For stretching and bending of bonds in the molecule very small amount of energy is required which correspond to larger wavelengths. These wavelengths lie between the microwave and visible region of electromagnetic spectrum. Infrared radiations, like any electromagnetic radiations are characterized by properties of frequency (υ) and wavelength (λ) that related by the speed of light (c).

Infrared spectra of metal complexes are different than the corresponding ligands to certain extent. The change in vibrational frequency can be related to change in molecular symmetry or group frequency or both. Infrared spectra are usually recorded as frequency measurement called wave number (cm^{-1}) which is inverse of the wavelength λ. Generally infrared spectra are recorded in the region 4000-400cm^{-1}.

The infrared absorption occurs not only in organic molecule but also with covalently bonded metal complexes. Infrared spectra are used to study the surrounding environment of organic ligands and their bonding with the metal ion. By correlating the spectra of ligands with that of their metal complexes, the bonding character in the metal complexes can be deduced.

The characterization of metal chelates by their vibrational spectra is usually carried out by taking into account following considerations with respect to their free ligand spectra.

1) Change in the position of bands.
2) Appearances of new bands.
3) Splitting of bands into multiplets.
4) Change in relative intensities of bands.

The change in the position of a band is observed due to change in stretching vibration mode of bond involving co-ordinated atom. Additional bonds on chelationfavour appearance of new peaks. Replacement of a bond by newer one causes replacement of earlier peaks by new peaks. The interaction of the functional group along with the surrounding ions is important and can be identified by absorption spectra of metal complexes in the IR region.

3.3.2 Infrared spectral studies of ligand:

The infrared spectral studies of ligands and their metal complexes were recorded on a Jasco FT-IR-4100 spectrometer using KBr pellets. Present study deals with the metal complexes of Mo(VI), Ru(III), Rh(III), Pd(II) metal ions. The data presented in the Table 3.3.1 is discussed by assigning various bands in the spectra with respect to prominent bond stretching vibration modes in the ligands. The absorption pattern in infrared spectra exhibits complex nature due to various vibrational modes. However, some of them such aromatic >C=C<, azomethine >C=N-, aryl azomethine >C-N-, M-N and M-X groups of ligands that are involved in the complex formation are discussed.

1) **Azomethine (C=N) stretching frequency:**

The ligand Ethylenediamine (L1) and 2-aminopyridine (L2) generally exhibits azomethine (C=N) stretching vibrational band in the region 1689-1471 cm-1 Rawet et.al reported C=N stretching band at 1665 cm-1 and 1650 cm^{-1} in the IR spectra of complex derived from metal with ligands respectively. Kappe et.al studied reactions of 3- acetyl-4-hydroxy-2(1H) -quinolone and nitrogen bases and found ν(C=N) stretching frequency in the range 1550-1605 cm-1.Stadllaure et.al have assigned ν(C=N) stretching frequency in the range of 1580-1600 cm-1. Kotawale et.al. have assigned (C=N) frequencies in the heterocyclic Schiff bases derived from substituted salicylaldehyde, 2 hydroxy -11-napthaldehyde and amino pyridines in the range 1621 -1608 cm-1. Mane et. al assigned 1670-1660 cm-1 frequencies in the spectra of Schiff bases of dehydroacetic acid and aromatic amines to C=N stretching vibrations. The various vibrations are observed for azomethine group of conjugated system. In many Schiff bases of dehydroacetic acid and aromatic amines, C=N stretching vibrations are dependent on the substituents on it, mostly causing resonance interaction and hydrogen bonding. In the present work ,the

broad band (strong /medium) appeared in the region 1565-1650 cm^{-1} in the spectra of all ligands is assigned to (C=N)azomethine stretching frequency.

2) Aromatic ring C=C frequency:

The IR bands due to aromatic ring C=C stretching vibrations are often seen around 1600-1585cm^{-1} for the complexes drived from anilines diamines, amino acids, amino phenol, aminoalcohol and dehydroacetic acid assigned to C=C and aromatic ring. Mane et.al reported the strong to medium intense bands were assigned appeared in the range 1562 to 1576 cm^{-1} in the IR spectra of ligands derived from O-phenyldiamine and dehydroacetic acid. The band appeared in the region 1467 to 1569 cm-1 in the Infrared spectra of metal complexes in the present inverstigation are assigned to C=C aromatic ring stretching vibration modes.

3) Aryl azomethine C-N stretching frequency:

Percy and Thorton studied N-aryl salicyaldeimines and suggested that the appearance of two IR bands in the regions 1350-1375 cm^{-1} and 1470-1450 cm-1were attributable to aromatic azomethine C-N stretching vibrations. Maria et. al assigned the band in the rigion 1330-1315 cm^{-1} in the IR spectra of Schiff base metal complexes derived from 4,6 diamine1,2 dihydro-2-thiopyrimidine to C-N stretching vibration mode. The band in the region 1360-1350 cm^{-1} appeared in the IR spectra of transition metal complexes derived from 4-amino phenol, 4- amino benzoic acid and dehydroacetic acid were assigned to stretching frequency of arylazomethine C-N group by Shirodkar et.al. In the present study the C-N stretching frequency appears in the region1320 to 1433 cm^{-1}.

4) New bands and other observed changes:

Apart from these, a band in the region 426-541 cm^{-1} suggests the presence of ν (C-Cl) which lies in the expected range 450-700 $cm^{-1}$of halide. The C-N group in ligand is confirmed due to the presence of stretching vibrational band at 1262-1352 cm^{-1} which lies in the expected range 1250-1350 cm^{-1}.

A lot of work has been done on the synthesis and characterization of complexes. Vibrational modes of the ligands (L1-L2) have been assigned on the basis of values reported in the literature.

3.3.3 Infrared Spectral Studies of Metal Complexes:

Infrared spectral study is useful in the determination of surrounding organic groups and their bonding with metal in the complex. An organic chelating group of the inorganic complexes have tendency to absorb light within the infrared region, it gives a wide importance to IR spectral studies. Also, no two different groups have ability to absorb light at single wavelength (i.e. different groups absorb light at different wavelengths) hence IR plays significant role in every structural determination of complexes.

1) Mo(VI) complexes:

The infrared absorption frequencies of the ligands and their metal complexes along with their assignments are listed in Table.3.3.1 The FTIR spectra of the Mo(VI) complexes are given in Figures 3.3.1 and 3.3.2. In all these a broad band in the range 3400-3432 cm^{-1} assignable to co-ordinated or uncoordinated water molecules associated with the complexes.

i) Azomethine(C=N) and aromatic (C=C) frequencies:

In the metal complex Mo-L1 and Mo-L2, band at 1565 and 1634 due to C=N and band at 1541 and 1518 due to C=C. In the spectra of the ligands the band centered at 1633 cm^{-1} can be attributed to the azomethine stretching frequency, which decreases to 1612-1570 cm^{-1} in their metal complexes suggesting the co-ordination of azomethine nitrogen to the metal

New Bands and other observed changes :

The bands in the 583**,** 538 cm^{-1} regions may be assigned to ν(M-N) vibration and 460 and 426 cm^{-1} (M-Cl) respectively.

2) Ru(III) Complexes:-

The IR spectra of some representative Ru (III) complexes were recorded, the salient features of these complexes are summarized in Table 3.3.1 and the original spectra of these complexes are presented in Fig.3.3.3 and Fig. 3.3.4. for Ru-L1 and Ru-L2 respectively.

i) Azomethine C=N and Aromatic C=C frequency:

In the IR spectra of Ru (III) complexes, it can be seen that ν (C=N) stretching vibrational frequencies appeared in the region 1650 cm-1 for L1 and 1647 cm-1 for L2. These are

shifted towards lower frequency side than corresponding free ligands. The lowering in frequency indicates the co-ordination through nitrogen of azomethine C=N group.

The medium to strong bands in the region 1555 (Ru-L1) and 1467 (Ru-L2) cm-1 in the IR spectra of Ru(III) complexes are assigned to aromatic ν (C=C) stretching vibrations. These bands in the corresponding free ligands appeared almost in the same region due to non-involvement of C=C group. The band due to (C=C) aromatic ring vibrations may remain same or shift as its position in a ring changes due to the distribution of electrons and molecular environment of metal ion.

Medhi et.al. synthesized ruthenium(III)complexes and reported that co-ordination of azomethine nitrogen to the metal ion leads to reduction in electron density of the azomethine linkage, which results in a downward shift by 1430 cm-1 of (C=N) bond.

ii) New bands and other observed changes:

The bands in the 439 (Ru-L1) and 451 (Ru-L2) cm-1 region may be assigned to (M-N) vibrations Medhi etal. Synthesized ruthenium (III) complexes and reported that infrared spectra of the complexes exhibited bands around 449 cm-1,assignable to ν(M-N) stretching vibration. Also the medium to strong bands observed in the region 1208 to 1258 cm-1 in the spectra of ruthenium complexes are assigned to ν(C-O) stretching vibrations.

Easwaremoorthy et al synthesized Ru(III) bipyridine complexes and reported that infrared spectra of the complexes exhibited band in the range 526 (Ru-L1) and 526 (Ru-L2) cm^{-1}, assignable to ν(M-Cl) stretching vibration. Arounaguiri et.al have synthesized Co(III), Ni(II), Ru (III) complexes of 1-10- phenanthroline family of ligands and reported that infrared spectra of the complexes exhibited band in the range 545-568 cm-1, assignable to ν (M-Cl) stretching vibration.

3) Rh (III) complexes:

The IR spectra of Rh(III)complexes of ligands are presented in Fig 3.3.5 and Fig.3.3.6 and their absorption frequencies are tabulated in Table.3.3.1.

i) Azomethine (C=N) and aromatic C=C Frequencies:

In the spectra of Rh (III) complexes, co-ordination of complex to the metal ion through the nitrogen atom is expected to reduce the electron density in the azomethine link and

lower the ν(C=N) absorption frequency. In the IR spectra of Rh(III) complexes the band appeared in the region 1594 (Ru-L1) and 1585 (Ru-L2) cm-1are assigned to (- C=N) stretching vibration. The band in the corresponding free ligand is found in the region 1581-1652 cm-1. The shift of this band to lower frequency indicates that the compleaxation takes place through azomethine C=N group. In the IR spectra of Rh(III) complexes, the strong band appears in the range, 1563 (Ru-L1) and 1478 (Ru-L2) cm-1 can be assigned to(C=C) stretching vibrational mode. These bands are found to remain unchanged or slightly shift their position than that of their parent ligands indicates the non-involvement of (C=C) group in complex formation.

ii) New Bands and other observed changes:

The band in the 519 (Ru-L1) and 441 (Ru-L2) cm^{-1} region may be assigned to ν(M-N) and 441 (Ru-L1) and 541 (Ru-L2) (M-Cl) vibration respectively. Ajrawy etal synthesized Rh(III) complexes with tetradentate N donor ligands and reported that the infrared spectra of complexes exhibited band in the range 440-520 cm-1 and 440-510 cm-1assigned to ν (Rh-O) and ν(Rh-N) stretching vibrations, respectively.

Sonaba Raj etal. synthesized some Rh(III) complexes and reported that infrared spectra of the complexes exhibited bands in the range 600-526 cm-1 region, assignable to ν(M-N) stretching vibration. In the present study the medium to strong bands the medium to strong band observed in the region1271-1350 cm^{-1} shifts upward by 25-43cm^{-1} in the spectra of complexes are assigned to ν(C-O) stretching vibrations.

4) Pd (II) Complexes:-

The salient features of some Pd(II) complexes are summarized in the Table 3.3.1 and the original spectra of these complexes are presented in Fig.3.3.7 and Fig 3.3.8.

i) Azomethine (C=N) and aromatic (C=C) frequencies:-

In the spectra of Pd (II) complexes, co-ordination of the metal ion through the nitrogen atom is expected to reduce the electron density in the azomethine link and lower the ν(C=N) absorption frequency. In the IR spectra of Pd (II) complexes the band appeared in the region 1638 (Ru-L1) and 1627 (Ru-L2) cm^{-1} are assigned to (- C=N) stretching vibration. The shift of this band to lower frequency indicates that the complexation takes place through azomethine C=N group. In the IR spectra of Rh(III) complexes, the strong

band appears in the range, 1569 (Ru-L1) and 1567 (Ru-L2) cm-1 can be assigned to (C=C) stretching vibrational mode. These bands are found to remain unchanged or slightly shift their position than that of their parent ligands indicates the non-involvement of (C=C) group in complex formation.

ii) New bands and other observed changes:-

The bands observed in the region 555 and 505 cm^{-1} were due to ν (Pd-N) for L1 and L2 and 497 and 457 cm^{-1} due to (Pd-Cl) for L1 and L2 respectively.

Table 3.3.1 Infrared Absorption Frequencies (cm-1) of Metal Complexes (Assignment of band frequencies to bond vibration modes)

Complex	Bond vibrational modes (Stretching) Band position				
	C=N	C=C	C-N	M-N	M-X
Mo-L1	1565	1541	1320	583	460
Mo-L2	1634	1518	1344	538	426
Ru-L1	1650	1555	1351	439	526
Ru-L2	1647	1467	1324	451	526
Rh-L1	1594	1563	1433	519	441
Rh-L2	1585	1478	1350	441	541
Pd-L1	1638	1569	1352	555	497
Pd-L2	1627	1567	1262	505	458

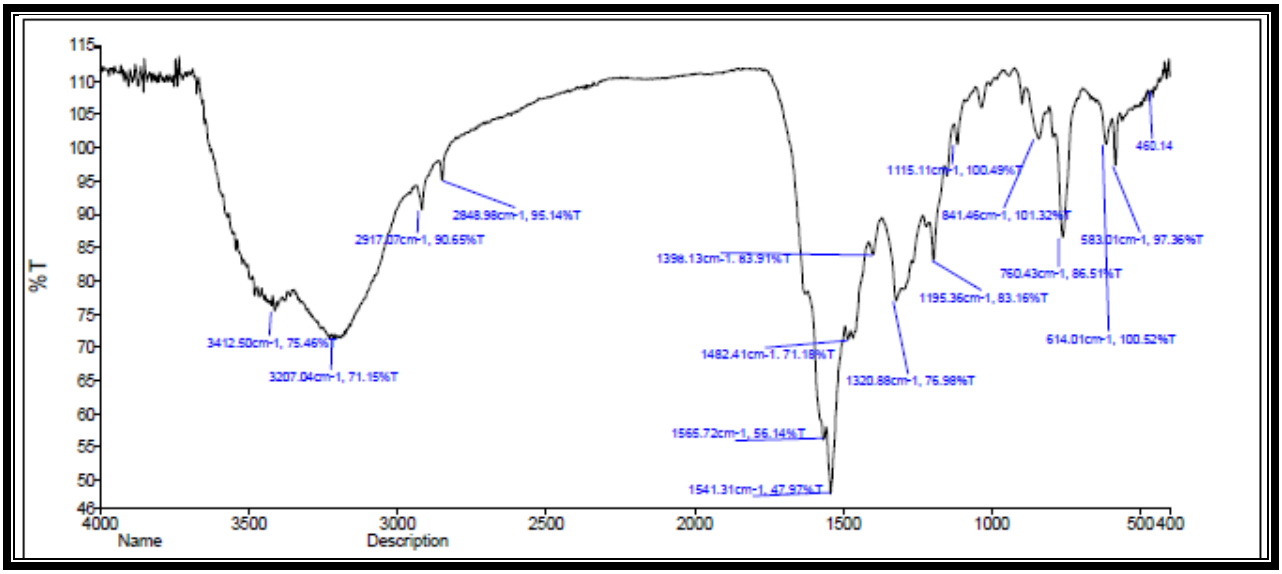

Fig. 3.3.1 Infra Red Spectra of Mo(VI)-L1 complex

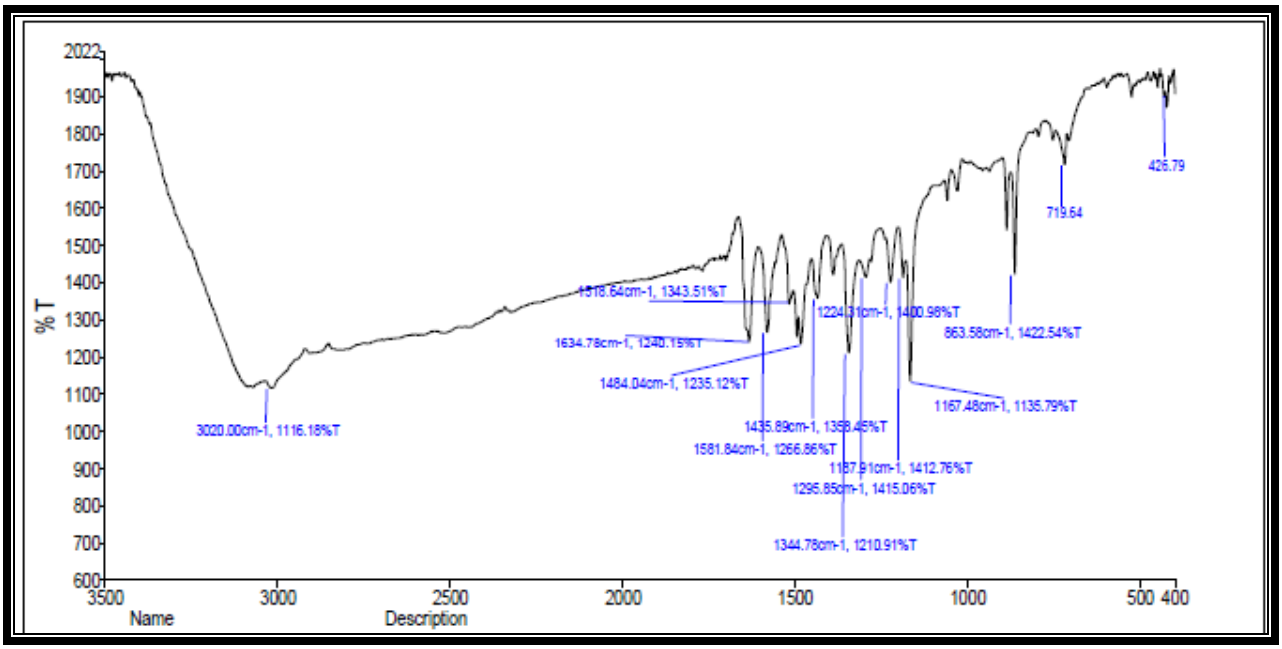

Fig.3.3.2 Infra Red Spectra of Mo(VI)-L2 complex

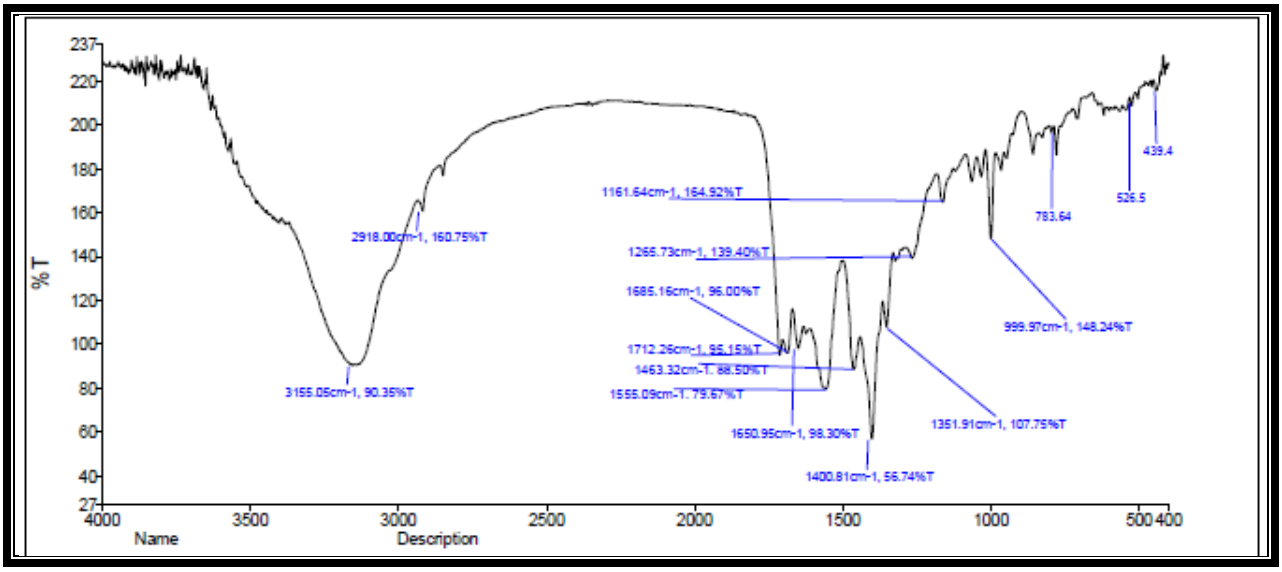

Fig.3.3.3 Infra Red Spectra of Ru(III)-L1 complex

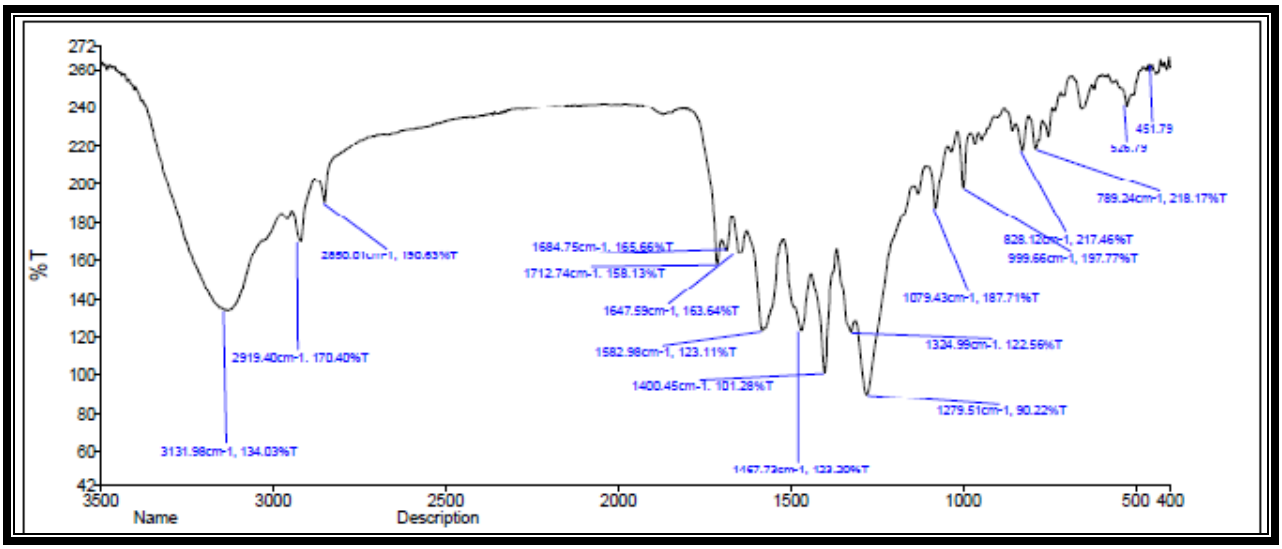

Fig.3.3.4 Infra Red Spectra of Ru(III)-L2 complex

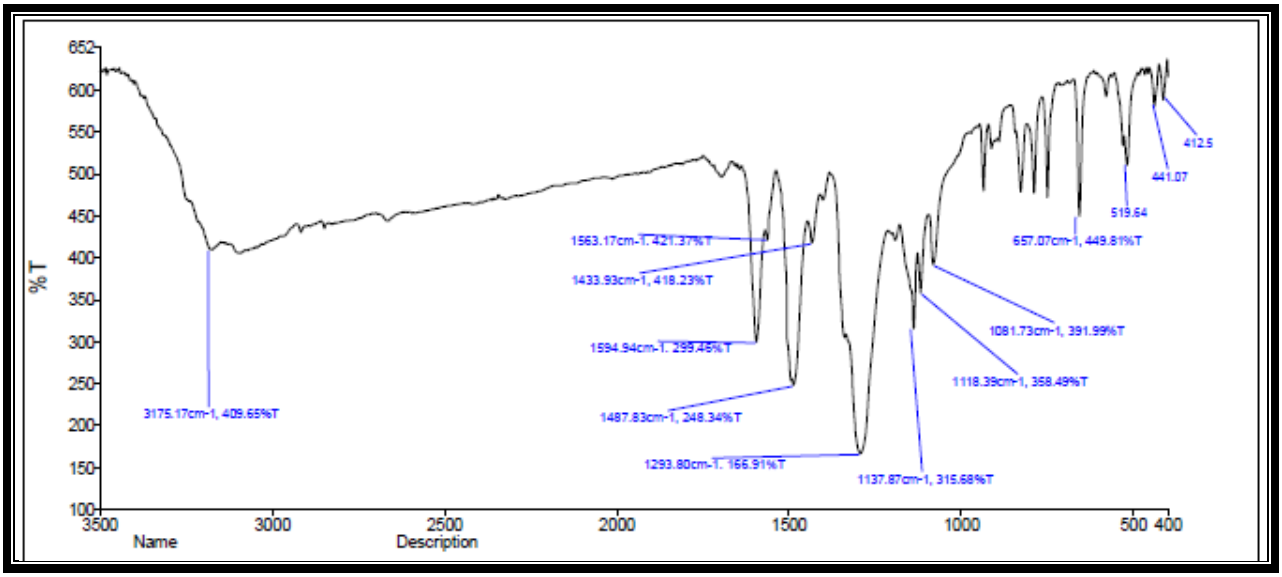

Fig.3.3.5 Infra Red Spectra of Rh(III)-L1 complex

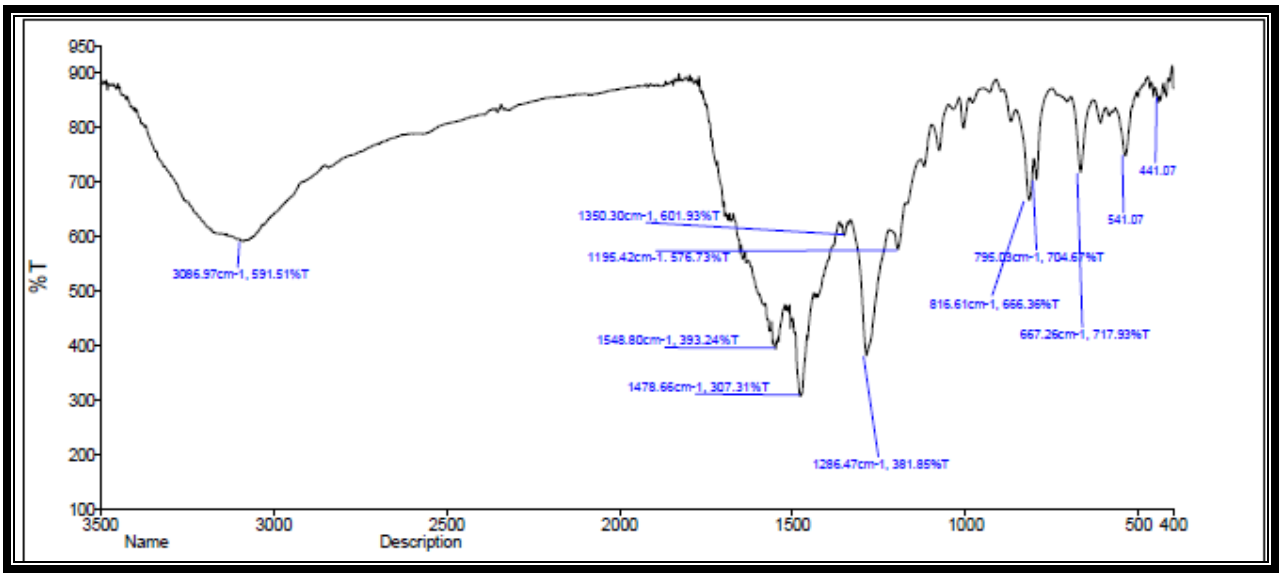

Fig. 3.3.6 Infra Red Spectra of Rh(III)-L2 complex

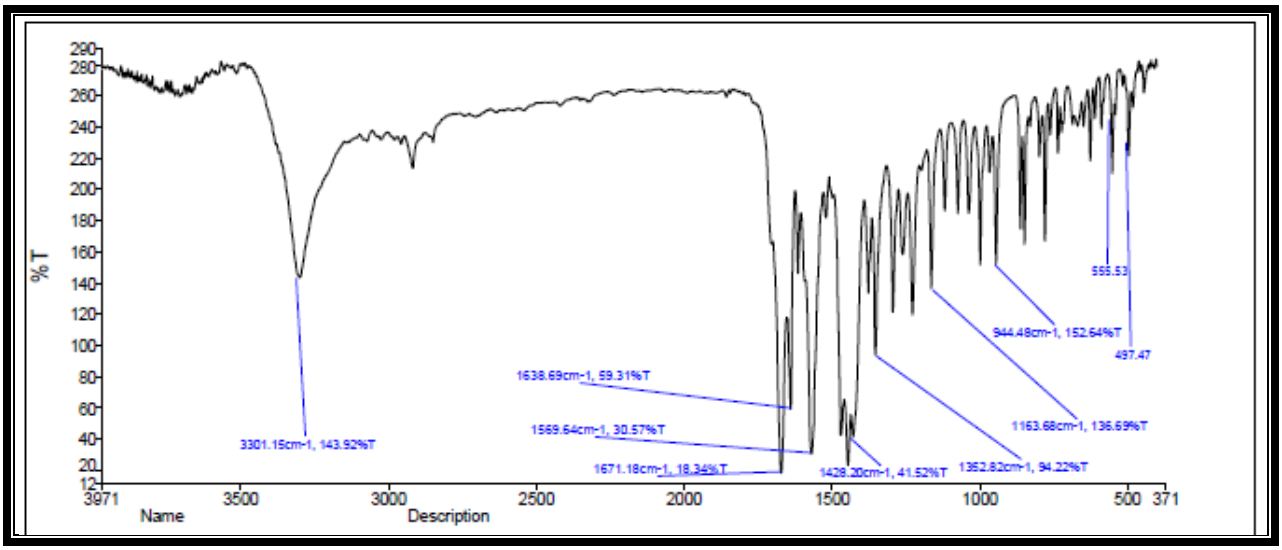

Fig.3.3.7 Infra Red Spectra of Pd(II)-L1 complex

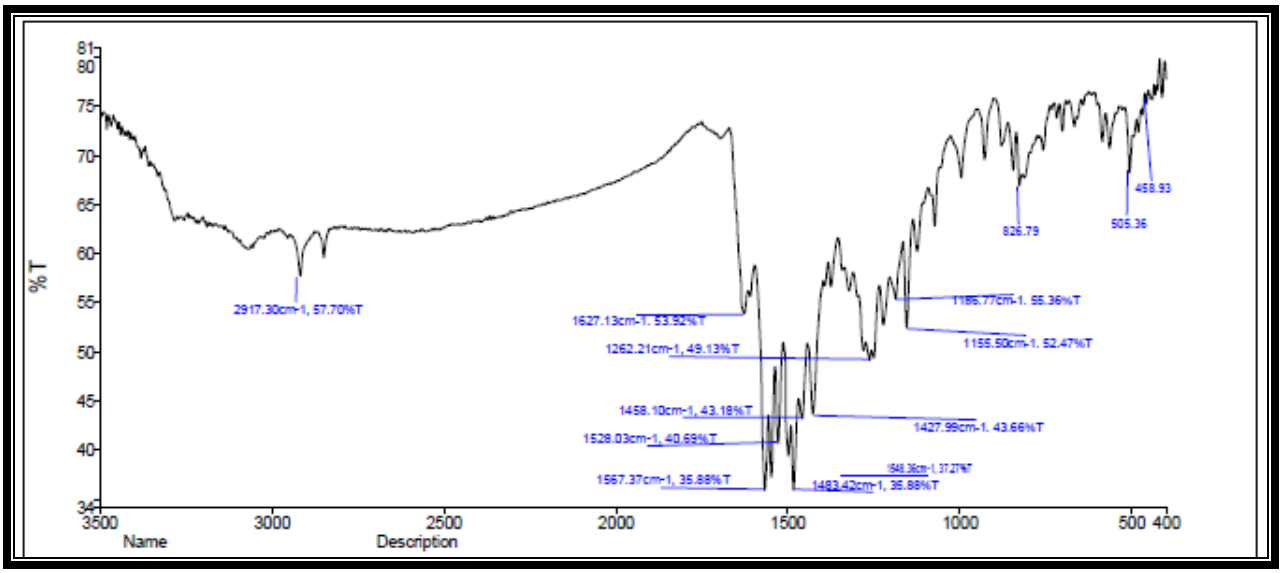

Fig.3.3.8 Infra Red Spectra of Pd(II)-L2 complex

3.4 Section D:
Thermo-gravimetric Analysis Of Metal Complexes (TGA-DTA)

3.4.1 Theoretical Consideration:

Thermogravimetry is a process in which a substance is decomposed in the presence of heat, which causes bonds of the molecules to be broken. This technique is widely applied to study the thermal behavior of metal complexes. Thermal analysis, including mainly thermogravimetry (TG) and differential thermal analysis (DTA) are widely used techniques in qualitative and quantitative evaluation of various compounds.

Thermal properties are important for kinetic studies of thermal decomposition process, energy of activation (Ea), free energy changes (ΔF), order of reaction (n), pre-exponential factor (z), and entropy of activation (ΔS) which directly govern the factors of thermal stability of any substance which can be determined by these methods.

Two alternative methods have been used in kinetic investigation of thermal decomposition of solids. In first approach weight loss-time/ temperature measurements are made and in second approach the sample is subjected to a controlled rising temperature. The first method is called isothermal/ static method and second one is called non-isothermal/ dynamic method.

In static method, determination of isobaric weight change, isothermal weight change is carried where as in dynamic method, thermogravimetry (TG), differential thermal analysis (DTA) and more recently inverted thermo gravimetric techniques are being used. In non-isothermal TG analysis, more information is extracted from a single TG-curve compared to many curves and hence non-isothermal TG analysis is plotted over isothermal TG analysis.

The simultaneous use of TG,DTA and DSC was made in the present study of metal complexes with a view to understand stoichiometry, thermal stability, the presence and nature of water molecules. The water in inorganic compounds may be classified as lattice and co-ordinated water. There is no definite border line between the two. The former term denotes water molecules trapped in the crystalline lattice; either by weak bonds to the anion or by weak ionic bonds to the metal or both where as the later denotes water molecules bonded to the metal through partial covalent bonds or co#ordinate bonds. According to Freeman and co-workers.

the water eliminated below 1500 c can be considered as lattice water and above 1500 c as water

Co-ordinated to metal ion.

We have used dynamic method; 5-10 mg of the sample was treated with increase in temperature by 10°c per minute from 40°Cto 1000°C in an inert nitrogen atmosphere. Considering percentage loss in weight, thermal decomposition behavior of Mo(VI), Ru (II), Rh (II), Pd (II) complexes of some selected ligands are discussed on the basis of their simultaneous TGA-DTA curves as follows. All the synthesized compounds showed multi stage decomposition pattern.

3.4.2 Thermal decomposition study of metal complexes

1) Mo(VI) complexes :

The Mo(VI) complexes of ligands L1, L2 were subjected to thermal decomposition studies. The thermal decomposition curves of these complexes are shown in Fig.3.4.1 and Fig.3.4.2.

The Mo(VI) complex of ligand L1 in which two lattice and one coordinated water molecules are removed with mass loss of 6.64 % (calcd.6.51%) between 50-110 ^{o}C. An endothermic peak in the range 90-110 ^{o}C (ΔTmax 100 ^{o}C) in the DSC curve corresponds to the ionic dehydration. Second endothermic peak observed in the range 450-500 ^{o}C (ΔTmax 471.25 ^{o}C) in the DSC curve corresponds to the loss of ligand along with coordinated chloride ion. The mass of final residue corresponds to stable Molybdenum oxide MoO_3.

The Mo(VI) complex Ligand L2 in which one lattice and one coordinated water molecules are removed with mass loss of 4.27 % (calcd.4.12 %) between 50-200 ^{o}C. An endothermic peak in the range 90-120 ^{o}C (ΔTmax 110 ^{o}C) in the DSC curve corresponds to the dehydration. Second endothermic peak observed in the range 470- 510 ^{o}C (ΔTmax 502.52 ^{o}C) in the DSC curve corresponds to the loss of ligand along with coordinated chloride ion.. The mass of final residue corresponds to stable Molybdenum oxide MoO_3.

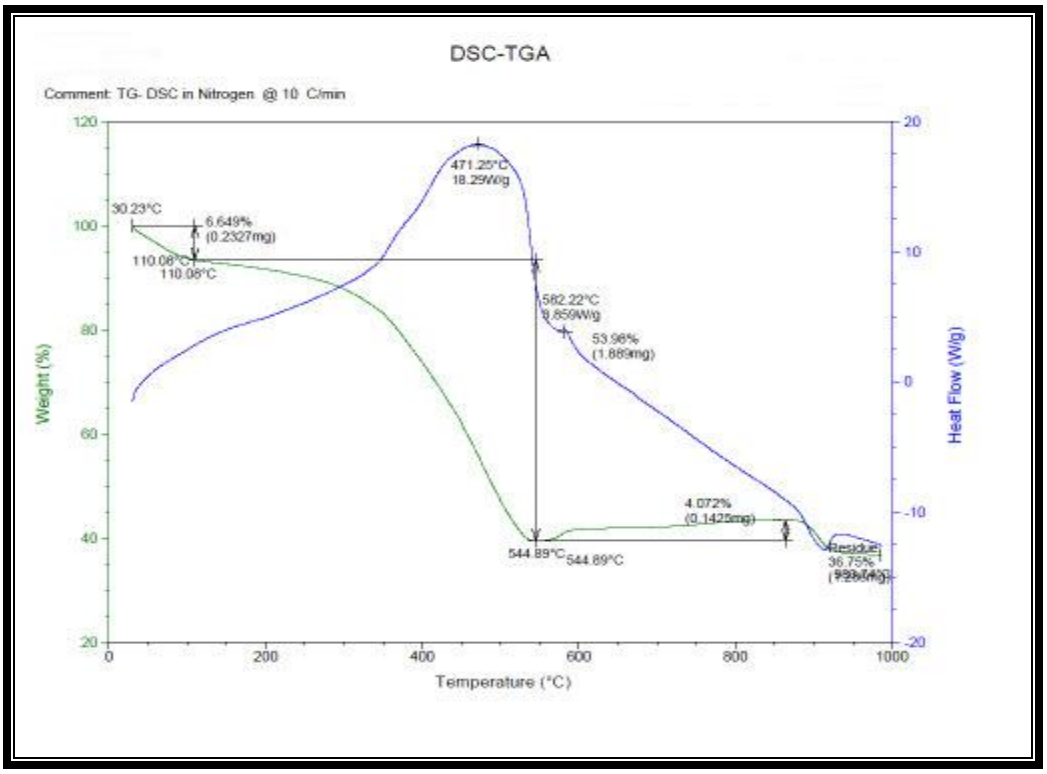

Fig. 3.4.1 TGA-DTA curves of Mo(VI) complex of Ligand L1

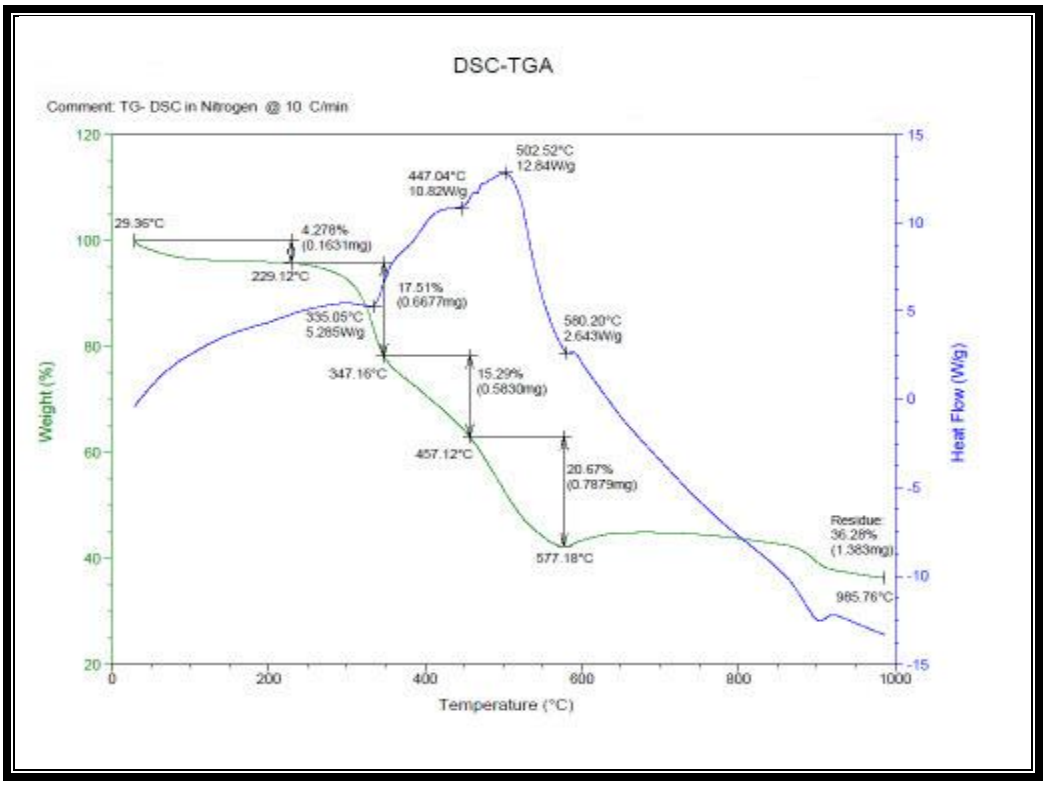

Fig.3.4.2 TGA-DTA curves of Mo(VI) complex of Ligand L2

2) Ru(III) complexes:

The Ru(III) complexes of ligands L1 and L2 were subjected to thermal decomposition studies. The thermal decomposition curves of these complexes are shown in Fig.3.4.3 and 3.4.4 respectively.

On the TGA curve of the Ru(III) complex of ligand L1 in which one water molecule and one chloride ion are removed with mass loss of 7.49 % (calcd. 7.78 %) between 50-180 ^{o}C .An endothermic peak in the range 140-150 ^{o}C (ΔTmax 145 ^{o}C) in the DSC curve corresponds to the coordinated dehydration and dechlorination step.Second endothermic curve observed in the range 425-475^{o}C (δmax 464.19 ^{o}C) in the DSC curve corresponds to the loss of ligand. The mass of final residue corresponds to stable ruthenium oxide.

On TGA curve of the Ru(III) complex of ligand L2 in which one water molecule and one chloride ion are removed with mass loss of 7.51 % (calcd. 7.58 %) between 50-140 ^{o}C . An endothermic peak in the range 120-140 ^{o}C (ΔTmax 130 ^{o}C) in the DSC curve corresponds to the coordinated dehydration and dechlorination. Second endothermic peak observed in the range 390-450 ^{o}C (ΔTmax 401.64 ^{o}C) in the DSC curve corresponds to the loss of ligand. The mass of final residue corresponds to stable ruthenium oxide.

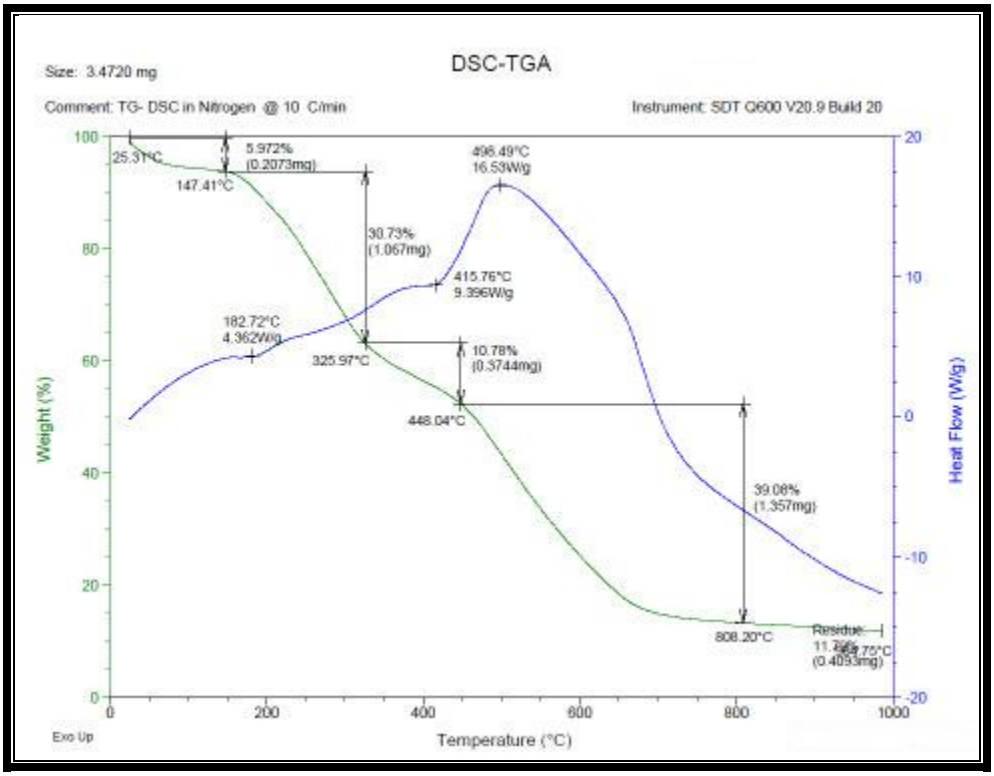

Fig.3.4.3 TGA-DTA curves of Ru(III) complex of Ligand L1

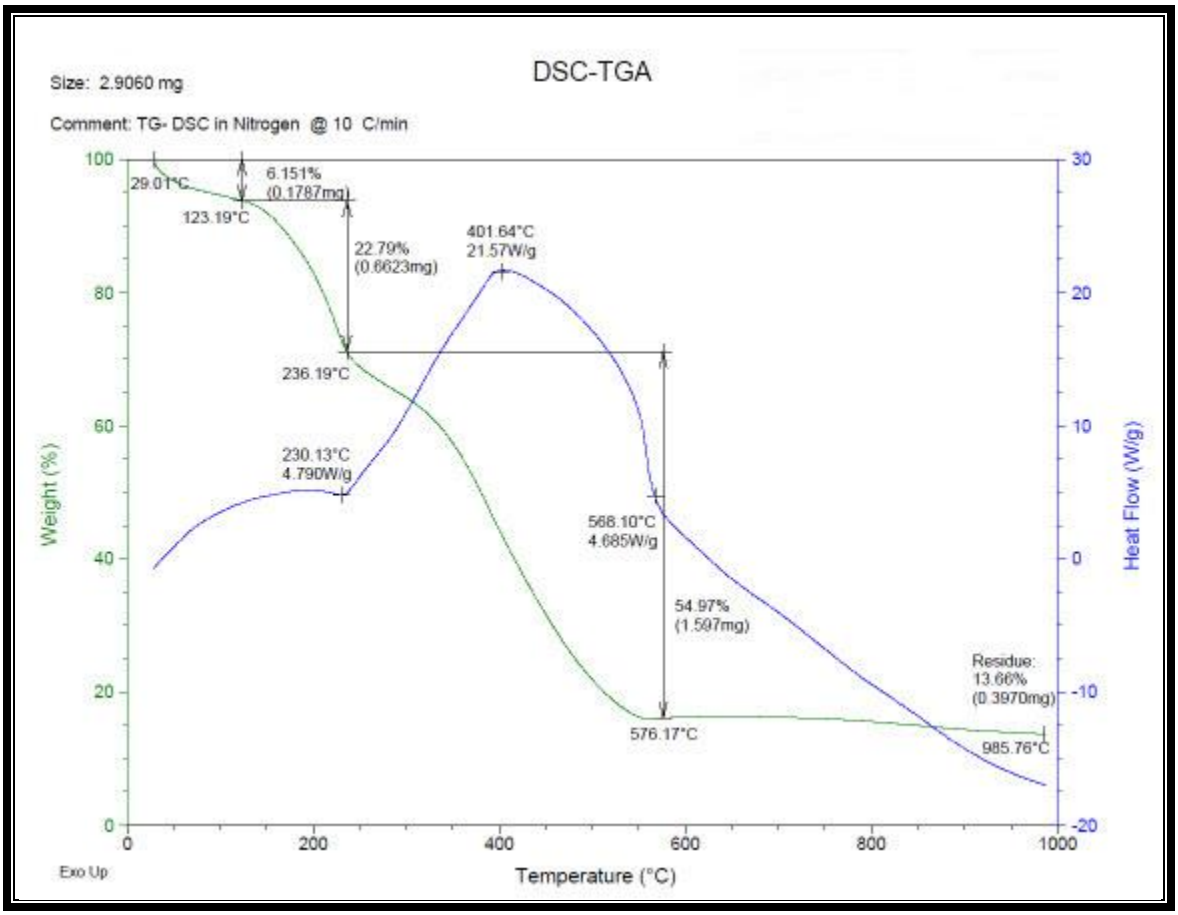

Fig.3.4.4 TGA-DTA curves of Ru(III) complex of Ligand L2

3) Pd(II) complexes:

The Pd (II) complexes of ligands L1 and L2 were subjected to thermal decomposition studies. The thermal decomposition curves of these complexes are shown in Fig.3.4.5 and 3.4.6 respectively.

On TGA curve of the Pd(II) complex of Ligand L1 in which two ligand molecules are removed with mass loss of 79.65 % (calcd.83.25 %) between 250-700 ^{o}C. An endothermic peak in the range 350-400 ^{o}C (ΔTmax 372.38 ^{o}C) in the DSC curve corresponds to the decomposion of ligand. The mass of final residue corresponds to stable PdO.

On TGA curve of the Pd(II) complex of ligand L2 in which two ligand molecules are removed with mass loss of 73.29 % (calcd.74.30 %) between 200-800 ^{o}C . An

endothermic peak in the range 450-500 ^{o}C (ΔTmax 483.35 ^{o}C) in the DSC curve corresponds to the decomposion of ligands. The mass of final residue corresponds to stable PdO.

In the TGA curve of the PdL1 complex, estimated mass loss of 20.4%.was observed. The weight loss is attributed to loss of ligated part. For this step the exothermic peak with CTmax=428.6 $^{\circ}$C in the DSC was observed.

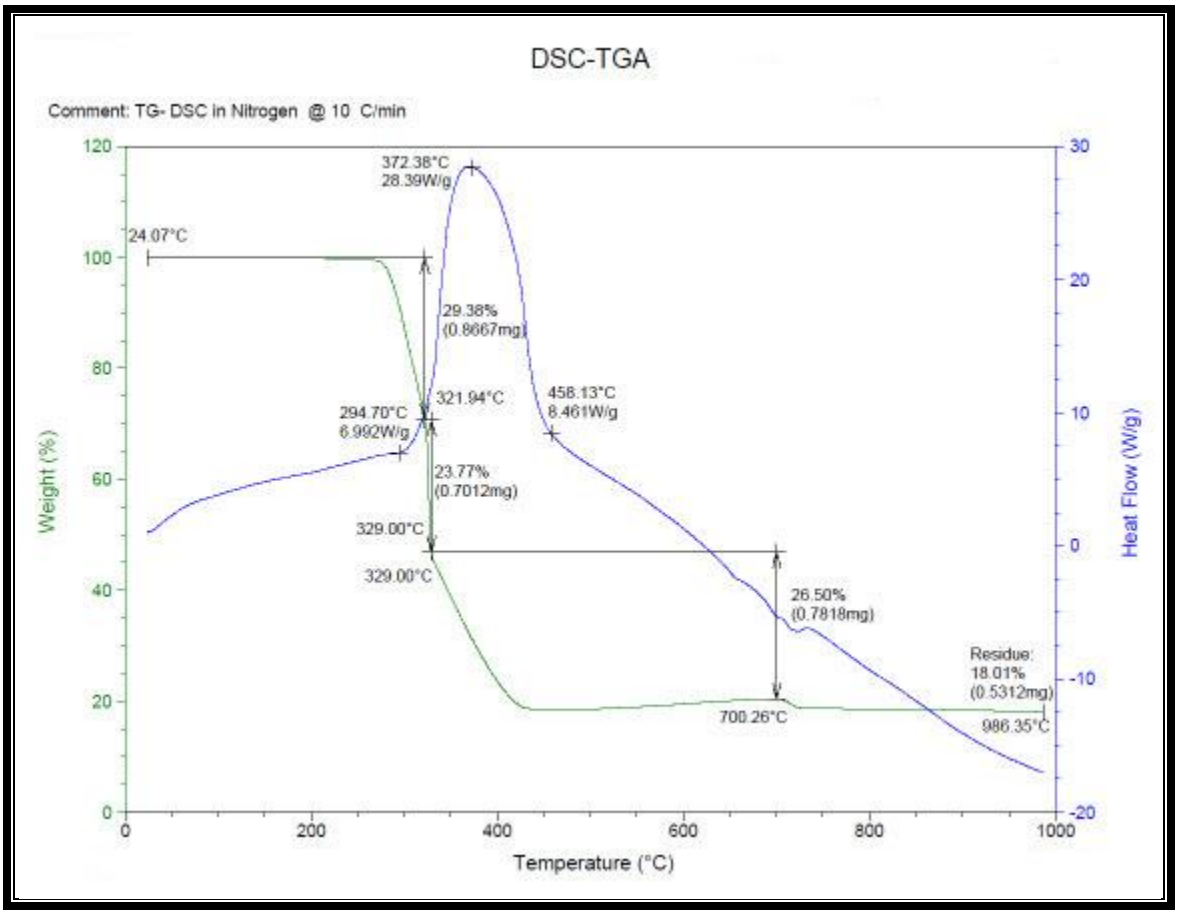

Fig.3.4.5 TGA-DTA curves of Pd(II) complex of Ligand L1

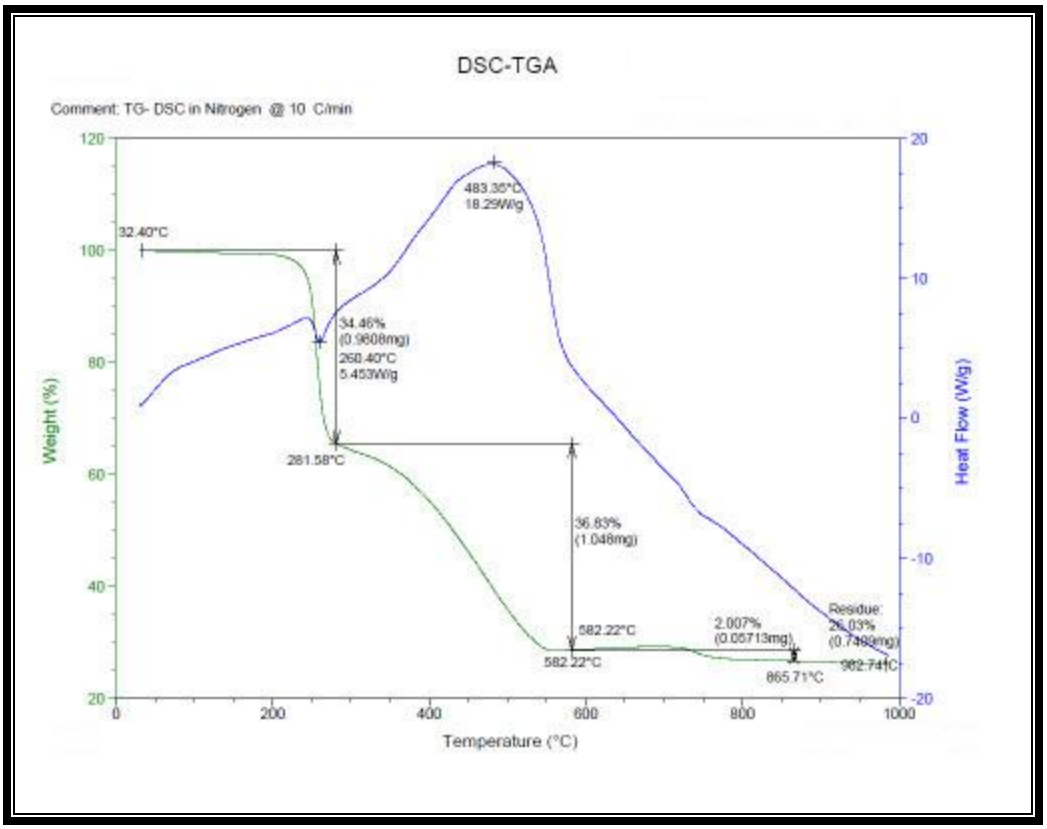

Fig.3.4.6 TGA-DTA curves of Pd(II) complex of Ligand L2

3.5 Section E:
X-Ray Diffraction Study of Metal Complexes

3.5.1 Theoretical Considerations:

X-ray crystallography is a technique that determines the arrangement of atoms within a crystal. Diffraction pattern can be described in terms of three dimensional array called lattice points. The simplest array of points from which a crystal can be created is called unit cell. It is possible to diffract X-ray by means of crystals because of the wavelength of X-ray is of about the same order as the inter atomic distances in crystal. The X-ray intersects with inner most electronic cloud in the atoms and provides information about internal arrangement of the atoms in the crystal [1-2]. The intensity of diffracted beam is related to structure of crystal. The ionic distribution in the sample can be determined by interpreting the XRD patterns and this direct tool for assigning the crystal pattern for the complexes.

The X-ray powder diffractograms of representative metal complexes synthesized were used for crystal structure characterization and determination of lattice dimensions. The observed data of compounds under investigation was compared with other literature data having analogous cell and subsequent index to similar geometry.

The X-ray diffractograms of respective metal complexes were scanned in the range 20-1000 at λ = 1.543 A. The diffractograms and associated data depict the 2θ value for each peak, relative intensity and observed inter planer spacing (d-values). The information gathered from diffractogram and associated data was used for indexing the pattern and to find out the unit cell dimensions and space group. The unit cell data of metal complexes along with the powder diffraction data are given in the respective table. The positions of each reflection with intensity are recorded. Inter planer spacings were calculated from 2θ values using the relation $\eta\lambda=2d\sin\theta$.

The computer programme used for indexing data was powder_XRD. The preliminary data in the form of 2θ and intensities fed to the computer programme and all differences (d-obs) are calculated as required. All the possible combination of h k l planes and d values observed are arranged in the decreasing order. In this, all the essential features of X-ray programme are presented and in addition, it calculates the deviation in lattice

parameters a, b, c in A° and α, β and γ in degree and minutes with better combination of h, k, l values. When the system of compound is unknown the observed data is first tested with the isometric chart and Hul_Devy's curve for tetragonal and hexagonal system. If the tests are proved to be negative then the data is subjected to programme bar and an attempt is made to index it in an orthorhombic system. The failure of all these tests is an indication for the existence of lower symmetry and then data can be indexed on either monoclinic or triclinic system. The precise lattice parameters and the deviations are obtained from powder X programme.

3.5.2 X-ray diffraction studies of metal complexes:

The X-ray powder diffractogram of the metal complexes were used for the structural characterization and determination of lattice dimensions. The observed data of complexes under investigation was compared with other literature data having analogous cell and subsequently indexed to similar geometry. The original diffraction patterns of complexes are presented in Figures.

1) X_ray Diffraction Studies of Mo (VI) Complex:

The Mo(VI) complex of ligand L1 was subjected to X-ray powder diffraction studies. The powder diffractogram of this complex is presented in (Fig.3.5.1) and x-ray diffraction data are presented in (Table 3.5.1 and 3.5.2). The diffractogram of Mo(VI) complex of LC shows 6 reflections with maxima at 2θ= 15.682 A^0 and intensity 994.60 a.u corresponding to d value 5.64317Aº. The observed & calculated densities are 1.67&0.88 g-cm^3 respectively. The standard deviation observed is 0.0067% which lies in permissible range. The unit cell of Mo(VI) complex yielded values of lattice constants a = 16.92Aº, b=10.35Aº, c=3.5Aº with α=90.000, β=90.000, c=90.000 with unit cell volume = 610.71081A^{o3}. In concurrence with these cell parameters the conditions such as a≠b≠c and α=β=γ=90º required for sample to be orthorhombic were tested and found to be satisfactory Hence, It can be concluded that Mo(VI) complex of ligand L1 have orthorhombic crystal system.

Table 3.5.1 Indexed X-ray diffraction data of Mo(VI) complex of ligand L1

Peak No.	2θ (observed)	2θ (calculated)	d (observed)	d (observed)	Miller indices of places	Relative intensities

					h	k	l	(%)
1	9.974	10.013	8.86243	8.82553	1	1	0	18.249
2	13.521	13.502	6.54371	6.55043	2	1	0	24.14
3	15.680	15.690	5.64632	5.54312	3	0	0	100
4	17.924	17.923	4.94423	4.94545	1	2	0	50
5	30.092	30.094	2.96723	2.96073	3	0	1	16.0572
6	41.042	41.012	2.19882	2.19891	5	2	1	14.2856

Table 3.5.2 Unit cell data and Crystal Lattice Parameters

a= 16.92973	Volume (V) = 610.71081
b= 10.35203	Density (obs) = 1.678
c= 3.4	Density (cal) = 0.88
α= 90.00	Z=4
β=90.00	Crystal system = Orthorhombic
γ=90.00	Porosity = 8.7%
Standard deviation (%)=0.0067	Particle size = 114.43A^{o}

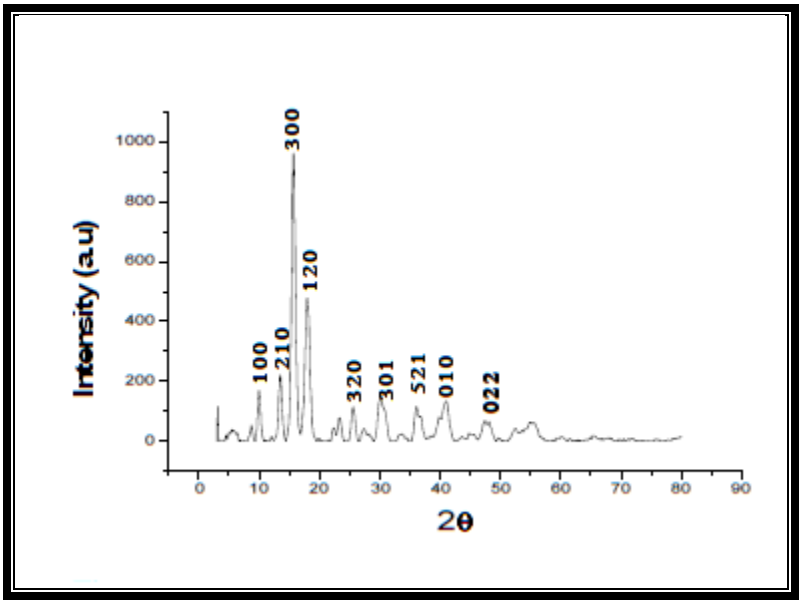

Fig.3.5.1 X-ray diffractogram of Mo(VI) complex with L1

2) X_ray diffraction studies of Ru(III)complexes:_

The Ru(III) complexes of ligand L1 were subjected to X-ray powder diffraction studies. The X-ray diffraction pattern of representative Ru(III) complex was shown in Fig.3.5.2. The unit cell data, crystal lattice parameters and diffraction data are presented in Table 3.5.3 and 3.5.4. The diffractogram of Ru (III) of L1 shows 12 reflections with maxima at 2θ=32.274 and it's intensity 1226 a. u. corresponding to d value 2.7712Aº. The observed and calculated density of Ru(III) complex of L1 ligand is 1.62 and 1.42 g-cm^3 respectively. The unit cell data of Ru(III) complex yielded values of lattice constants a=22.43 Aº, b = 3.4 Aº, c= 14.92 Aº and unit cell volume V = 823.431(Aº3). The standard deviation observed is within permissible range i.e. 0.046%.

In concurrence with these cell parameters, the conditions such as a ≠b≠c and α=β=90, γ =120 required for a sample to be monoclinic were tested and found to be satistafctory. Hence, it can be concluded that Ru(III) complex of Ligand L1 have monoclinic crystal system.

Saurabh Dave, Nidhi Bansal[5-6] reported $RuCl_3C_26H_{21}N_2O_3$ Ru (III) complex and yielded values of lattice constants a= 35.63 Aº,b=14.35Aº, c= 13.7450Aº and α = 90º β = 11.20Aº, γ= 90ºAº with unit cell volume V=65.54 (A^{o3}) respectively with monoclinic crystal system[4].

The Ru(III) complexes of ligand L2 were subjected to X-ray powder diffraction studies. The X-ray diffraction patterns of these complexes are shown in Fig 3.5.3 and the unit cell data, lattice parameters obtained are represented in Table 3.5.5 and 3.5.6.

In concurrence with these cell parameters, the conditions such as a≠b≠c and α=β=γ=900 required for sample to be tetragonal and found to be satisfactory. Hence, it can be concluded that Ru(III) complexes of ligands L2 have tetragonal crystal system.

Carl_Erik et al[7]synthesized Ru(III) complexes and assigned tetragonal system on the basis of observed lattice parameters, a=4.4919Aº, b=24.1266Aº, c=3.10065Aº, with unit cell volume = 62.28A^{o3}.

Table 3.5.3 Indexed X-ray diffraction data of Ru(III) complex of ligand L1

Peak No.	2θ (observed)	2θ (calculated)	d (observed)	d (observed)	Miller indices of places			Relative intensities (%)
					h	k	l	
1	5.474	5.483	16.12345	16.10045	-1	0	0	10.827
2	5.928	5.912	14.89423	14.92482	-1	0	1	9.489
3	12.698	12.706	6.96521	6.96111	1	0	1	15.31
4	22.610	22.613	3.92943	3.92908	-5	0	1	18.812
5	25.919	25.931	3.43475	3.43312	0	1	0	43.43
6	26.194	27.148	3.27652	3.28293	-2	1	1	13.99
7	28.245	28.234	3.15664	3.15794	-2	1	0	100
8	32.263	32.273	2.77162	2.77145	-2	1	3	8.71
9	39.894	39.882	2.25803	2.25863	6	0	1	13.632
10	46.465	46.465	1.95223	1.95421	-4	0	7	16.12
11	52.434	52.438	1.74352	1.74352	-2	0	7	15.02
12	57.938	34.04	1.59043	3.08	-1	0	0	13.02

Table 3.5.4 Unit cell data and Crystal Lattice Parameters

a= 22.43	Volume (V) = 823.431
b= 3.4	Density (obs) = 1.61
c= 14.92	Density (cal) = 1.43
α= 90.00	Z=4
β=134.1554	Crystal system = Monoclinic
γ=90.00	Porosity = 11.02%
Standard deviation (%)=0.046	Particle size = 191.53Aº

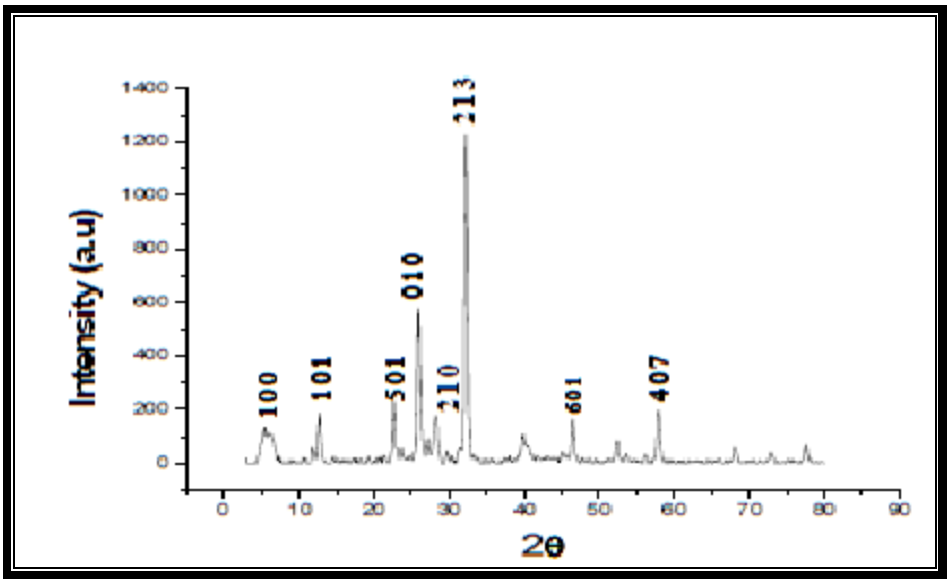

Fig.3.5.2 X-ray diffractogram of Ru(III) complex with L1

Table 3.5.5 Indexed X-ray diffraction data of Ru(III) complex of ligand L1

Peak No.	2θ (observed)	2θ (calculated)	d (observed)	d (observed)	Miller indices of places			Relative intensities (%)
					h	k	l	
1	5.350	5.383	16.42123	6.40321	0	0	1	9.872
2	12.742	4.67	6.87363	15.723	0	0	2	17.032
3	22.792	22.793	3.89732	3.89821	2	0	0	24.572
4	26.101	26.102	3.41123	3.41052	2	1	1	26.14
5	32.432	32.437	2.75534	2.75643	2	2	0	100
6	46.652	46.654	1.94522	1.94532	2	1	7	11.423
7	58.063	58.043	1.58734	1.58733	4	0	6	17.32

Table 3.5.6 Unit cell data and Crystal Lattice Parameters

a= 7.72	Volume (V) = 996.3825 A^{o3}
b= 7.7	Density (obs) = 0.95
c= 16.40843	Density (cal) = 0.72
α= 90.00	Z=2

β=90.00	Crystal system = Tetragonal
γ=90.00	Porosity = 21%
Standard deviation (%)=0.0012	Particle size = 178.48Aº

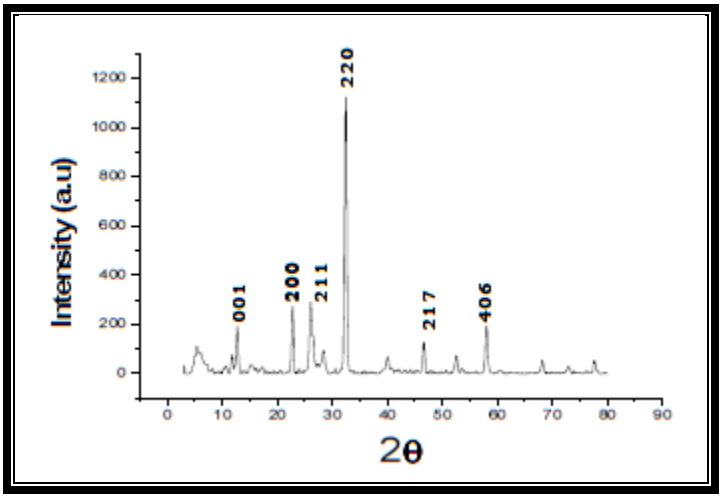

Fig.3.5.3 X-ray diffractogram of Ru(III) complex with L2

3) X-ray Diffraction Studies of Rh(III) Complexes :

The Rh(III) complexes of ligand L1 & L2 were selected for X-ray powder diffraction studies. The powder diffractogram of these complexes are presented in (Figs.3.5.4 and 3.5,5) and X_ray diffraction data are presented in Tables 3.5.7 and 3.5.8 for L1 and Table 3.5.9 and3.5.10 for L2. The diffractogram of Rh(III) complex of L1 & L2 shows 13 & 9 reflections with maxima at 2θ = 32.471Aº and 9.06Aº respectively, it's intensity observed at 1099 a.u& 142.01a.u with d values 2.75 Aº and 9.7Aº. The standard deviation observed is within permissible range 0.012 & 0.018 % respectively. The observed and calculated densities are 1.75 and 1.674 g-cm^{-3} respectively, for Rh(III) complex of ligand L2 The Observed and calculated densities are 0.9 and 0.7 respectively. The unit cell of Rh(III) complex yielded values of lattice constants, a=16.44Aº, b=4.0598Aº, c=14.29215Aº and a=20.473Aº,b=4.851Aº, c=12.590Aº with unit cell volume 945.93 & 970.47A^{03} respectively.

In concurrence with these cell parameters, the conditions such as a≠b≠c and α=90.0, β=123.790, γ=120 required for sample to be monoclinic were tested and found to be

satisfactory. Hence, it can be calculated that Rh(III) complex of ligand L1& L2 have monoclinic crystal system.

Soumik Mandal et al.[10] synthesized Rh(III) complexes derived from 1_methyl _ 2_ imidazole carboxy aldehyde & 8_aminoqunoline. They were characterized by X_ ray crystal structure analysis. The complexes were found to be crystallized in monoclinic system having lattice parameters a=1097.6Aº, b=10.43Aº, c=10.27 Aº and unit cell volume 19.390A^{03}which satisfied conditions required for monoclinic crystal system that is $\alpha=\beta=90.0$, $\gamma\neq90.0$.

Table 3.5.7 Indexed X-ray diffraction data of Rh(III) complex of ligand L1

Peak No.	2θ (observed)	2θ (calculated)	d (observed)	d (observed)	Miller indices of places			Relative intensities (%)
					h	k	l	
1	5.427	5.414	16.26132	16.30213	-1	0	0	13.2
2	6.165	6.162	14,32687	11.23	1	0	0	7.1
3	11.803	11.782	7.49124	7.49913	-2	0	1	5.44
4	12.426	12.236	7.11652	6.692	0	0	1	5.824
5	12.692	11.964	5.96976	6.235	1	0	1	6.54
6	22.478	22.764	3.90306	3.90280	0	1	1	15.8
7	26.76	26.068	3.41444	3.41536	1	0	1	19.7
8	31.653	31.637	2.82598	2.82546	0	1	1	19.84
9	32.464	32.478	2.75512	2.75451	-2	0	4	100
10	40.012	40.009	2.25164	2.25173	7	0	1	6.64
11	46.654	46.642	1.94573	1.94583	-1	2	2	13.84
12	52.551	52.543	1.74006	1.74030	-7	1	5	7.4
13	58.071	58.072	1.58723	1.58713	-1	0	9	19.38

Table 3.5.8 Unit cell data and Crystal Lattice Parameters

a= 16.44123	Volume (V) = 945.93 A^{o3}
b= 4.059806	Density (obs) = 1.5
c= 14.29215	Density (cal) = 1.04
α= 90.00	Z=4
β=97.46	Crystal system = Monoclinic
γ=90.00	Porosity = 32%
Standard deviation (%)=0.012	Particle size = 186.65A^{o}

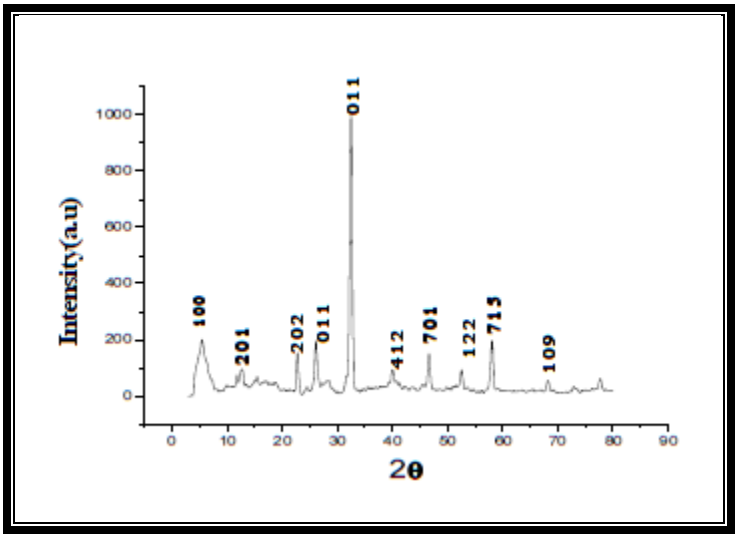

Fig.3.5.4 X-ray diffractogram of Rh(III) complex with L1-Lb

Table 3.5.9 Indexed X-ray diffraction data of Rh(III) complex of ligand L2

Peak No.	2θ (observed)	2θ (calculated)	d (observed)	d (observed)	Miller indices of places			Relative intensities (%)
					h	k	l	
1	5.571	5.558	15.84827	15.88657	-1	0	0	62.67
2	7.022	7.016	12.57781	12.58796	-1	0	1	24.63
3	9.062	9.044	9.75214	9.76997	0	0	1	100
4	18.143	18.145	4.88508	4.88497	0	0	2	38.641

5	19.121	19.121	4.64036	4.64027	1	1	0	38.64
6	19.785	17.234	4.48372	4.234	1	0	0	24.63
7	26.267	26.276	3.39004	3.39007	-6	0	2	28.16
8	32.630	32.644	2.74126	2.7404	-6	1	3	96.76
9	40.846	40.847	2.20745	2.20739	-4	1	5	42.23

Table 3.5.10 Unit cell data and Crystal Lattice Parameters

a= 20.47302	Volume (V) = 970.47453 A^{o3}
b= 4.851857	Density (obs) = 0.97
c= 12.59057	Density (cal) = 0.7
α= 90.00	Z=2
β=129.1064	Crystal system = orthorhombic
γ=90.00	Porosity = 50%
Standard deviation (%)=0.018	Particle size = 182A^{o}

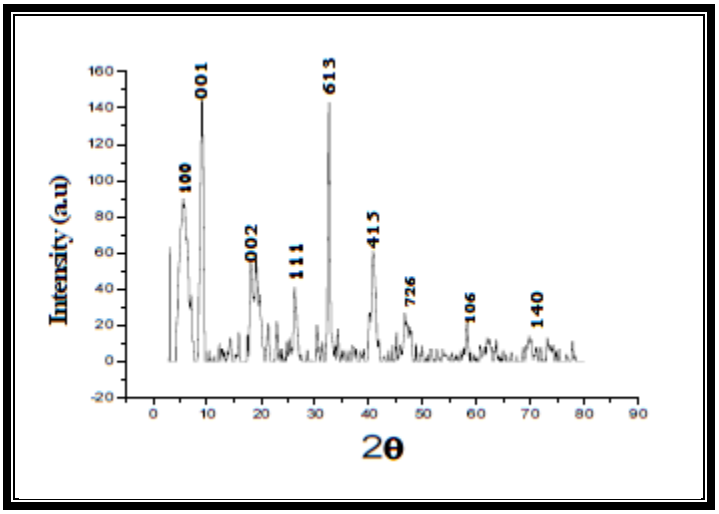

Fig.3.5.5 X-ray diffractogram of Rh(III) complex with L2-Ld

4) X_ray diffraction of Pd(II) complexes:_

The Pd (II) complex of Ligand L1 was subjected to X-ray powder diffraction studies. The powder diffractogram of complex is presented in (Fig.3.5.6) and X-ray diffraction data is presented in Table. 3.5.11 and 3.5.12. The diffractogram of Pd (II) complex of ligand L1 showed 10 reflections at maxima 2θ = 19.731 and it's intensity 2763 a.u. corresponding to d value 5.439Aº. The observed & calculated densities are 1.0 & 0.9 respectively. The standard deviation observed for Pd (II) complex is 0.064% which is within permissible limit.

The unit cell of Pd(II) complex yielded values of lattice constant. a=20.98Aº, b=8.68Aº, c= 4.63Aº and unit cell volume V = 846.82A^{o3}. In concurrence with these cell parameters the conditions such as a=b≠c and α=β=γ= 90 for sample to be orthorhombic were tested and found to be statisfactory. Hence, it can be concluded that Pd(II) complex of ligand L1 show orthorhombic crystal system.

Mehta et al.[17-18]synthesized Pd(II) complexes derived from thiosemicarb_ azone as a ligand, the complexs were found to be crystallized in orthorhombic crystal system with unit cell data a = 20.6267Aº, b=23.63Aº, c= 23.6779Aº with calculated and observed densities. 28Aº and 1.256gcm^{-3} respectively, the % porosity is 1.99. The unit cell volume of Pd (II) complex was found to be 12289.62A^{03}.

The diffractogram of Pd(II) complex of L2 showed 16 reflections with maxima at 2θ=19.73Aº and it's intensity 778 a.u corresponding to d value 4.48277Aº. The standard deviation observed for Pd(II) complex is 0.032% which is observed within the permissible limit. The observed and calculated densities of this complex are1.0 and 0.72 gm^{-3} respectively. The unit cell of Pd(II) complex yielded values oflattice constants a=13.94675Aº, b=7.6684Aº, c=9.7928Aº with unit cell volume V=531.443 (A^{03}).

In concurrence with these cell parameters, the conditions such as a≠b≠c and α=γ=90.0, β≠90.0 required for sample to be monoclinic were tested and found to be satisfactory. Hence, it can be calculated that Pd(II) complexes of ligand L2 have monoclinic crystal system.

Sehreineret et al.[11]reported Pd(II) complexes derived from 2 (Diphenylphosphino) benzaldehyde, 2-formylphenyldiphenylphosphine and characterized by X-ray crystal

structure analysis. The complexes were found to crystallized in monoclinic system having lattice parameter a=10.17A^0, b=2081.3A^0, c=1220.5A^0 and unit cell volume 2.520 A^{03}.

MauroV.de Almeida, etal[12_13]synthesized and characterized palladium Schiff base complexes derived from allyl_amine and vinylamine. The complexes were found to be crystallized in monoclinic system having lattice parameter=14.0A^0, b=7.29A^0, c=17.5A^0 and unit cell volume 1760.5A^{03} with calculated density 1.610gcm^{-3}.

Debasis Das et al[14] synthesized & characterized Pd(II) complexes of Schiff base ligands and reported monoclinic crystal system having unit cell lattice constant values of a=16.9353A^0, b=9.627A^0, c=20.667A^0, z=8, calculated density 1.637gcm^{-3}.with unit cell volume = 3369.4A^{03}.

Table 3.5.11 Indexed X-ray diffraction data of Pd(II) complex of ligand L1

Peak No.	2θ (observed)	2θ (calculated)	d (observed)	d (observed)	Miller indices of places			Relative intensities (%)
					h	k	l	
1	8.410	8.420	10.50468	10.49247	2	0	0	29.89
2	11.003	11.022	8.03442	8.02116	1	1	0	196
3	16.284	16.263	5.43906	5.44760	3	1	0	100
4	19.078	19.075	4.64853	4.64884	0	0	1	20.99
5	19.731	19.757	4.49590	4.48992	4	1	0	22.65
6	21.663	21.663	4.09896	4.09813	0	1	1	17.23
7	22.140	22.146	4.01134	4.01245	2	2	0	18.6
8	25.451	25.447	3.49680	3.49750	6	0	0	17.37
9	28.107	28.103	3.17220	3.17249	0	2	1	29.8
10	39.814	2.34	2.24234	1.24	0	1	0	23.84

Table 3.5.12 Unit cell data and Crystal Lattice Parameters

a= 20.98	Volume (V) = 846.82 A^{o3}
b= 8.68	Density (obs) = 1.0
c= 4.63	Density (cal) =0.9

α= 90.00	Z=3
β=90.00	Crystal system = orthorhombic
γ=90.00	Porosity = 9.4%
Standard deviation (%)=0.064	Particle size = 142.34A^{o}

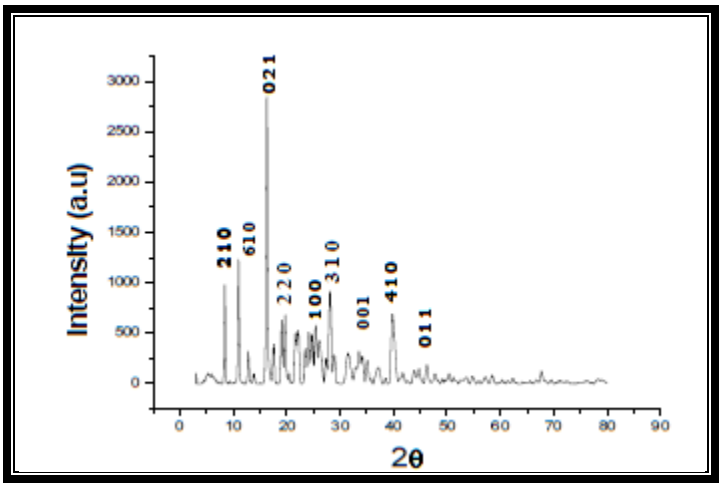

Fig.3.5.6 X-ray diffractogram of Pd(II) complex with L1

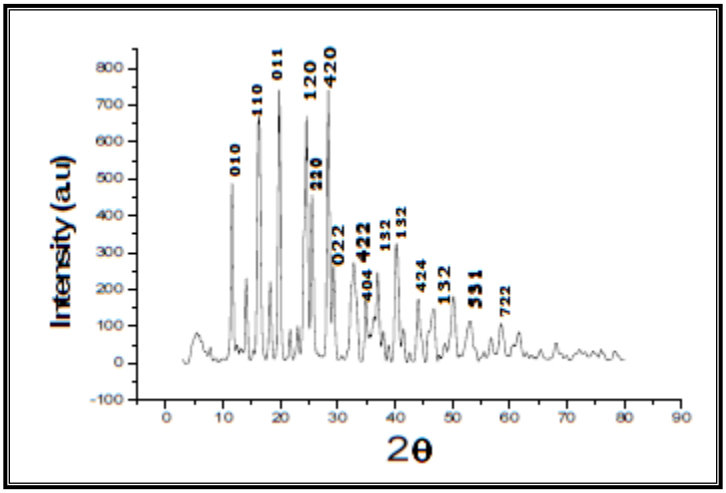

Fig.3.5.7 X-ray diffractogram of Pd(II) complex with L2

Table 3.5.13 Indexed X-ray diffraction data of Pd(II) complex of ligand L2

Peak No.	2θ (observed)	2θ (calculated)	d (observed)	d (observed)	Miller indices of places			Relative intensities (%)
					h	k	l	
1	11.564	11.530	7.64674	7.66847	0	1	0	65.29
2	14.055	14.043	6.29634	6.30224	-1	1	0	29.94
3	16.220	16.234	5.46019	5.45685	0	1	1	86.50
4	18.224	18.226	4.86372	4.86303	-2	0	2	28.79
5	19.789	19.775	4.47724	4.48582	-2	1	0	100
6	24.562	24.553	3.62163	3.62277	1	2	0	88.56
7	25.522	22.36	3.78743	4.56	1	0	0	59.64
8	28.335	28.229	3.14720	3.15110	-2	2	0	98.07
9	29.266	29.274	3.04922	3.04811	-4	1	1	34.190
10	32.349	32.346	2.76524	2.76543	-4	0	0	26.60
11	32.798	32.797	2.72865	2.76842	0	2	2	35.21
12	34.923	34.914	2.56726	2.56775	-4	2	2	25.04
13	36.923	36.939	2.43224	2.43151	-4	0	4	32.64
14	40.240	40.214	2.23936	2.24073	-1	3	2	43.04
15	44.056	44.067	2.05367	2.05342	-4	2	0	23.90
16	50.176	50.186	1.81679	1.81654	-5	3	1	21.9

3.5.14 Unit cell data and Crystal Lattice Parameters

a= 13.94675	Volume (V) = 531.443 A^{o3}
b= 7.6684	Density (obs) = 1
c= 9.7928	Density (cal) = 0.72
α= 90.00	Z=3
β=127.51	Crystal system = Monoclinic
γ=9.7928	Porosity = 28%
Standard deviation (%)=0.032	Particle size = 135.97A^{o}

4. Chapter -IV

Antimicrobial activity of metal complexes

4.1 Section A:

4.1. Antifungal activity:

Fungi are a kingdom of eukaryotic organisms. They are heterotrophic and digest their food externally, absorbing nutrient molecules into their cells. Yeasts, molds and mushrooms are examples of fungi. Fungi often have important symbiotic relationship with other organisms. Mycorrhizal symbiosis between plants and fungi is particularly important, over 90% of all plant species engage in some kind of mycorrhizal relationship with fungi and are dependent upon this relationship for survival. Fungi are also used extensively by humans, yeasts are responsible for fermentation of beer and bread and mushroom farming and gathering is a large industry in many countries. Fungi and bacteria are the primary decomposers of organic matter in most terrestrial ecosystem. Fungi were originally classified as plants, however, they have since been separated as they are heterotrophs. This means they do not fix their own carbon through photosynthesis, but use carbon fixed by other organism for metabolism. Fungi are now thought to be more closely related to animals than to plants, and are placed with animals in the monophyletic group of opisthokonts. The kingdom fungi included some of the most important organisms, both in terms of their ecological and economic role. By breaking down dead organic material, they continue the cycle of nutrients through ecosystems. In addition, most vascular plants could not grow without the symbiotic fungi, or mycorrhizae, that inhabit their roots and supply essential nutrients. Other fungi provide numerous drugs (such as penicillin and other antibiotics), foods like mushrooms, truffles and morels, and the bubbles in bread, champagne, and beer. Fungi absorb their food while animals ingest it, also unlike animals, the cells of fungi have cell walls. For these reasons, these organisms are placed in their own kingdom, Fungi, or Eumycota.

The external factors such as the composition of the medium used for fungal cultivation, pH value and the temperature influence and the composition of fungal cell walls.

Fungi also cause a number of plant and animal diseases: in humans, ringworm, athlete's foot, and several more serious diseases are caused by fungi. Because fungi are more chemically and genetically similar to animals than other organisms, this makes fungal diseases very difficult to treat. Plant diseases caused by fungi include rusts, smuts, leaf rots and stem rots and may cause severe damage to crops.

In the present study three fungi were used (1) *Aspergillus flavus* (2) *Curvularia lunata* and 3) *Penicillium notatum*, because of their immense economic importance in industry, agriculture, medicine, food, and nutrition.

4.1.1 Aspergillus flavus

Thom and Raper recognized more than 78 species of *Aspergillus. Aspergillus flavus* is a plant, animal, and human pathogen that produces the carcinogen, aflatoxin. *Aspergillus flavus* is a fungus. It grows by producing thread like branching filaments known as hyphae. Filamentous fungi such as *A. flavus* are sometimes called molds. A network of hyphae known as the mycelium secretes enzymes that break down complex food sources. The resulting small molecules are absorbed by the mycelium to fuel additional fungal growth. The unaided eye cannot see individual hyphae, but dense mats of mycelium with conidia (asexual spores) often can be seen. The ear of maize below shows the growth of the fungus covering four maize kernels. When young, the conidia of *A. flavus* appear yellow green in color. As the fungus ages the spores turn a darker green. In nature, *A. flavus* is capable of growing on many nutrient sources. It is predominately a saprophyte and grows on dead plant and animal tissue in the soil. For this reason it is very important in nutrient recycling. *Aspergillus flavus* can also be pathogenic on several plant and animal species, including humans and domestic animals. The fungus can infect seeds of corn, peanuts, cotton, and nut trees. The fungus can often be seen sporulating on injured seeds such a maize kernels. Often, only a few kernels will be visibly infected. Growth of the fungus on a food source often leads to contamination with aflatoxin, a toxic and carcinogenic compound. *Aspergillus flavus* is also the second leading cause of aspergillosis in humans. Patients infected with *A. flavus* often have reduced or compromised immune systems. Finegold et al. reported twelve cases of aspergillosis, which closely resemble to those of tuberculosis. The epidemiology of *Aspergillus flavus* differs depending on the host species. The fungus overwinters either as mycelium or as resistant structures known as sclerotia. The sclerotia either germinate to produce additional hyphae or they produce conidia (asexual spores), which can be dispersed in the soil and air. These spores are carried to the maize ears by insects or wind where they germinate and infect maize kernels. Unlike most fungi, *Aspergillus flavus* is favored by hot dry conditions. The optimum temperature for growth is 37^{o}C, but the fungus readily

grows between the temperatures of 25-42ºC, and will grow at temperatures from 12-48ºC. Such a high temperature optimum contributes to its pathogenicity on humans.

4.1.2 Curvularia lunata

Curvularia is a dematiaceous filamentous fungus. Most species of Curvularia are facultative pathogens of soil, plants, and cereals in tropical or subtropical areas, while the remaining few are found in temperate zones. As well as being a contaminant, Curvularia may cause infections in both humans and animals. The genus Curvularia contains several species, including Curvularia brachyspora, Curvularia clavata, Curvularia geniculata, Curvularia lunata, Curvularia pallescens, Curvularia senegalensis, and Curvularia verruculosa. Curvularia lunata is the most prevalent cause of disease in humans and animals. Curvularia spp. are among the causative agents of phaeohyphomycosis. Wound infections, mycetoma, onychomycosis, keratitis, allergic sinusitis, cerebral abscess, cerebritis, pneumonia, allergic bronchopulmonary disease, endocarditis, dialysis-associated peritonitis, and disseminated infections may develop due to Curvularia spp. Curvularia lunata is the most commonly encountered species. Importantly, the infections may develop in patients with intact immune system. However, similar to several other fungal genera, Curvularia has recently emerged also as an opportunistic pathogen that infects immuno compromised hosts. Curvularia produces rapidly growing, woolly colonies on potato dextrose agar at 25°C. From the front, the color of the colony is white to pinkish gray initially and turns to olive brown or black as the colony matures. From the reverse, it is dark brown to black

4.1.3 Penicillium notatum

Penicillium chrysogenum is a mold that is widely distributed in nature, and is often found living on foods and in indoor environments. It was previously known as Penicillium notatum. It has rarely been reported as a cause of human disease. It is the source of several -lactam antibiotics, most significantly penicillin. Penicillium is known as the blue-green mold on bread, fruits, and nuts. It is mostly found on rotting tangerines. It is also used for the production of green and blue mould cheese. The name Penicillium comes from the word "brush"; this refers to the appearance of spores in Penicillium. Like the many other species of the genus *Penicillium*, P. chrysogenum reproduces by dry chains of spores (or conidia) from brush-shaped conidiophores. The conidia are typically

carried by air currents to new colonization sites. In P. chrysogenum the conidia are blue to blue-green, and the mold sometimes exudes a yellow pigment. However, P. chrysogenum cannot be identified based on color alone. Observations of morphology and microscopic features are needed to confirm its identity. P. chrysogenum has been used industrially to produce penicillin and xanthocillin X, to treat pulp mill waste, to produce the enzymes polyamine oxidase, phospho-gluconate dehydrogenase, and glucose oxidase. Penicillium grows at its peak during the spring and winter, but the mold has no seasonal variation. It is a well-known group of brushed-shaped microorganisms belonging to the fungimycin family, and has no known sexual state. Penicillium is heterotrophic. This means that it gets nutrients through food digestion.

4.1.4 Factors affecting on fungal growth

1) Temperature:

For any particular organism the minimum and maximum temperatures are the lowest and highest at which growth occurs. The optimum temperature at which the growth rate is high is 20 – 30^{o}C

2) P^{H} of the medium:

Enzyme activity is also known to be conditioned by the composition of the medium, although different enzymes have different PH optima for their activity. The general favorable range lies between PH = 4 to PH = 8.

3) Humidity

Generally 95 to 100% relative humidity supports best growth of most fungi and those below 80-85% are inhibitory for them.

4) Concentration

A few workers have studied the effect of concentration of essential trace elements on the growth of fungi. They recorded that different fungi required different concentrations of trace elements for their optimum growth. Concentrations of essential trace elements higher than the optimum have been found to be inhibitory for the growth of different fungi studied by them.

4.1.5 Previous related study

Metal complexes is an important biological active compound. Studies have shown both antibiotic and antifungal effects of this compound. The compound is widely used in food

technology. It is used to enhance vitamin 'C' stability in vegetable, food processing and as a preservative. In aqueous solution, even at low concentration (0.02 – 0.2 %) dehydration acetic acid shows a strong antiseptic effect. Coordination of such compounds with metal ions such as copper, nickel, iron often enhances their activities as reported for pathogenic fungi.

From the documented literature, it is evident that, various metal complexes moiety exhibited appreciable antifungal acitivity and the activity varied with different amine moiety and metal ions in the complexes. Literatutre survey also unrevels the fact that, there is no attempt on the study of fungicidal and bactericidal activity of transition metal complexes. Since the antimicrobial activities increases due the presence of a, unsaturated system, an attempt is made to study the antifungal and antibacterial activity of some metal complexes of Mo, Ru,Rh and Pd. The fungicidal activities were screened *in vitro* against (1) *Aspergillus flavus* (2) *Curvularia lunata* and 3) *Penicillium notatum*

4.1.6 Experimental

1)Preparation of G.N. of Medium

The Glucose - Nitrate (G.N.) medium was prepared by dissolving 10.00 g of glucose, 2.5 g of potassium nitrate, and 1.0 g of potassium hydrogen phosphate, 0.5 g of magnesium sulphate and 0.001g of Rose Bengal in one lire of sterile distilled water. For the growth of fungi, glucose is the source for carbohydrate while potassium nitrate is for nitrogen, while potassium hydrogen phosphate and magnesium sulphate are the activators for growth.

2) Preparation of sets of test sample and control flasks

All the eight ligands and their five different metal complexes were used for testing fungicidal activity by using fungi (*Aspergillus flavus, Curvularia lunata* and *Penicillium notatum species*). Two different concentration levels 125 ppm and 250 ppm were used. The nine sets of each fungi were prepared, each set with control, one each with a ligand and five with metal complexes in GN media. The narrow necked 100 ml conical flasks were used. The sets were prepared in the following manner.

1. In control, 25 ml of GN media and 5ml of DMF (Dimethyl formamide) was taken in 100 ml conical flask.

2. Accurately weighed ligand in 5 ml DMF and 25 ml of GN were taken in 100 ml conical flask.

3. 25 ml of GN and accurately weighed complexes in 5 ml DMF were taken separately in 100 ml conical flasks.

All the flasks were plugged with non-absorbent cotton and then thoroughly mixed aseptically by autoclaving at 15 lbs pressure for 30 minutes. This effected total sterilization.

3)Inoculation and Incubation

The autoclave flasks were transferred to the inoculation chamber and exposed to UV light. The stock culture of fungi *Aspergillus flavus, Curvularia lunata* and *Penicillium notatum* were collected from the culture unit of the Department of Microbiology. The cell culture of test fungi in the form of spore suspension were prepared by adding 10ml of sterile distilled water to a seven days old culture of *Aspergillus flavus, Curvularia lunata* and *Penicillium notatum species*. The media were inoculated with five drops of the spore suspension. The autoclaved media flasks of control ligand and complexes were then incubated for seven days at $25^oC + 2^oC$ at room temperature.

4) Collection of microbial biomass

After desired incubation (seven days), the fungal biomass contents were filtered through previously weighed Whatman No.41 filter paper dried at $65^oC + 5^oC$ in oven previously. The mycelial biomass was dried along with the filter paper in a oven and mycelial dry weight (MDW) was recorded by subtracting the weight of filter paper47. Each treatment was replicated three times in all experiments. The mycelial dry weight (MDW) was corrected each time by subtracting the dry weight obtained from uninoculated flask under similar experimental conditions. The yield of MDW in mg at 125 ppm and 250 ppm are presented in Table 4.11.

4.1.7 Results and Discussion

It can be seen from the Tables No. 4.1.1, that the ligands and their metal complexes arrested the growth of all the three fungi *Aspergillus flavus, Curvularia lunata* and

Penicillium notatum. A considerable increase in fungitoxicity of metal complexes as compared to those of ligands is observed for both 125 and 250 ppm concentrations. At 125 ppm concentration, the percentage inhibition of *Aspergillus flavus, Curvularia lunata* and *Penicillium notatum* growth due to the ligands was found to be 15 - 40% while that due to their complexes was enhanced to 20 - 50 %. At 250 ppm concentration, the percentage inhibition of *Aspergillus flavus, Curvularia lunata* and *Penicillium notatum* growth due to the ligands was found to be 30 – 60 % while that

due to their complexes was enhanced to 35 – 100 %. In all the cases, the chelates exhibited toxicity as compared to their respective free ligands. Further, it is inferred that, the percentage inhibition of all the fungi *Aspergillus flavus, Curvularia lunata* and *Penicillium notatum* growth increases with increase in concentration of the test compounds.

The inhibition of growth of test fungi observed for all the complexes was not due to either metal ions or ligand alone, but was due to cumulative effect of both metal ion and ligand in the complexes. Hence, the complexes show synergistic combination. The fungicidal activity of any compound is a complex phenomena governed by combination of steric, electronic and pharmacokinetic factors. A possible mode of enhanced toxicity of the complexes could be speculated in the light of “Chelation theory”. It is postulated that, chelation reduces the charge on the metal ion considerably, mainly because of the partial sharing of its positive charge with the donor groups and possible electron delocalization over the whole chelate ring. This increases the lipophilic character of metal chelate which favors its permeation through lipid layers of fungus membrane. The antifungal activity of complexes are given below.

Table 4.1.1 Antifungal activity of metal complexes. Yield of mycelia dry weight in mg (% inhibition)

Compound	Aspergillus flavus		Curvularia lunata		Penicillium notatum	
	125 ppm	250 ppm	125 ppm	250 ppm	125 ppm	250 ppm
Control	97	98	71	69	86	86
Mo-L1	20	13	26	18	38	17
Ru-L1	22	15	28	20	32	16
Rh-L1	38	16	22	16	28	18
Pd-L1	32	16	38	18	34	20
Mo-L2	24	18	30	18	40	24
Ru-L2	28	12	34	26	26	17
Rh-L2	23	16	26	14	36	19
Pd-L2	35	14	36	16	26	14

4.2 Section B:

4.2 Antibacterial Activity

Microorganisms are the cause of many infectious diseases. The organisms involved include bacteria, causing diseases such as plague, tuberculosis and anthrax; protozoa, causing diseases such as malaria, sleeping sickness and toxoplasmosis; and also fungi causing diseases such as ringworm, candidiasis or histoplasmosis. However, all microorganisms do not produce diseases. The microorganisms capable of producing diseases in animal or human being are pathogenic organisms. Bacteria are microscopic and are relatively simple and primitive form of cellular organisms known as 'Prokaryotic'. The Danish physician Chriatian Gram, discovered a stain known as Gram stain, which divide all bacteria into two classes, "Gram positive" and "Gram negative". Bacteria can be classified according to their morphological characteristic as lower and higher bacteria. The lower bacteria have unicellular structure e.g. cocii, bacilli etc. The higher bacteria are filamentous organisms few being sheathed having certain cells specified for reproduction.

The biological and medicinal potency of coordination compound has been established by various microbial activities. This characteristic property has been related to the ability of the metal ion to form complexes with the ligands containing sulphur, nitrogen and oxygen atoms. The environment around the metal centre "as coordinated geometry" number of coordinated ligands and their donor group is the key for metalloprotein to carry out a specific physiological function. Manganese plays an important role in several biological redox-active system, a number of copper proteins including enzymes have been reported and protein containing iron participate in oxygen transpot. The preparation of model complexes having similar stereospecific feature is perhaps the most important step to understand the structure and behavior of these biological system.

4.2.1 Escherichia coli

Escherichia coli (**E. coli**), is one of the main species of bacteria living in the lower intestines of mammals, known as gut flora. When located in the large intestine, it actually assists with waste processing, vitamin K production, and food absorption. Discovered in 1885 by Theodor Escherich, a German pediatrician and bacteriologist, The E. coli strain

O157:H7 is one of hundreds of strains of the bacterium that causes illness in humans.2 As with all Gram-negative organisms, *E. coli* are unable to sporulate. Thus, treatments which kill all active bacteria, such as pasteurization or simple boiling, are effective for their eradication, without requiring the more rigorous sterilization which also deactivates spores. As a result of their adaptation to mammalian intestines, *E. coli* grow best *in vivo* or at the higher temperatures characteristic of such an environment, rather than the cooler temperatures found in soil and other environments. *E. coli* can generally cause several intestinal and extra-intestinal infections such as urinary tract infections, meningitis, peritonitis, mastitis, septicemia and Gramnegative pneumonia. The enteric *E. coli* are divided on the basis of virulence properties into enterotoxigenic (ETEC, causative agent of diarrhea in humans, pigs, sheep, goats, cattle, dogs, and horses), enteropathogenic (EPEC, causative agent of diarrhea in humans, rabbits, dogs, cats and horses); enteroinvasive (EIEC, found only in humans), verotoxigenic (VTEC, found in pigs, cattle, dogs and cats); enterohaemorrhagic (EHEC, found in humans, cattle, and goats, attacking porcine strains that colonize the gut in a manner similar to human EPEC strains) and enteroaggregative *E. coli*
(EAggEC, found only in humans).

4.2.2 Staphylococcus aureus,

Staphylococcus aureus, the most common cause of *staph infections*, is a spherical bacterium, frequently living on the skin or in the nose of a healthy person, that can cause a range of illnesses from minor skin infections (such as pimples, boils, and cellulitis) and abscesses, to life-threatening diseases such as pneumonia, meningitis, endocarditis, Toxic shock syndrome (TSS), and septicemia. *S. aureus* was discovered in Aberdeen, Scotland in 1880 by the surgeon Sir
Alexander Ogston in pus from surgical abscesses.3 *S. aureus* is a Gram-positive coccus, which appears as grape-like clusters when viewed through a microscope and has largened, round, golden-yellow colonies, often with _-hemolysis, when grown on blood agar plates. The golden appearance is the etymological root of the bacteria's name: *aureus* means "golden" in Latin.

4.2.3 Previous related study

The antibacterial activity of Schiff bases derived from dehydroacetic acid and thiocarbohydrazide were done by Rao et al. using paper disc method at concentration 500 and 1000 g/mL in DMF against *E.Coli* and *S.aureus.* It is observed that the ligand showed 8.2 and 42.5 % inhibition at 500 and 1000 _g/mL against *E.Coli* and 6.8 and 41.5 % against *S.aureus* at the same concentration. The complexes also show a minimum percentage inhibition of 9.5 % at 500 g/mL and 40.5 – 100 % inhibition at 1000 g/mL against *S.aureus.* Salunke23 synthesised transition metal complexes of aryl azo Schiff bases of dehydroacetic acid and aromatic amines. Some of the ligands and Cu complex are found to show moderate activity against *E.Coli.*

In the present study, the antibacterial activity of the test compounds were assessed against *Staphylococcus aureus* (gram positive) and *Escherichia Coli* (gram negative) organisms.

4.2.4 Experimental

1)Preparation of media

The nutrient agar prepared by dissolving bacteriological peptone (1g/L), beef extract (5 g/L), sodium chloride (5 g/L) in distilled water and the pH of the solution adjusted to 7.4 by sodium hydroxide (1M) or hydrochloric acid (1M). These solutions were filtered and agar (20 g/L) were added. Then it was sterilized for 30 minutes at 15 lb pressure.

2) Test organism

The test organisms were selected from both gram positive and gram negative organisms to test the antibacterial activity. The stock cultures were collected from the culture unit of the Department of Microbiology, These organisms were cultured on agar slants and incubated for 24 hrs at 32 – 34^{o}C. From these slants a suspension were made using sterile saline solution (saline solution was prepared by dissolving 0.9 gm of sodium chloride in 100 ml distilled water and then sterilized).

3) Method of testing

Bactericidal activities were evaluated by the paper disc plate method. The nutrient agar medium and 5mm diameter paper discs (Whatman No. 1) were used. The compounds

were dissolved in DMF making known stock solution. A known volume of stock solution is diluted in ethanol making 500 and 1000 ppm concentration. The filter paper discs were soaked in different solutions of the compounds and then placed in the Petri plates previously seeded with the test organisms (*Staphylococcus aureus* and *Escherichia Coli*). The plates were incubated for 24 -30 hrs and the inhibition zone around each disc were measured. The standard drug ciprofloxacin (500 and 1000 ppm) and the solvent used were

also tested for their activity under the same conditions. All these experimental procedures were repeated thrice with three replicates for each compound. The average values obtained for the ligand and there metal complexes are tabulated in Table 4.2.1.

4.2.5 Results and Discussion

The synthesized complexes were tested for their antibacterial activity against *Escherichia Coli* and *Staphylococcus aureus.*

It can be seen from the Table 4.2.1 that their metal complexes possess antibacterial activity. The ligands show weak activity with 8 – 13 mm zone of inhibition at 500 ppm and 10 – 15 mm zone of inhibition at 1000 ppm concentration for both the organisms.

The antibacterial activity is dependent on the molecular structure of the compound, the employed solvent and the bacterial strain under consideration. However standard drug ciprofloxacin showed very high activity with 24 mm zone of inhibition at 500 ppm and 26 ppm at 1000 ppm concentration under the same conditions.

The antibacterial data reveals that the metal complexes showed enhanced activity compared to the free ligand. Such increased activity of metal chelates can be explained on the basis of chelation theory and overtone's concept. According to overtone's concept of cell permeability, the lipid membrane that surrounds the cell favors the passage of only lipid soluble materials due to which liposolubility is an important factor that decides antimicrobial activity. On chelation, the polarity of metal ion will be reduced to a greater extent due to the overlap of positive charge of metal ion with donor groups. Further, it increases the delocalization of the pi-electrons over the whole chelation ring and enhances the lipophilicity of the complexes. This increased lipophilicity enhances the penetration of the complexes into lipid membrane and blocking the metal binding sites on the enzymes of microorganisms. These complexes also disturb the respiration process of

the cell and thus block the synthesis of proteins which restrict further growth of the organism. The antibacterial activity of metal complex are shown below.

Table 4.2.1 Antibacterial activity of metal complexes.

Compound	Diameter of inhibition zone (mm), Conc. In ppm.			
	Escherichia Coli		*Staphylococcus aureus*	
	500	1000	500	1000
Mo-L1	18	19	20	17
Ru-L1	15	17	18	15
Rh-L1	16	17	16	18
Pd-L1	19	20	17	16
Mo-L2	18	18	16	15
Ru-L2	15	18	19	16
Rh-L2	14	16	18	15
Pd-L2	15	18	16	17
ciprofloxacin	24	26	24	26

References

References

1. J. E. Huheey, Inorganic chemistry, Harper and Row, New York,(1983) 359.
2. G. B. Kauffman ed., “Coordination Chemistry”, A Century of Progress Amer. Chem. Soc., Washington, (1994).
3. F. J. C. Rossotti and H. Rossotti, “The Determination of Stability Constants” McGraw Hill Book Co., New York (1961).
4. W. H. Brock, K. A. Jensen, C. K. Jorgensen and G. B. Kauffman, “The origin and dissemination of the term ligand in Chemistry” Ambix 27 (1981), 171.
5. Morgan and Dew, J. Chem. Soc., 117 (1920), 1456.
6. P. Pfeiffer, Angew. Chem., 53 (1940), 93.
7. A. Z. Werner, Inorg. Chem., 3 (1893), 267.
8. G. N. Lewis, J. Am. Chem. Soc., 38 (1916), 762.
9. L. Pauling, “The nature of Chemical bond”, 3rd Edn, Cornell University press, Ithaca, New York, 162 (1960).
10. H. Bethe, Ann. Physik., 5 (1929), 133.
11. J. H. Van Vleck, Z. Physik., 73 (1931), 565.
22. G. A. Melson, Eds, Coordination chemistry of Macrocyclic compounds; Plenum New York, (1979).
23. R. M. Izatt, and christensen, J. J., Eds. "Synthesis of Mcrocycles the Design of selective complexing agents, progress in macrocyclic chemistry; willey interscience"; New York, (1987), 3.
24. L. F. Lindoy, "The chemistry of macrocyclic ligand complexes"; Cambridge university press; Cambridge (1989).
25. K. Dally, In synthetic multidentate Macrocyclic compounds; R. M. Izatt, J. J Christensen; Eds. Academic press; New York, (1978).
26. Y. K. Gupta, S. C. Agrawal, S. P. madnwat Ram Narain, Res. J.chem.sci, 2(4) (2012) 68.
27. J. Parekh, P. Inamdar,, R. Nair, S. Baluja, S. chanda, J. serb.chem.soc ; 70 (2005) 115.
28. D. Sinha, A. K. Tiwari, S. Sing, G. Shukla, P. Mishra, H. Chandra, A. K. Mishra, Eur.J.med.chem, 43 (2008) 160.

29. Y. Kumar, V. Gupta and S. Singh, Journal of pharmacy Research, Elsevier, 7 (6) (2013) 491.
30. J. Houch Zhu, B. Qiz,Zhou, M. Li, Y. Liu, Wahan univ.J.Nat sci; 15 (2010) 71.
31. N. Aggrawal, R. kumar, P. Durja, D. S. Rawal, J.Agric, Food chem., 57 (2009) 8520.
32. S. Adsule, V. Barve D. Ahmed, J.med.chem; 49 (2006) 7242.
33. Y. Elerman, M. K. Kabak, A. Z. Elmali, Nature fresh. Jiut chem. soc, 357 (2002) 651.
34. F. Lions and Barry Aust. J. Chem., 22 (1969) 17.
35. P. G. Avaji, C. H. V. Kumar, S. A. Patil, K. N.Shivnanada and C. Nagarjun, Eur.J.med.chem; 44 (2009) 3552.
36. H. G. Brugsch, J. occup .med; 7 (1965) 394.
37. B. Dash, P. K. Mahapatra, D. Panda, & J. M. Patnaik, J.Indian chem. Soc, 61 (1984) 1061.
38. N. R. Rao, P. V. Rao, G. V. Reddy, M. C. Ganorkar, Indian J chem, 26 A (1987) 887.
39. P. Mishra, P. N. Gupta, & A. K. Shankya, J. Indian chem. Soc, 68 (1991) 539.
40. N. Manav, A. K. Mishra, and N. K. Kaushik, Spectrochemica acta part A :Molecular Spectroscopy 60 A (2004) 3087.
41. A. S. Abel-Surrah, M. Kutteunen, Current Medicinal Chemistry, 13 (2006) 1337.
42. A. Jakson, J. Davis, R. J. Pither, Rodger, A. Inorg.Chem; 20 (2001) 3964.
43. E. H. Jame, A. K. Ellen, and L. K. Richard, “Inorganic chemistry”, Harper Collins, Fourth Edn; 97 (1993).
44. F. P. Dwyer, E. Mayhew, M. F. Roe, and R. Schilman, J.Cancer Res.19 (1965) 195.
45. J. A. Crim, H. G. Petering, J. Medicinal. Chem.13 (1976) 763.
46. E. J. Frihant, J. C. Bailer, J. Inorg.Nucl.Chem; 241 (1962) 205.
47. Kaul, Bansilal, Sandoz-Patent. Gmbh, Frg.Ger.Offin.D.E; 3413603, Al, 12 (1985).
48. Leung et al; 2013; Zhong et al; 2014; Liu et al; 2014; Ma et al; 2014 and Leung et al; (2012).
49. J. T. Mullhaupt, N. A, Stephenson, P. C. Stephenson, and Notaro Frank; Eur.Pat. appl. EP.711598A2, (1996).

50. M. M. T. Khan, S. B. Halligudi, S. Shukla and Z. A. Shaikh, J.Mol, Catal; 57 (1990) 301.
51. M. M. T. Khan, S. B. Halligudi, N. S. Rao, J. Mol,Catal; 63 (1990) 137.
52. Y. Aoyama, T. Fujisawa, T. Walanav, H. Toi and H. Ogashi, J. Am, Chem Soc; 108 (1986) 943.
53. E. Kimura, R. Machida and M. Kochima, J.Am.Chem, Soc; 106 (1990) 247.
54. P. K. Bhattacharya, Proc, Ind, Acad, Sci;(Chem.sci), 102 (1990) 247.
55. R. S. Brown, M. Zamakani, J. L. Sho, J.Am, Chem, Soc; 106 (1984) 5222.
56. S. A. Patil, V. H. Naik, A. D. Kulkarni, and P. S. Badami, Spectrochimica Acta A ,75 (2010) 347.
57. K. Sharma, R. Sing, N. Fahmi, R. V. Singh, Spectrochemica Acta A, 75 (2010) 422.
58. A. A. Al-Amiery, Y. K. Al-Majedy, H. Abdul Reazak, and H. Abood, (2011)"Bioinorganic chemistry and applications", (2011), 1-6, Article ID 483101.
59. J. Wiecek, D. Kovala-Demertiz, Z. Ciunik, M. Zervou, and M. A. Demertizis, 1 (2010) 9.
60. K. O. Ferraz, S.M.S.V. Wardell, J. L. Wardell, S. R. W Louro, and H. Beraldo, Artenia salina, Spectrochimica Acta A, & 3, 140.
61. A. E. Graminha, A. A. Bastida, I. C. Mendes, L. R. Teixeria, and H. Beraldo, Spectrochemica Acta A, 69, 1227.
62. N. Raja, and R. Ramesh, Spectrochemica Acta A, 75 (2010) 713.
63. A. Praveen Kumar, P. R. Reddy and V. K. Reddy, Jour.of The Korean Chem Soc, 51 (2007) 331.
64. C. Jayabalkrishnan, R. Kaevembu, and K. Natarajan, International J. of Che.Sci. 32 (2002) 1099.
65. I. D. Kostas, D. A. Heropoulos, D. Kovala-Demertzi, J. Tetrahedron Letters, 47 (2006) 4403.
66. J. S. Sttamler, J. D. Crapo, Fridovich, D.S. Patent CA-1, Pct. Appl. WO. 9639409A1, 12 Dec; 66 (1996).
67. M. E. Marmion, S. R. Woulfe, W. L. Neumann, D. L. Nosco, and E. Deutsch, Nuclear Med. Bio; 26 (7) (1999) 755.

68. R. C. Agarwal, B. Prasad, and B. N. Yadav, J. Inorg. Met Org.Chem, 23 (1993) 1061.
69. C. V. Sastri, D. Eswaramoorthy, L. Giribabu, and B. G. Maiya, Journal of Inorganic Biochemistry, vol. 94, no. 1-2 (2003) 138.
70. B. Forood, B. T. Flatt, C. Chassaing, and A. K. Katritzky, United States Patent US 6458789 B1, Lion Bioscience AG, 2002.
71. L. E. Kapinos and H. Sigel, Inorganica Chimica Acta, vol. 337 (2002) 131.
72. C. Yenikaya, M. Poyraz, M. Sarı, F. Demirci, H. Ilkimen, Polyhedron, vol. 28 (2009) 3526.
73. M. Odabas¸oˇglu, O. B¨uy¨ukg¨ung¨or, G. Turgut, A. Karadaˇg, E. Bulak, Journal of Molecular Structure, vol. 648, no. 1-2 (2003) 133.
74. K. Pavani and A. Ramanan, European Journal of Inorganic Chemistry, no. 15 (2005) 3080.
75. B. Dojer, A. Pevec, P. ˇSegedin et al., Inorganica Chimica Acta, vol. 363, no. 7 (2010) 1343.
76. M. A. S. Goher and T. C. W. Mak, Inorganica Chimica Acta, vol. 85, no. 2 (1984) 117.
77. B. Kozlevˇcar, N. Lah, D. ˇZlindra, I. Leban, and P. ˇSegedin, Acta Chimica Slovenica, vol. 48, no. 3 (2001) 363.
78. L. Li and F. Yuan, Synthesis and Reactivity in Inorganic, Metal-Organic, and Nano-Metal Chemistry, vol. 42, no. 2 (2012) 205.
79. K. Sakai,N. Akiyama, and M.Mizota, Acta Crystallographica Section E: Structure Reports Online, 59(7) (2003) 459.
80. M. M. Mashaly, Synthesis and Reactivity in Inorganic and Metal-Organic Chemistry, 34(1) (2004) 115.
81. S. Nieto, J. P´erez, L. Riera, V. Riera, and D. Miguel Chemical Communications, no. 22 (2009) 3279.
82. N. Lah, P. ˇSegedin, and I. Leban, Structural Chemistry, vol. 13(3-4) (2002) 357.
83. N. Kanematsu, M. Ebihara, and T. Kawamura, Inorganica Chimica Acta, vol. 292(2) (1999) 244.

84. S. A. Al-Jibori, Q. K. A. Al-Jibori, H. Schmidt, K.Merzweiler, C.Wagner, and G. Hogarth, Inorganica Chimica Acta, vol. 402 (2013) 69.
85. P. L. Andreu, J. A. Cabeza, V. Riera, Y. Jeannin, and D.Miguel, Journal of the Chemical Society, Dalton Transactions, no. 7 (1990) 2201.
86. S. Caglar, I. E. Aydemir, E. Adig¨uzel, B. Caglar, S. Demir, and O. Buyukgungor, Inorganica Chimica Acta, 408 (2013) 131.
87. E. Clot, J. Chen, D.-H. Lee et al., Journal of the American Chemical Society, 126(28) (2004) 8795.
88. B. Dojer, A. Pevec, M. Jagodi˘c, M. Kristl, and M. Drofenik, Inorganica Chimica Acta, 383 (2012) 98.
89. A.Moghimi, S.M.Moosavi, D. Kordestani et al., Journal of Molecular Structure, 828(1–3) (2007) 38.
90. J. H. K. Yip, Suwarno, and J. J. Vittal, Inorganic Chemistry, 39(16) (2000) 3537.
91. F. A. Mautner, A. Egger, B. Sodin et al., Journal of Molecular Structure, 969(1–3)(2010) 192.
92. L.Mei, L. S. Tai, J. Li, F. H. Tao, L. X. Liang, and Y. S. Zhong, Russian Journal of Coordination Chemistry, vol. 37(2) (2011) 153.
93. G. Sharma and A. K. Narula, Journal of Materials Science: Materials in Electronics, vol. 26 (2) (2015) 1009.
94. D. Neill, M. J. Riley, C. H. L Kennard, Acta Crystallogr. Sect. C Cryst. Struct. Commun., 53 (1997) 701.
95. L. J. Farrugia, P. Macchi, A. Sironi, J. Appl. Cryst. 36 (2003) 141.
96. P. V. Bernhardt, M. J. Riley, Aust. J. Chem., 56 (2003) 287.
97. Enemark JH, Cooney JJA, Wang J-J, Holm RH (2004) Chem Rev 104:1175–1200
98. Lyashenko G, Saischek G, Judmaier ME, Volpe M, Baumgartner J, Belaj F, Jancik V, Herbst-Irmer R, Mo¨sch-Zanetti NC (2009) Dalton Trans 29:5655–5665
99. Yin GC (2010) Coord Chem Rev 254:1826–1842
100. Hille R, Hall J, Basu P (2014) Chem Rev 114:3963–4038
101. Cindric´ M, Novak TK, Krajlevic´ S, Krajl M, Kamenar B (2006) Inorg Chim Acta 359:1673–1680

102. Cartuyvels E, Van Hecke K, Van Meervelt L, Go¨rller-Walrand C, Parac-Vogt TN (2008) J Inorg Biochem 102:1589–1598
103. Cindric´ M, Veksli Z, Kamenar B (2009) Croat Chem Acta 82(2):345–362
104. Djordjevic C, Puryear BC, Vuletic N, Abelt CJ, Sheffield SJ (1988) Inorg Chem 27:2926–2932
105. Dickman MH, Pope MT (1994) Chem Rev 94:569–584
106. Thiel WR (1997) J Mol Catal A: Chem 117:449–454
107. Jia M, Thiel WR (2002) Chem Commun 20:2392–2393
108. Pereira CCL, Balula SS, AlmeidaPaz FA, Valente AA, Pillinger M, Klinowski J, Goncalves IS (2007) Inorg Chem 46:8508–8510
109. Brito JA, Teruel H, Muller G, Massou S, Gomez M (2008) Inorg Chim Acta 361:2740–2746
110. Abrantes M, Amarante TR, Antunes MM, Gago S, Paz FAA, Margiolaki I, Rodrigues AE, Pillinger M, Valente AA, Goncalves IS (2010) Inorg Chem 49:6865–6873
111. Pisk J, Agustin D, Vrdoljak V, Poli R (2011) Adv Synth Catal 353:2910–2914
112. Pisk J, Prugovecki B, Matkovic-Calogovic D, Poli R, Agustin D, Vrdoljak V (2012) Polyhedron 33:441–449
113. Amarante TR, Neves P, AlmeidaPaz FA, Pillinger M (2012) AA Valente. I Inorg Chem Comm 20:147–152
114. Rayati S, Rafiee N, Wojtczak A (2012) Inorg Chim Acta 386:27–35
115. Masteri-Frhani M, Kashef Z (2012) J Magn Magn Mater 324:1431–1434
116. Grivani G, Akherati A (2013) Inorg Chem Comm 18:90–93
117. Djordjevic C, Puryear BC, Vuletic N, Abelt CJ, Sheffield SJ (1997) Inorg Chem 36:1798–1805
118. Das S, Bhowmick T, Punni-Yamurthy T, Dey D, Nath J, Chaudhuri MK (2003) Tetrahedron Lett 44:4915–4917
119. Gharah N, Chakraborty S, Mukherjee AK, Bhattacharyya R (2004) Chem. Comm. 22:2630–2632
120. Bregeault J-M, Vennant M, Salles L, Piquemal J-Y, Mahha Y, Briot E, Baka-la PC, Atlamsani A, Thouvenot R (2006) J MolCatal A Chem 250:177–189

121. Mancka M, Plass W (2007) Inorg Chem Commun 10:677–680
122. Gharah N, Chakraborty S, Mukherjee AK, Bhattacharyya R (2009) Inorg Chim Acta 362:1089–1100
123. Madeira F, Barroso S, Namorado S, Reis PM, Royo B, Martinsm AM (2012) Inorg. Chim Acta 83:152–156
124. Bagherzadeh M, Amini M, Parastar H, Jalali-Heravi M, Ellern AA, KeithWoo L (2012) Inorg Chem Commun 20:86–89
125. Carrasco CJ, Montilla F, Alvarez E, Herbert M, Galindo A (2013) Polyhedron 54:123–130
126. Sensato FR, Custodio R, Longo E, Safont VS, Andres J (2003) J Org Chem 68:5870–5874 127. Pontes da Costa A, Reis PM, Gamelas C, Romao CC, Royo B (2008) Inorg Chim Acta 361:1915–1921
128. Bagherzadeh M, Tahsini L, Latifi R, Ellern A, KeithWoo L (2008) Inorg Chim Acta 361:2019–2024
129. Bagherzadeh M, Mehdi Haghdoost M, Amini M, Derakhshandeh PG (2012) Catal Commun 23:14–19
130. E. M. Boon, J. K. Barton. Curr. Opin. Struct. Biol., 12 (2000) 320.
131. J. P. Paris, W. W. Brandt. J. Am. Chem. Soc., 81 (1959) 5001.
132. B. Norden, P. Lincoln, B. Akerman, E. Tuite. Met. Ions Biol. Syst., 33 (1996) 177.
133. K. E. Erkkila, D. T. Odom, J. K. Barton. Chem. Rev., 99 (1999) 2777.
134. Y. Xiong, L.-N. Ji. Coord. Chem. Rev., 185 (1999) 711.
135. C. V. Kumar, J. K. Barton, N. J. Turro. J. Am. Chem. Soc., 107 (1985) 5518.
136. H. L. Huang, Z. Z. Li, Z. H. Liang, J. H. Yao, Y. J. Liu. Eur. J. Med. Chem., 46 (2011) 3282.
137. H. L. Huang, Z. Z. Li, X. Z. Wang, Z. H. Liang, Y. J. Liu. J. Coord. Chem., 65 (2012) 3287.
138. X. W. Liu, Y. D. Chen, L. Li. J. Coord. Chem., 65 (2012) 3050.
139. Y. J. Liu, Z. H. Liang, Z. Z. Li, J. H. Yao, H. L. Huang. J. Organomet. Chem., 696 (2011) 2728.
140. J. M. Perez, A. G. Quiroga, E. I. Montero, C. Alonso, C. Navarro-Ranninger. J. Inorg. Biochem., 73 (1999) 235.

141. I. Kostova. Recent Pat. Anti-Cancer Drug Discovery, 1, 1 (2006).

142. P. Nagababu, M. Shilpa, M.B. Mustafa, P. Ramjee, S. Satyanarayana. Inorg. React. Mech., 6 (2008) 301.

143. P. Nagababu, S. Satyanarayana. Polyhedron, 26 (2007) 1686.

144. Significant literature references. Early Transition Metals: a) M. C. Wood, D. C. Leitch, C. S. Yeung, J. A. Kozak, L. L. Schafer, Angew. Chem., Int. Ed., 46 (2007) 354; b) C. Müller, C. Loos, N. Schulenberg, S. Doye, Eur. J. Org. Chem. (2006) 2499; c) H. Kim, P. H. Lee, T. Livinghouse, Chem. Commun. (2005) 5205; d) T. O. Nguyen, B. Y. -W. Man, R. Hodgson Aus. J. Chem. 64 (2011) 741; e) Z. Liu, H. Yamamichi, S. T. Madrahimov, J. F. Hartwig J. Am. Chem. Soc., 133 (2011) 2772; f) L. D. Julian, J. F. Hartwig, J. Am. Chem. Soc., 132, (2010) 13813; g) K. D. Hesp, M. Stradiotto, Chem. Cat. Chem. 2 (2010) 1192; h) C. F. Bender, R. A. Widenhoefer, Org. Lett., 8 (2006) 5303: i) S. Hong, T. J. Marks Acc. Chem. Res. 37 (2004) 673; j) G. A. Molander, J. A. C. Romero, Chem. Rev., 102 (2002) 2161.

145. a) J. S. Ryu, G. Y. Li, T. J. Marks, J. Am. Chem. Soc., 125 (2003) 12584; b) T. E. Müller, K. C. Hultzsch, M. Yus, F. Foubelo, M. Tada, Chem. Rev., 108 (2008) 3795.

146. D. R. Coulson, Tetrahedron Lett., 12 (1971) 429.

147. D. Selent, D. Scharfenberg-Pfeiffer, G. Reck, R. Taube, J. Organomet. Chem., 415, (1991) 417.

148. R. Taube, In Applied Homogeneous Catalysis, 2nd ed., Vol. 1 (Eds. B. Cornils, W. A. Hermann), Wiley-VCH, Weinheim, (2002) 513.

149. A. L. Casalnuovo, J. C. Calabrese, D. Milstein, J. Am. Chem. Soc. 110 (1988) 6738.

150. a) J. J. Brunet, G. Commenges, D. Neibecker, K, Philippot, L. Rosenberg, J. Organomet. Chem., 522 (1996) 117; b) ibid., Inorg. Chem, 33 (1994) 6373–6379; c) ibid., J. Organomet. Chem. 469 (1994) 221; d) J. J. Brunet, D. Neibecker, K. Philippot, Tetrahedron Lett., 34 (1993) 3877.

151. A. M. Monta˜na and C. Batalla, Current Medicinal Chemistry, 16(18) (2009) 2235.

152. A. S. Abu-Surrah and M. Kettunen, Current Medicinal Chemistry, 13(11) (2006) 1337.

153. F. L. Wimmer, S. Wimmer, P. Castan, S. Cros, N. Johnson, and E. Colacio-Rodrigez, Anticancer Research, 9(3) (1989) 791.
154. G. Zhao, H. Lin, Y. Ping et al., Journal of Inorganic Biochemistry, 73(3) (1999) 145.
155. H. Mansuri-Torshizi, T. S. Srivastava, H. K. Parekh, and M. P. Chitnis, Journal of Inorganic Biochemistry, 45(2) (1992) 135.
156. A. S. Abu-Surrah, T. A. K. Al-Allaf, L. J. Rashan, M. Klinga, and M. Leskel¨a, European Journal of Medicinal Chemistry, 37(11) (2002) 919.
157. T. A. K. Al-Allaf and L. J. Rashan, European Journal of Medicinal Chemistry, 33(10) (1998) 817.
158. T. A. K Al-Allaf, L. J. Rashan, M. T. Ayoub, and M. H. Adday, U.K. Patent No.2 304 712, (1997).